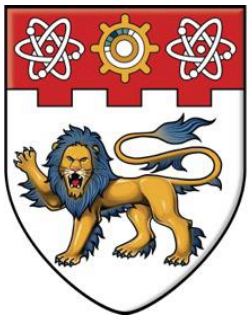

NANYANG TECHNOLOGICAL UNIVERSITY

THE CELLULAR THERMAL SHIFT ASSAY: A NOVEL STRATEGY TO STUDY DRUG TARGET ENGAGEMENT AND RESISTANCE DEVELOPMENT IN CANCER THERAPY

USHA SREEKUMAR LEKSHMY KUNJAMMA

2017

Supervisor: Prof. Pär Nordlund

School of Biological Sciences - Division of Biomedical Structural Biology
61 Biopolis Drive, Proteos – Singapore 138673

THE CELLULAR THERMAL SHIFT ASSAY: A NOVEL STRATEGY TO STUDY DRUG TARGET ENGAGEMENT AND RESISTANCE DEVELOPMENT IN CANCER THERAPY

USHA SREEKUMAR LEKSHMY KUNJAMMA

School of Biological Sciences

A thesis submitted to the Nanyang Technological University in partial fulfillment of the requirement for the degree of Doctor of Philosophy

2017

ACKNOWLEDGEMENTS

The four years of PhD life has been an amazing experience. This work wouldn't have been possible without the undying support of many people. I would like to take this opportunity to express my heartfelt gratitude to all those who have contributed to this journey of mine.

First and foremost, I would like to express my sincere gratitude my supervisor Prof. Pär Nordlund for giving me the opportunity to work on this project. Thank you Pär for all your invaluable guidance and support as well as for providing me a great work environment.

I am grateful to Dr. Andreas Larsson for the supervision and all the discussions that has helped in the progress of my research. Andreas, it has been a great pleasure working with you and thank you for all your guidance and encouragement. Thanks to Dr.Anna Jansson and the team members (present and past) of the fragment based drug design team: Dr.Christofer Björkelid, Dr. Kim Young-Mee, Dr.Chen Dan, Lim Pei Yiing and Yeung Kit for your suggestions and support.

I would like to thank all the CETSA team members (present and past): Dr. Lim Yan-Ting, Dr. Dai Lingyun, Dr. Radoslaw Mikolaj Sobota, Dr. Nayana Prabhu Padubidhri, Dr. Wang Loo Chien, Dr. Chen Liyan, Dr. Chris Soon Heng Tan, Dr. Yu Han, Dr. Sun Wendi, Dr. Lavanya Sundararaman, Veerappan Saranya, Zhao Tianyun, Go Ka Diam and Brenda Puspita for sharing your expertise. Yan Ting, thank you very much for your guidance and for always finding time for the project discussions.

Thanks to all the present and past members of the Nordlund group and protein production platform (PPP) for helping me and contributing to my research.

My acknowledgement also goes to the Resistant Cancer Cell Line (RCCL) collection (University of Kent) for providing the drug resistant cell lines for my study.

I gratefully acknowledge all my dear friends for their continuous encouragement. Special thanks to Saranya Veerappan and Manikandan Krishnamoorthy for your generous care and support especially during my thesis writing time. Thank you Sriram Swaminathan for the words of encouragement.

Finally, I acknowledge the people who mean everything to me, my family, without their prayers and support this journey would have been impossible.

I am forever grateful to my parents E.R Sreekumar and Usha Sreekumar. Thank you acha and amma for being my pillar of strength, believing in me and giving me the freedom to choose what I desired. I bow down to you for all the unconditional love, care and sacrifice you have made to shape my life. Thanks to my baby sister Vani Sreekumar, your jokes and funny conversations have certainly helped in uplifting my mood whenever I am down.

I would like to thank my grandparents Unnikrishnan Nair and Omanaamma for their selfless love and encouragement. Appooppan and ammachi, thank you for always being proud of even my smallest achievements.

I can't thank enough my husband Hariharan Sivaraman for being my backbone. Hari, you always stand by me and keep motivating me to chase my dreams. I am truly blessed to have you as my best friend for life. Thank you for your enormous love and support.

I express my gratitude to my parents-in-law Sivaraman Rajagopalan and Mohanambigai Sivaraman and brother-in-law Karthikeyan Sivaraman. Thank you appa, amma and anna for your unwavering love and understanding.

I am thankful to all my beloved people in the Eruppakkattu family and Cherukara family for your support and constant encouragement.

I thank God, the Almighty for being with me in each and every step of my life.

TABLE OF CONTENTS

LIST OF FIGURES

LIST OF TABLES

ABBREVIATIONS

1-MNA	1-Methylnicotinamide
5FdU	5-Fluorodeoxyuridine
5FU	5-Fluorouracil
ABC	ATP-binding cassette
ADMET	Absorption, distribution, metabolism, elimination and toxicity
AICARFT	5-aminoimidazole-4-carboxamide ribonucleotide formyltransferase
AlphaScreen	Amplified luminescent proximity homogeneous screen
AML	Acute myeloid leukemia
Arg	Arginine
ATP	Adenosine triphosphate
BCL	B-cell lymphoma
BCRP	Breast cancer resistance protein
BRET	Bioluminescence resonance energy transfer
BSA	Bovine serum albumin
cAMP	Cyclic adenosine monophosphate
CD	Clinical candidate
CDK	Cyclin-dependent kinase
cDNA	Complementary DNA
CETSA	Cellular thermal shift assay
CH_2THF	5,10-Methylenetetrahydrofolate
Cys	Cysteine
dAMP	Deoxyadenosine monophosphate
dC	2'-deoxycytidine
dCMP	Deoxycytidine monophosphate
DDR	DNA damage response
DHFR	Dihydrofolate reductase
DMSO	Dimethyl sulfoxide
DNA	Deoxyribonucleic acid
dNMP	deoxyribonucleoside monophosphate
dNTP	Deoxynucleoside triphosphate
DSC	Differential scanning calorimetry
DSF	Differential scanning fluorimetry

DSLS	Differential static light scattering
dT	deoxythymidine
dTTP	Deoxythymidine triphosphate
dU	Deoxyuridine
dUMP	Deoxyuridine monophosphate
dUTP	2'-deoxyuridine 5'-triphosphate
EA	Enzyme acceptor
ED	Euclidean distance
EDTA	Ethylenediaminetetraacetic acid
EFC	Enzyme fragment complementation assay
EGFR	Epidermal growth factor receptor
ELISA	Enzyme-linked immunosorbent assay
FBS	Fetal bovine serum
FDA	Food and Drug Administration
FdUMP	5-Fluoro-2′-deoxyuridine 5′-monophosphate
FLIM	Fluorescence-lifetime imaging microscopy
FPGS	Folyl polyglutamate synthetase
FR	Folate receptor
FRET	Fluorescence resonance energy transfer
GARFT	Glycinamide ribonucleotide formyltransferase
GF	Gel filtration
hCA	Carbonic anhydrase (human)
HCl	Hydrochloric acid
HIF1	Hypoxia-inducible factor 1
His	Histidine
hPARP	Poly (ADP-ribose) polymerase (human)
HRP	Horseradish peroxidase
hTNKS2	Tankyrase 2 (human)
HTS	High throughput screening
IDH1	Isocitrate dehydrogenase 1
IMAC	Immobilized metal affinity chromatography
ITC	Isothermal titration calorimetry
ITDR	Isothermal dose response
KB	Kinase buffer

LC	Liquid chromatography
MAD	Median absolute deviation
MDR	Multidrug resistance
MetAP2	Methionine aminopeptidase 2
MPM	Malignant pleural mesothelioma
mRNA	Messenger RNA
MRP	Multidrug resistance protein
MS	Mass spectrometry
MW	Molecular weight
MX	Methotrexate
NNMT	Nicotinamide N-methyltransferase
NX	Nolatrexed
PBS	Phosphate-buffered saline
PCFT	Proton-coupled folate transporter
PCR	Polymerase chain reaction
PDB	Protein data bank
PET	Positron emission tomography
Pgp	P-glycoprotein
PSM	Peptide spectrum matches
PSN	Penicillin-Streptomycin-Neomycin
PX	Pemetrexed
RFC	Reduced folate carrier
RNA	Ribonucleic acid
RPM	Revolutions per minute
RU	Response units
RX	Raltitrexed
SAH	S-Adenosyl-L-homocysteine
SAM	S-Adenosyl methionine
SDS-PAGE	Sodium dodecyl sulfate polyacrylamide gel electrophoresis
SG	Stargazer
SPR	Surface plasmon resonance
Tagg	Aggregation temperature
TBS	Tris-buffered saline
TBST	TBS with 0.05% Tween 20

TCEP	Tris(2-carboxyethyl)phosphine
TEAB	Triethylammonium bicarbonate
Tm	Melting temperature
TMP	Thymidine monophosphate
TMT	Tandem Mass Tag
TPA	Thermalpercipitation assay
TPP	Thermal proteome profiling
TS	Thymidylate synthase
U	Uridine
UDP	Uridine diphosphate
UMP	Uridine monophosphate
UTR	Untranslated region
VEGF	Vascular endothelial growth factor

ABSTRACT

The drug binding to its target molecule determines the efficacy of therapeutics. Therefore, it is important to study drug target engagement in cells. This is often difficult because drug binding cannot be directly measured inside cells. We have developed a technique called cellular thermal shift assay (CETSA) for studying drug binding to target proteins in cells and tissues. This assay is based on the biophysical principle of ligand-induced thermal stabilization of target proteins.

In this thesis, I have used CETSA for various applications. The assay was employed to study drug binding in cancer cell lines for a set of important clinical targets and to monitor processes of drug transport and activation in cells. We showed that CETSA has the potential to monitor drug resistance development during cancer therapy using antifolate and fluoropyrimide drug resistant cell lines. CETSA enables to understand the effects of drug usage and find out the most effective drug in targeting proteins in cancer patients.

Thermal precipitation assay (TPA) was developed in parallel to CETSA that uses the same principle to perform high throughput fragment screening at very low protein concentration. TPA was used for fragment screening of different clinically relevant targets.

The CETSA method combined with quantitative mass spectrometry detection permits the monitoring of a wide range of drug targets and the downstream effectors. We have used this strategy to study the interactions of metabolites with the human proteome. The method was validated with known nucleotide-protein interactions and most importantly, novel interactions were discovered.

These studies show that CETSA is likely to become a valuable tool for drug research and development.

CHAPTER 1: INTRODUCTION

1. Cancer: An overview

Cancer is a serious health problem in humans worldwide and it is the second major cause of death in the United States. Cancer involves the uncontrollable proliferation and spread of abnormal cells. This happens due to many external as well as internal factors. The external factors include exposure to chemicals or radiation, specific infections and usage of tobacco. The internal factors causing cancer are, for example, inherited and random mutations, hormones and immune conditions. Dietary factors, lack of physical exercise, infections, obesity and environmental pollutants are also known to increase the risk of cancer [1, 2]. All these factors may work together to promote carcinogenesis in humans.

The changes in the mechanisms regulating cell proliferation on one hand, and cell death including apoptosis, on the other, are important features of cancer development.

The processes involved in tumorigenesis are not completely understood but accumulated mutations reprogram the cells to drives the process where each successive generation of tumour cells are more adjusted to violate the laws that regulate the proliferation of normal cells [3].

A linear progression model was proposed by Fearon and Vogelstein to report the tumorigenesis process in colon cancer (Figure 1A) [4]. In this study, they suggest that malignant tumours gradually develop from benign tumours. The benign tumour gets converted in to less aggressive lesions and eventually become more fatal neoplasms. This model suggests that both epigenetic changes such as DNA methylation that affects expression of genes and genetic changes such as adenomatous polyposis coli (APC) mutations are also related to the evolution of neoplasms. The lethal neoplasms are preceded by less aggressive lesions with expected genetic modifications. Therefore, if these genetic defects can be detected in an early stage, therapies can potentially be explored to prevent development of advanced tumours. The recognition of mutated genes in cancers is critical not only to understand their mechanism of action but also to identify targets for therapeutics [3].

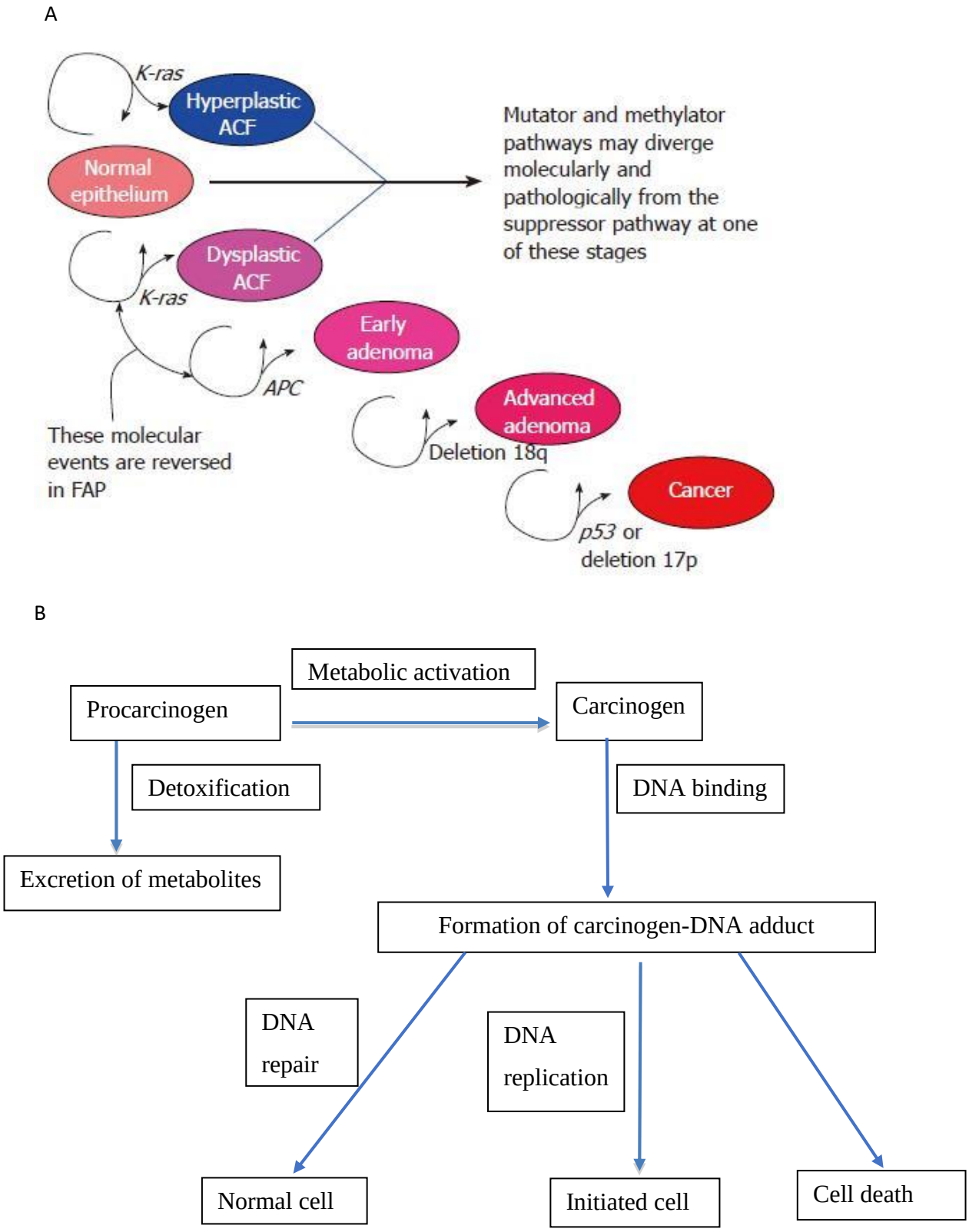

Figure 1: Mechanisms of carcinogenesis

The linear progression model of tumorigenesis proposed by Fearon and Vogelstein (A) [5].

Possible consequences of carcinogen metabolic activation (B) [3].

Carcinogenesis is the process caused by genetic mutations due to chemical or physical agents (Figure 1B). Carcinogenesis can be classified in to three stages that are initiation, promotion and progression [6]. The occurrence of a genetic mutation triggers initiation, and promotion happens due to increased multiplication of the initiated cells. In the progression stage, more genetic mutations accumulate that lead to malignancy. The active metabolites of most carcinogens bind to the DNA and forms adducts that can be eliminated only by DNA repair mechanisms [7]. If these adducts are not reversed, it leads to permanent mutations in the genome that can cause activation of the oncogenes or inactivation of the tumour suppressor genes.

Promotion is the process where chemical agents promote the proliferation of initiated cells. The promoting agents do not form any DNA adducts or damage the DNA but they can activate cell proliferation. [3].

Progression step involves the acquiring of additional mutations that causes malignancy. DNA damage is caused also by environmental factors such as ultra violet radiation, chemical agents and ionizing radiation. These factors can cause DNA lesions such as base alterations, deletion or addition of DNA sequences; cross-links, single-strand and double-strand breaks and insertion of incorrect bases [3].

2. Molecular biology of cancer

The characteristics that distinguish the tumour cells from healthy cells are the key to understand the behaviour of neoplasms. Such understanding can help in developing new targeted therapies for cancer. Several studies have been performed to understand phenotypic characteristics of tumour cells such as immortality, loss of cell cycle control, decreased reliance on growth factors that support cell proliferation, increase in genetic instability, loss of anchorage-dependent growth, decreased sensitivity to apoptotic cell death and angiogenesis [3,8]. These characteristics are described below.

2.1. Immortality:

Normal cells have a limited capacity to proliferate both *in vitro* and *in vivo*. On the other hand, cancer cells that are established in culture can divide and grow indefinitely and are therefore called immortalized cells. To become immortal, the cancer cells need to overcome mainly two mechanisms operative in normal cells. One of them is the inability of the DNA replication mechanism to effectively replicate the 5’ ends of the DNA that

causes chromosome shortening. Studies show that upregulation of telomerase activity also helps the tumour cells to proliferate indefinitely [9]. The other is the elimination of tumour suppressor activity that leads to loss of growth control [3].

2.2. Loss of cell cycle control:

Cell cycle regulation is important for control of proliferation and it consists of several steps that must be finished in a sequence wise and timely manner. The cell cycle regulatory machinery monitor, for example, the genome integrity, size of the cells, absence or presence of growth factors and the nutritional status of the cells. Cell division is divided in to G1, S, G2 and M phases (Figure 2). The DNA replication happens in the S phase and the segregation of the chromosomes take place in the mitotic phase, the M phase. Two groups of cell cycle proteins called cyclins and cyclin dependent kinases (CDKs) control the cell cycle process. The cyclin D1 is produced during the G1 phase and plays a critical role in the regulation of R point. Cyclin E is necessary to exit from the G1 phase and progress in to the S phase. Both these cyclins are upregulated in some tumours and therefore these proteins can be good therapeutic targets [10]. CDKs require the activation of an associated cyclin to function. The abundance of CDK proteins stay constant throughout the cell cycle mechanism but their activity changes at different stages of the cell cycle. Growth factors drive the proliferation while checkpoints along the cell cycle detect if the genome is intact and whether the previous steps of the cell cycle have been finished [10].

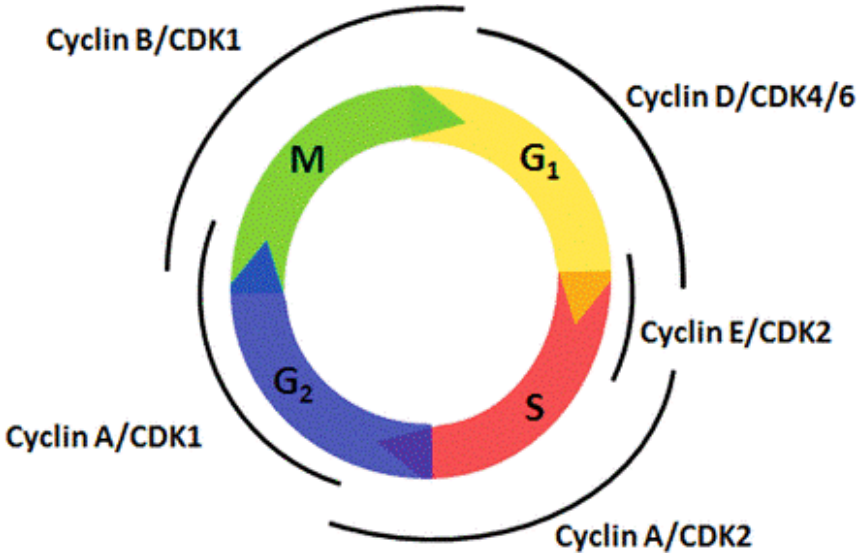

Figure 2: The cell cycle model

Different stages of cell cycle and the CDK/cyclin complexes required at each stage [11].

2.3. Decreased reliance on growth factors that support cell proliferation:

The cells growing in culture need various growth factors to support proliferation. In vivo the growth factors are provided extracellularly through the body circulation. The tumour cells also produce growth factors that bind and stimulate their own receptors - this phenomenon is termed as autocrine stimulation and generates a continuous self-produced proliferative signal. The growth factors and their receptors are therefore important targets for anti-cancer drugs. One example is the epidermal growth factor receptor (EGFR), which is upregulation in some tumour cells as proliferative drivers. Several approaches have been developed to inhibit EGFR activity in tumour cells such as monoclonal antibodies blocking EGFR activity, toxins fused to epidermal growth factor and small molecules inhibiting the activity of the receptor tyrosine kinase domain [3].

2.4. Decreased sensitivity to apoptotic cell death:

Apoptosis is a controlled process of cell death, which is important for balancing cell numbers in the human body. Impairment of the apoptotic processes plays a major role in diseases such as cancer. Morphological changes such as shrinkage of cells, swelling of cell membrane, chromatin condensation, degradation of DNA and nuclear fragmentation happens in apoptosis (Figure 3A).

Apoptosis is generally classified in to three phases that are the initiation phase, the decision phase and the degradation phase (Figure 3B). The signal transduction pathways that respond to both external and internal stimuli are activated in the initiation phase. The mitochondrial membrane loses its integrity in the decision phase where nucleases and proteases are released/activated to start the degradation phase. Cancer cells escape from apoptosis mainly through two mechanisms: overexpression of the Bcl-2 proteins and suppression of the Fas receptor. Overexpression of anti-apoptotic Bcl-2 proteins makes the cancer cells less sensitive to apoptosis and allows them to proliferate in conditions in which normal cells die [3]. The anti-apoptotic Bcl-2 proteins therefore constitute potential target for cancer therapy [12].

A

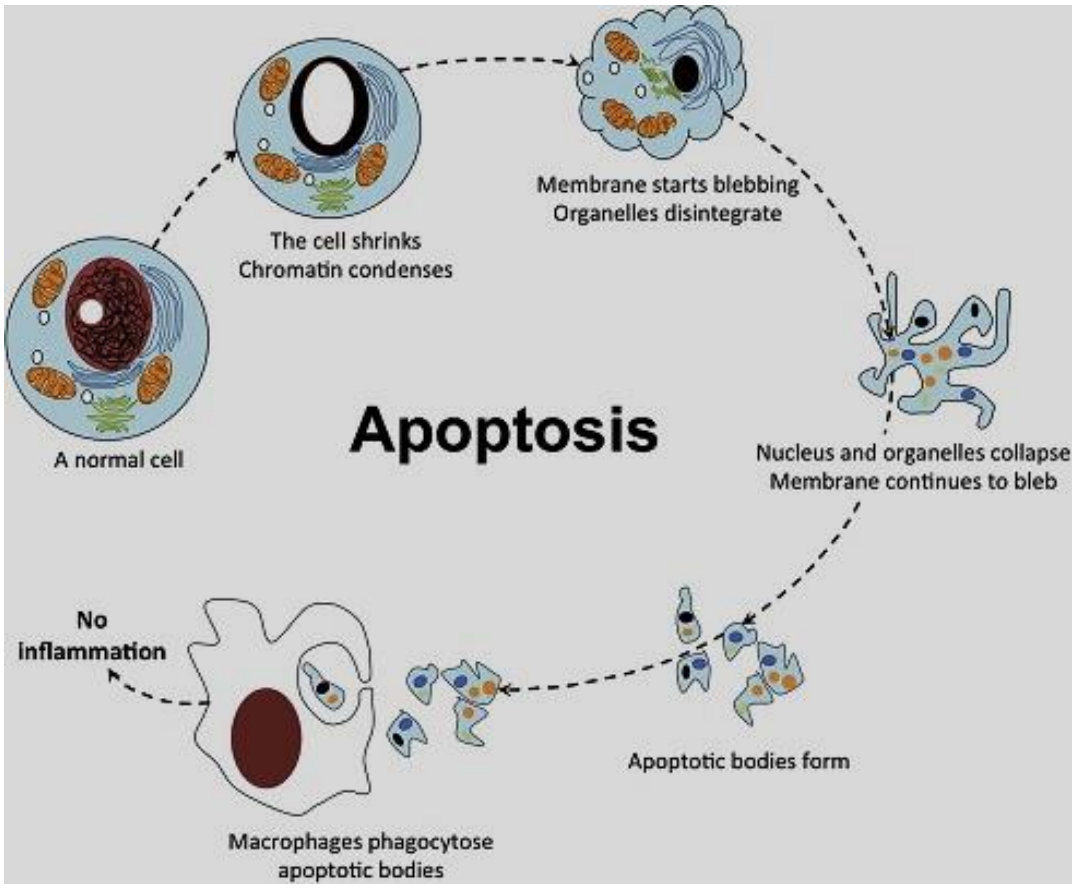

B

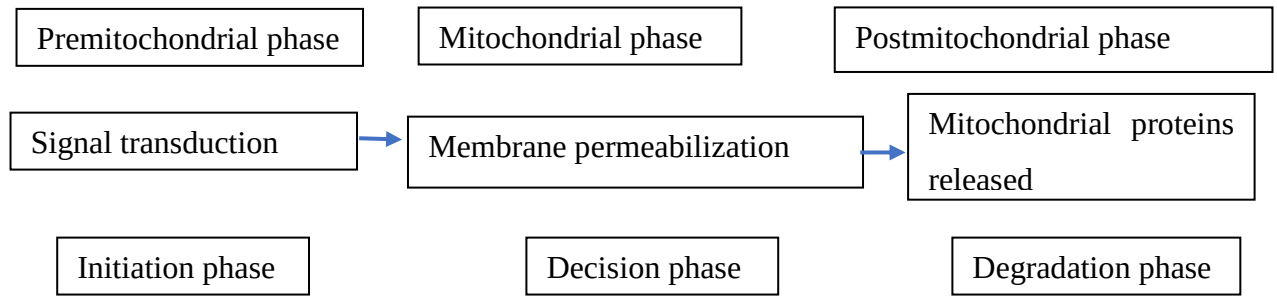

Figure 3: Mechanism of apoptosis

Structural changes in the cell during apoptosis (A) [13]. The three phases of mitochondria-mediated apoptosis (B) [3].

2.5. Angiogenesis:

Angiogenesis is the formation of new blood vessels from existing ones (Figure 4). Cancer cells require oxygen and other nutrients to grow and as the tumour size increases it requires more oxygen and other nutrients for survival. Without angiogenesis, the intracellular levels of oxygen reduce in cancer cells making the cells hypoxic. This leads to the overexpression of the hypoxia inducible factor (H1F1), which regulates the

expression of the VEFG growth factor that in combination with other cytokines causes tumour-neovascularization and allows the cells to proliferate [14]. VEGF is expressed by almost all tumour types and is high in concentration in hypoxic areas and around the blood vessels of the tumour. VEGF receptors are also present in the blood vessels of tumours [3,15].

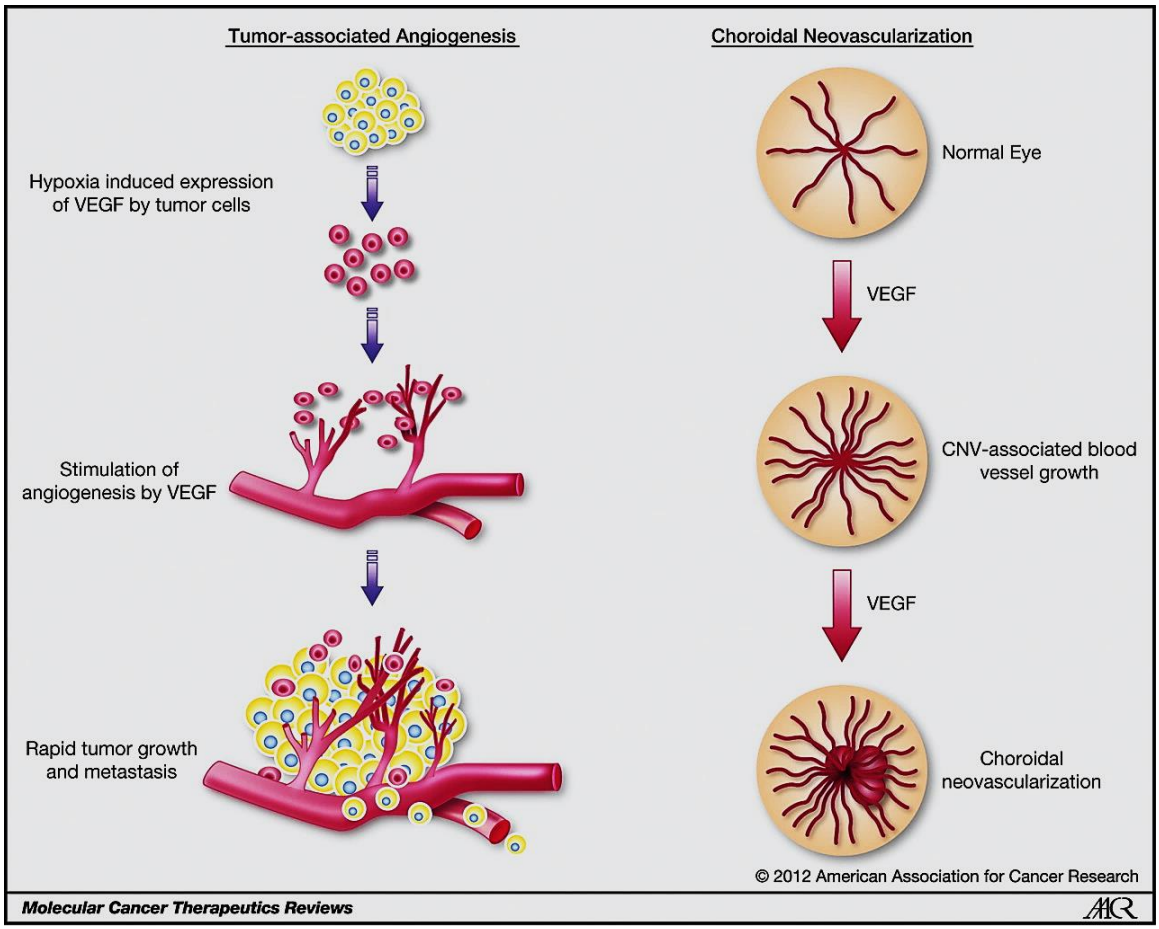

Figure 4: Schematic illustration of angiogenesis and neovascularization

The expression of VEGF induces angiogenesis and tumour progression [15].

2.6. Frequently mutated genes in cancer:

A study by *Kandoth, C. et al.* investigated the fundamental mechanisms causing the initiation and progression of cancer. This was done by performing whole genome sequencing of 3281 tumours from 12 different cancers. This study identified 127 significantly modified genes that are involved in different cellular mechanisms. These mechanisms are generally classified into 20 groups, including histones, histone modifiers, receptor tyrosine kinase signalling, transcription factors/regulators, cell cycle, mitogen-activated protein kinases (MAPK)

signalling, Wnt/β-catenin signalling, phosphatidylinositol-3-OH kinase (PI(3)K) signalling, ubiquitin-mediated proteolysis, splicing and genome integrity. The Wnt/β-catenin signalling pathways, PI(3)K and MAPK are identified consistently in conventional cancer studies. Particularly, newer classes such as transcription regulators, histones, proteolysis, metabolism and splicing appeared as exciting guidelines for the development of new targets for therapeutics. The frequently mutated genes in the cohort were TP53, PIK3CA and BRCA. Mutations were found also in chromatin re-modelling genes such as MLL2, MLL3 and MLL4 that are histone-lysine *N*-methyltransferases. This whole genome sequencing and analysis gave key insights to many enzymatic and cellular processes involved in tumorigenesis. The key findings of this study are summarised in figure 5. It was observed that combination of driver mutations and their distribution in a cancer type is different for individual patients. Therefore, to optimize treatment, it is very important to understand the clonal architecture of individual patient's tumour [16].

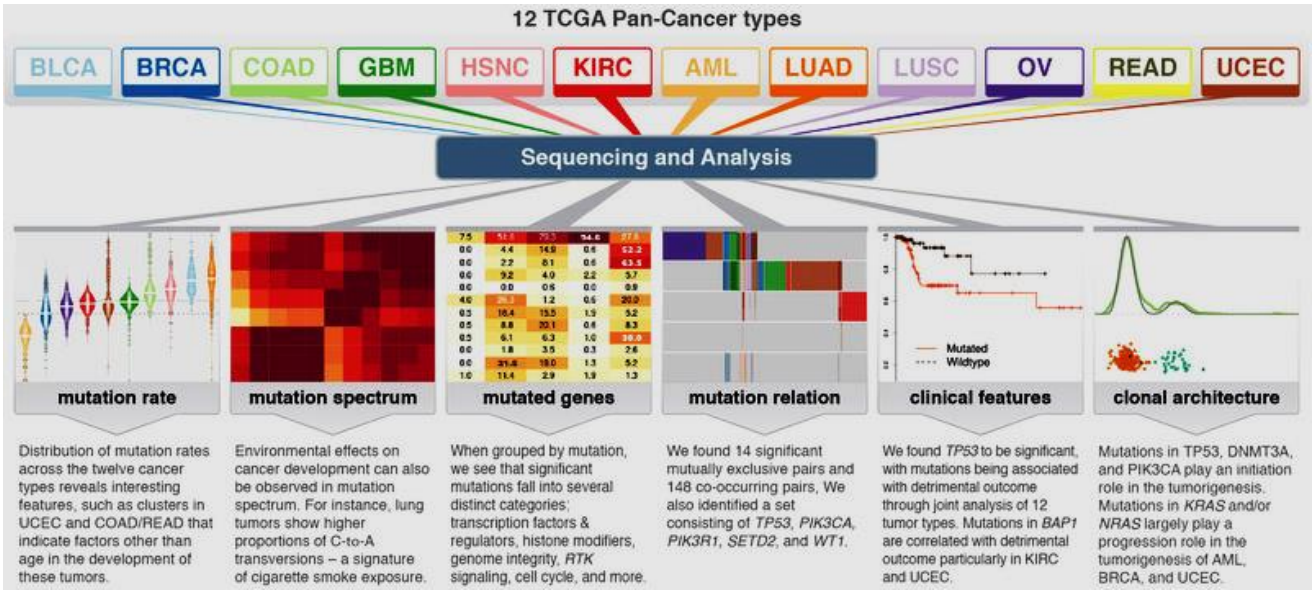

Figure 5: The whole genome sequencing of different cancer types.

The identified SMGs, different cellular processes associated to cancer and genes related to the progression of tumour [16].

2.7. Oncogenes and tumour suppressor genes:

These are specific genes that can control proliferation, differentiation and survival of cancer cells. The most commonly encountered oncogenes in human tumours are the ras gene family. Ras genes are present in approximately 20% of all human tumours, including 25% of lung carcinoma and 50% colon cancer. Ras oncogenes are not present in healthy cells but are generated in cancer cells due to mutations that form as the tumour develops [17].

The myc oncogene plays a key role in the progression of many human cancers. The activation of myc oncogene in cancer cells can happen from alterations such as chromosomal translocation or amplification of the myc gene. Recent findings in to the expression of myc oncogene in cancer have given rise to therapeutic opportunities [18].

PTEN and PI3 kinase are important regulators of the PI3 kinase pathway that regulates survival, growth and proliferation of cells. In human cancers, these proteins are frequently mutated, which leads to unregulated stimulation of PI3K signalling that causes tumorigenesis. The significance of these proteins in PI3K signalling makes them critical therapeutic targets of cancer [19].

The Adenomatous Polyposis Coli (APC) tumor suppressor gene is frequently mutated in different cancers such as colorectal, breast, lung and pancreatic [20]. APC mutations happen due to the loss of function with the protein missing the carboxy-terminal region. APC plays a critical role as a negative regulator of the Wnt/ β -catenin pathway. APC is considered an ideal therapeutic target because mutations in this gene can be identified at early stages of tumour development that makes it a gatekeeper of cancer progression [20].

Another important tumour suppressor that plays in the negative control of cell cycle in tumour progression is the Rb protein. The retinoblastoma protein family consists of Rb/p105, p107 and Rb2/p130 known as pocket proteins. The Rb protein can bind to the transactivation domain of the E2F, which represses gene transcription essential for transition from G1 to S phase. Loss of Rb function can cause cell cycle deregulation that leads to a malignant phenotype [21]. The p53 gene similar to the Rb gene is a tumor suppressor. It has a pro-apoptotic function and is a nuclear transcription factor. Loss of function mutations in the p53 gene is found in more than 50% of human cancers. Mutated p53 gene acts as an oncogene and in some instances cancer cells with p53 mutations show a chemo-resistant phenotype [22].

The activation of p53 gene causes cell cycle arrest to permit DNA repair and thus prevent the proliferation of cells with severe DNA damage. Thus, the tumor suppressive activity of the p53 gene is closely linked to its DNA-binding property [22].

3. Types of anticancer therapy

Surgical treatment:

This involves the surgical removal of tumour and remains a key approach in cancer therapy. This treatment strategy is economical, effective and easy to perform and can be curative for specific cancers such as some colorectal and breast cancers. However, surgery is not first line therapy for treating e.g. lymph node tumours, spinal, facial and pelvic osteosarcomas and thyroid cancer [23].

Radiotherapy:

This process involves the usage of ionizing radiation to destroy cancer cells. Gamma rays and x-rays can penetrate the tissue and destroy tumours even from deep layers. Radiotherapy causes DNA lesions that deregulate the cell division process and induce different types of cell death. The method is preferred in cases where the tumour is voluminous and inaccessible to surgery. Radiotherapy typically uses electromagnetic rays that penetrate the tumour and causes molecular lesions. This interferes with the cell proliferation finally causing cell death [24].

Chemotherapy:

This treatment technique uses chemicals that interfere with the cellular mechanisms causing cell death. For cancers that cannot be surgically removed these are important therapeutic strategies to prolong life, reduces painful symptoms and in special settings even cure cancer. Chemotherapy can include targeted drugs and more broad specific drugs as discussed in more detail below. Although sometimes curative, chemotherapy can be associated with severe adverse effects, which sometime is the cause of death. Acquired drug resistance also often develops. Still novel chemotherapy reagents, also in combination therapies, hold great hopes for improved cancer therapy [25].

Immunotherapy:

Recent development of therapies aimed at reactivating the immune system towards tumor cells have given hope of significant improved cancer therapies. Antigens exposed by cancer cells and recognized by cytolytic T lymphocytes can induce immune response that kills cancerous cells without destroying healthy tissues. This has led to the development of therapies, which activate the immune system based on monoclonal antibodies that inhibit checkpoint blockades, interferons, antiangiogenesis factors, cytokines, tumour necrosis factors and others. [26].

Targeted therapy:

The genetic modifications that distinguish cancer cells from normal cells can be denoted as molecular targets and the therapies that address these modifications are termed as targeted therapies or targeted drugs. Targeted cancer therapy includes drugs that cause cancer cell death by acting against cell survival signaling, and drugs that interfere with the microenvironment of the tumour. Majority of the current targeted therapies are small molecule drugs and monoclonal antibodies. Most monoclonal antibodies interfere with extracellular targets such as the receptor ligand binding sites, as they cannot penetrate the plasma membrane of the cell. On the other hand, small molecule drugs can diffuse in to the cells and interact with targets localized in the cells [27].

Antihormonal therapy is one of the commonly used targeted therapies in breast cancer and it works by depriving the cancer cells of ligand oestrogen receptor (ER) activation. This is done either by blocking oestrogen synthesis using inhibitors such as anastrozole or by using anti-oestrogens. Epidermal growth factor receptor (EGFR) plays an important role in tumorigenesis and therefore has been a key target for cancer therapy. EGFR is targeted using both small molecule drugs and monoclonal antibodies but in many cases a temporary response to treatment is observed. This lack of response is explained by several mechanisms such as mutations in the drug binding site and mutations affecting the downstream signaling molecules present in the EGFR activated pathway [27]. Another promising strategy for therapeutics that can keep cancer in dormancy for longer periods is re-activation of the immune system to fight against cancer cells. Inducing a targeted immune response against tumour cells can do this. Ipilimumab, the CTLA4 blocking antibody was the first approved immune checkpoint blockade therapy [27]. The approval of Ipilimumab by FDA created a breakthrough in the field of immunotherapy. Ipilimumab re-activates the patient's immune

system to fight against cancer by interfering with the immunological synapse immune checkpoint CTLA4 [27]. Although Ipilimumab induces prolonged clinical response, it is accompanied with severe side effects.

Recent advances in sequencing have helped in identifying several somatic mutations in a single cancer sample. This was established by molecular sequencing of the DNA from tumour biopsy samples and this lead to the discovery of novel therapeutic targets in various cancer types.

HER2 gene amplification is common in 18-30 % of total breast cancers. Identification of the role of HER2 in breast cancer led to the development of Herceptin, the first humanized monoclonal IgG1 antibody for treating HER2 amplified breast cancer [28]. Treatment with Herceptin reduces mitogen-activated protein kinase (MAPK) signaling and PI3K that leads to apoptosis in tumour cells via antibody-dependent cell-mediated cytotoxicity [29]. It showed initial improved responses but later caused either primary resistance or acquired resistance. To overcome this, novel class of inhibitors known as dimerization drugs were developed. Combination of these drugs with Herceptin increased the antitumour activity through the degradation of HER2 [30].

Imatinib mesylate (Gleevec) is a tyrosine kinase inhibitor used for treating patients with chronic myeloid leukemia. Gleevec inhibits the BCR-ABL protein by competitive inhibition at its ATP binding site. Despite of the initial positive results, drug resistance developed as a major hindrance to treatment using Gleevec. Majorly, point mutations in the kinase domain of the BCR-ABL lead to drug resistance that causes treatment failure [31].
Venetoclax is a bcl-2 selective inhibitor used for treating chronic lymphocytic leukemia. Drug resistance mechanisms associated to venetoclax resistance includes: upregulation of anti-apoptotic proteins that are not targeted by venetoclax and mutations in the target protein that could potentially affect venetoclax binding [32].

Inhibition of the CDK4/6 cell cycle kinases using palbociclib has led to an increase in the control of ER-positive breast cancer. In a study by *Herrera-Abreu et al*. exome sequencing of MCF-7 parent and palbociclib resistant cells was performed and multiple de novo mutations were identified in the resistance cells that could possibly cause drug resistance [33].

4. Drug discovery

There are huge efforts worldwide to develop novel cancer drugs when there is an urgent need for novel therapies for cancers that do not respond to available treatment strategies. Any new compound that has been identified, as a potential drug candidate need to be attributed to comprehensive safety and efficacy studies before being introduced to the market (Figure 6). The early stage of drug discovery typically consists of three steps that are identification and validation of the target protein/pathway, lead discovery and lead optimization/identification. The late stage of the process, often called drug development, involves preclinical efficacy and safety testing of the drugs, clinical studies and regulatory approval [34,35,36]. The drug discovery process is an intricate process, which is time-consuming and very expensive [37,38].

The drug discovery process in olden days can be divided in to three time periods: early drug discovery till 19th century, modern drug discovery in 19th century and drug discovery and drug development in 20th century and beyond.

In the early discovery period, natural products were widely used for treating diseases. The medicinal values of plant-extracts were exploited for healing diseases but this involved several steps of trial and error. Also, this approach lacked understanding of its chemical properties and synergistic effect in curing the disease [39,40,41]. In the modern drug discovery period, techniques were introduced to develop single entity drugs. For example, quinine was discovered earlier but it was isolated only in 1823 [42]. New methods and techniques were introduced over the last two decades of the 20th century. High-throughput screening (HTS) is one of these techniques, which enables detection of promising compounds out of vast libraries of compounds. A range of novel approaches to study target proteins and cellular process have also been critical to accelerate drug development [38,43,44].

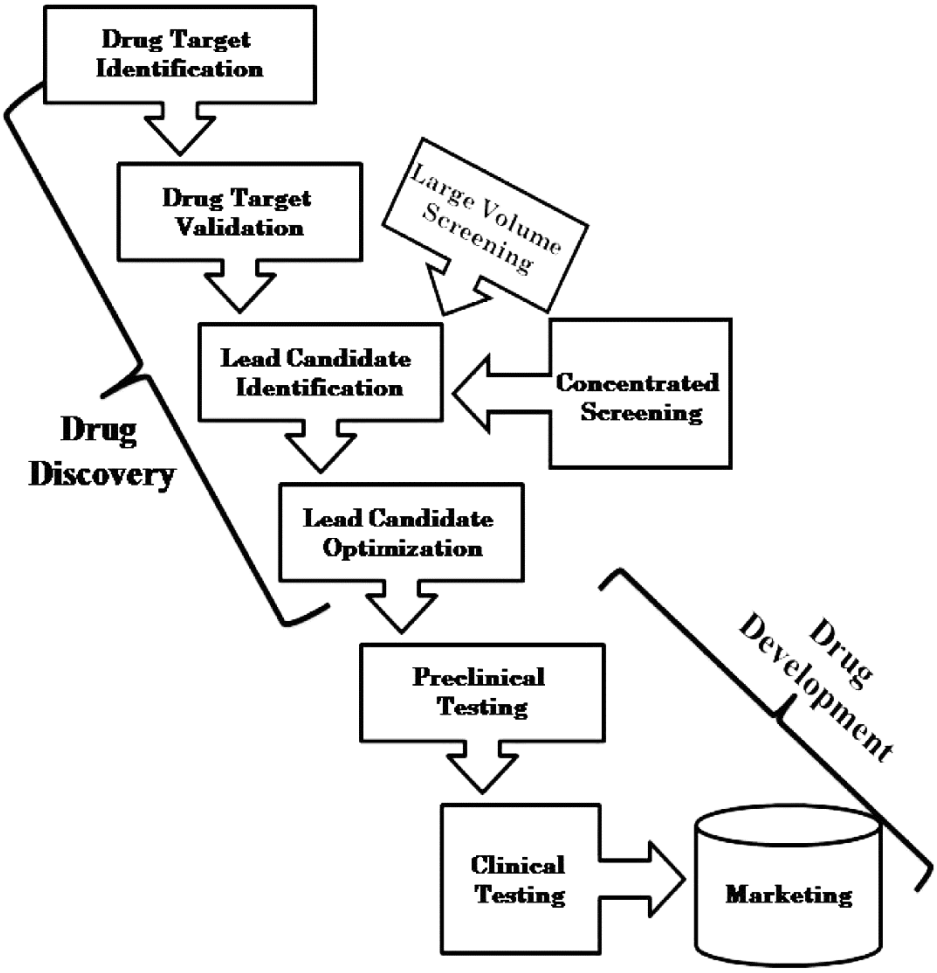

Figure 6: The steps involved in the drug discovery pipeline [45]

4.1. Steps involved in the drug discovery pipeline for targeted therapies

Target identification:

The first step in this drug discovery pipeline is the identification of protein targets that when inhibited, will show the appropriate modulation of cellular functions but also be druggable, i.e. have an appropriate binding site where the drug can bind [46]. The process of drug target identification has improved significantly after the development of genomic and proteomic approaches [35].

Target validation:

This process focuses on showing the relevance of the target protein in a disease condition and this is done using disease and animal models. The optimal way to study drug target

engagement is by using highly specific inhibitors with good pharmacological properties. Genetic techniques can be used for early target validation and the recently introduced Crispr technology bear promises for more distinct evaluation of potential drug targets at early stages [34].

Hit discovery and lead optimization:

Discovery of compounds that interact with the target proteins is the next step after the identification of drug targets. For intracellular targets, this involves the identification of small molecule hits and the development of them into potent drug candidates. The hits can be identified by screening the target protein in cells or in a purified form against large compound libraries. The hit compounds are then optimised for affinity in subsequent cycles. This can be done by structure-based design if the target protein structure is known or can be determined. Eventually the compounds are subjected to pharmacokinetic studies such as cell-membrane permeability, drug catabolism and toxicity studies [34,35].

Lead candidate optimization:

Optimization of the lead compounds that are found in the previous step is done at this stage. The lead compounds are modified to improve its'- efficacy, potency, pharmacodynamic and pharmacokinetic characteristics and this is done by performing chemical modifications in the compound structure [35]. Structure-based design can be carried out if the target structure is well known and this is an expensive step as the optimization of multiple parameters should be performed in this process. Therefore, the lead optimization process is considered to be the rate-limiting step in drug discovery [35].

Preclinical studies:

The lead compounds found in the discovery phase are subjected to to further optimization to eventually yield a clinical candidate (CD). A small set of lead variants are here tested in more advanced animal models for efficacy, safety, drug delivery, metabolism and elimination and eventually a CD is selected which need to be attributed to a standardized scale-up production process before clinical trials [35].

Clinical trials:

This is the most expensive stage in the entire drug discovery process. The pharmacological and metabolic effects of the drug candidates are studied in humans in this phase. Clinical trials

involve up to four phases and not all the drug candidates entering the clinical trials succeed and become approved drugs. In the phase I clinical trial, the tolerability, safety, pharmacokinetic and pharmacodynamic characteristics of the drug is studied in human volunteers which do not have to have the specific disease. In the phase II clinical trial, the same tests performed in phase I trial are performed in individuals with defined diseased conditions. The drug is assessed in the phase III clinical trial against standard therapy by testing it on hundreds to thousands of patients. Finally, if the drug is delivered the phase III clinical trials endpoints, it can be approved for public use [34,35]. The long term adverse effects of the drug are monitored across large patient population after the drug is launched in to the market and this forms the phase IV clinical trials [35].

5. Biophysical methods to measure protein-ligand interactions

5.1. Introduction to protein thermal stability

Proteins execute their biological function by folding in to a specific three-dimensional structure. Active proteins at room temperature are normally well folded. When proteins are subjected to higher temperatures, they unfold and lose their three-dimensional structure. Often unfolding can lead to protein aggregation/precipitation (Figure 7) [47,48]. Specific factors affect the thermal stability of proteins including its primary sequence and structure, solution/buffer conditions and ligand binding [49,50,51].

To study the effect of these factors on protein thermal stability, the protein is subjected to increasing temperature, and the unfolding event is monitored. The midpoint of this unfolding transition gives the melting temperature (Tm) of the protein [49]. If the aggregation is monitored a related aggregation temperature (Tagg) is obtained [50]. Typically, to study ligand binding the buffer conditions would be kept constant while a ligand would be added before the heating experiment. The difference in Tm of the protein in the two different conditions gives the thermal shift, ΔTm, and hence determines the change in thermal stability of the protein.

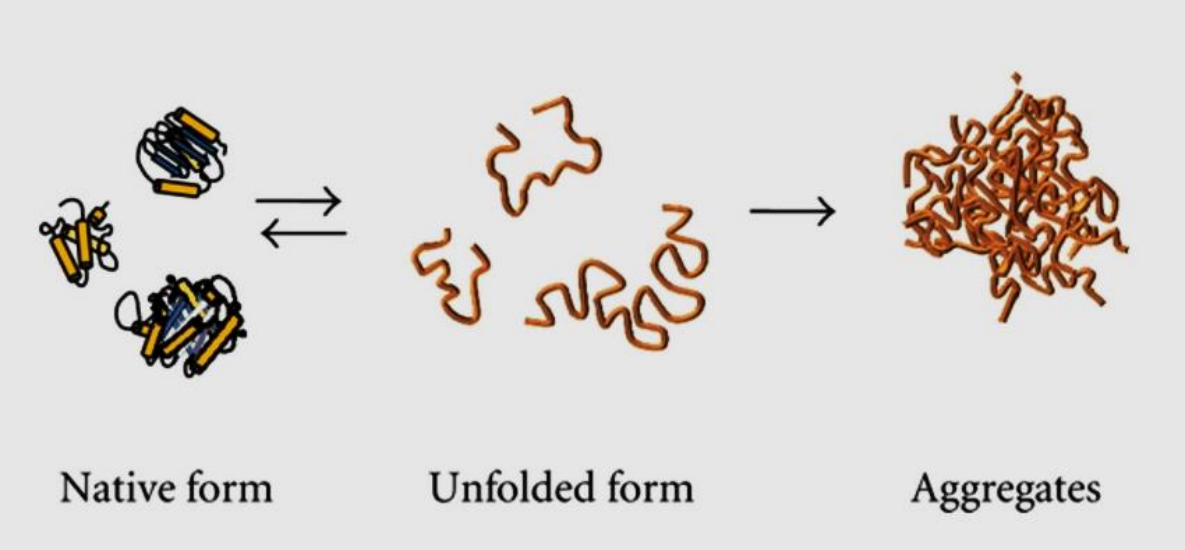

Figure 7: Protein unfolding and aggregation [52]

When a ligand binds to the active site of the protein, it stabilizes the protein and lowers the free energy ΔG of the system. This often stabilizes the protein towards thermal stress and delays the protein-unfolding event. Ligand induced thermal stabilization of proteins is an important biophysical principle and is used extensively in drug discovery, to identify and characterize small molecule inhibitors binding to target proteins [53,54].

5.2. History of thermal shift assays and its' role in drug discovery

Advances in genomics based target generation and combinational chemistry has led to an increasing demand for assay technologies, which can assist the drug discovery process. The attributes of thermal shift assays satisfy the needs of a general drug discovery assay. It uses the principle of ligand-induced thermal stabilization of proteins in which inhibitors, metal ions, cofactors, natural ligands, substrates and even other proteins induce thermal stability to proteins upon binding. The studies by Daniel Koshland (1958) and Kaj Ulrik Linderstrøm-Lang and Schellman (1959) first introduced the principle of increase in the thermal stability of proteins due to binding of low molecular weight ligands [55,56].

This phenomenon is dependent on the coupling of ligand binding and receptor melting reactions. Traditionally, differential scanning calorimeters were used to conduct thermal shift assays, which measure difference in heat capacity associated with the temperature-induced melting transitions of proteins. Other biophysical methods have also been historically used to perform thermal shift assays. These methods use temperature regulated optical

instrumentation, which measures temperature dependent changes in fluorescence, absorbance and circular dichroism [53].

Since the late 1990s, there has been a significant progress in the use of thermal shift assays for high throughput screening of large compound libraries [57]. Differential scanning fluorimetry, a commonly used thermal shift assay was first introduced by *Semisotnov et al.* and later in 2001 *Pantoliano et al.* used this technique for high throughput screening using a plate reader [53,58].

More recently, these biophysical assays have become a very important part of fragment-based drug discovery. These assays provide reliable ways to understand structure-activity relationships in the earlier stage of drug development process by performing quantitative measurements of indirect dose response effects (IC50) and direct binding (Kd) [57]. The ability to detect compounds with low binding affinity makes these assays capable for screening fragment libraries. A panel of thermal shift assays such as differential scanning fluorimetry, differential scanning calorimetry, differential static light scattering, magnetic resonance spectroscopy, surface plasmon resonance and isothermal titration calorimetry are widely used to study protein-ligand interactions.

5.3. Techniques to study protein unfolding

Protein unfolding can be measured by direct and indirect methods. The direct methods monitor the protein-unfolding event itself, while the indirect methods monitor the unfolding event typically through effects of protein aggregation/precipitation.

5.3.1. Differential scanning fluorimetry (DSF):

DSF is a method commonly known as thermofluor assay. It is a simple, fast and inexpensive technique for detecting the unfolding of a protein. DSF uses an environmentally sensitive dye for the fluorescence measurement for example, sypro-orange that has its fluorescence quenched in aqueous medium [59,60]. DSF is widely used to screen proteins for small molecule binders. When the protein-dye mix is heated, the protein unfolds and exposes the hydrophobic patches and the dye binds to this hydrophobic region. After binding, the dye starts emitting fluorescence that is plotted as a function of temperature [59]**.** As mentioned above, the midpoint of this unfolding transition of the protein is the melting temperature Tm and any change in the stability of the protein is determined by a shift in the Tm (Figure 8) [61].

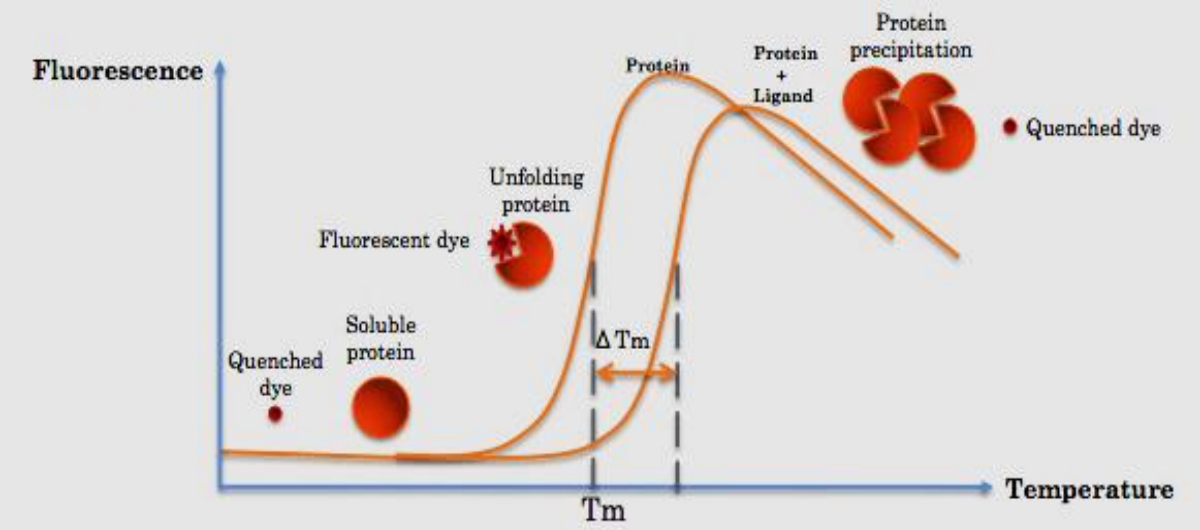

Figure 8: Differential scanning fluorimetry (DSF)

5.3.2. Thermal stability assays using cysteine reactive dyes:

DSF works very well to study the thermal stability and unfolding of soluble proteins. However, the method is not very efficient for membrane proteins. This is because of the highly hydrophobic nature of these proteins, which will substantially increase the background fluorescence in the measurement.

The thermal stability of both soluble and membrane proteins can be studied by looking at the covalent modification of native cysteine residues, as a read out for the protein unfolding event. The temperature-induced unfolding renders the cysteine residues embedded in the protein solvent-exposed. These residues can be modifiable with a diffusible fluorescent probe. The assay uses highly reactive thiol-specific fluorochrome N-[4-(7-diethylamino-4- methyl-3-coumarinyl)phenyl]maleimide (CPM) when this compound is not fluorescing in its unbound form. Due to their high packing value, cysteines are frequently located at helix-helix interaction sites and therefore are good sensors for the overall integrity of the membrane protein structure [62].

5.3.3. Differential scanning calorimetry (DSC):

DSC has been extensively used to study the unfolding of proteins. This method detects the heat change involved in thermal denaturation of the protein, when it is heated at a constant rate. A protein in solution is in equilibrium between its native (folded) and denatured (unfolded) conformations. DSC measures the enthalpy (ΔH) of unfolding that results from heat-induced denaturation. DSC can be used to study the factors affecting protein folding and

thermal stability, which includes hydrogen bonding, hydrophobic interactions, presence of small molecular ligands and the physical environment (Figure 9) [63].

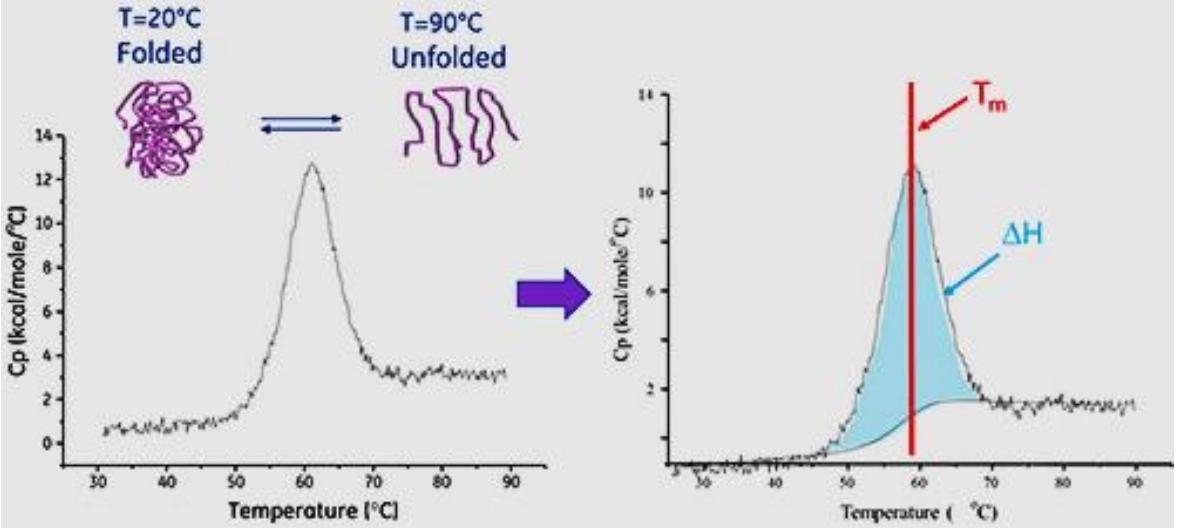

Figure 9: Differential scanning calorimetry (DSC)

(http://www.malvern.com/Assets/Techn_DSC_01.png)

5.3.4. Differential static light scattering (DSLS):

Protein-unfolding events often lead to protein aggregation. The protein-unfolding event can therefore be monitored indirectly through effects of aggregation and precipitation. Differential static light scattering (DSLS) is an indirect technique to study protein unfolding by monitoring protein aggregation.

DSLS is based on the measurement of the fluctuations in intensity of scattered light. The formation of aggregates leads to increased scattering of light, which is captured. The light scattering intensity is plotted against increasing temperature and the midpoint of the curve gives the aggregation temperature Tagg of the protein. The stabilization of the protein due to ligand binding gives a shift in the protein Tagg (Figure 10) [64].

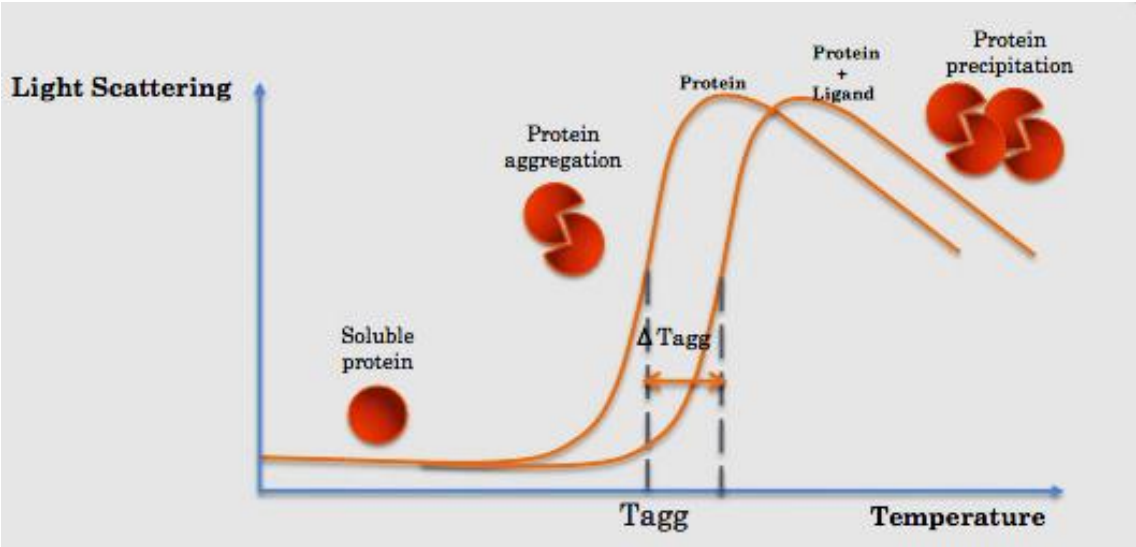

Figure 10: Differential static light scattering (DSLS)

5.4. Other biophysical concepts for studies of protein-ligand interactions

5.4.1. Surface plasmon resonance (SPR):

SPR is an optical technique used to understand molecular interactions. It detects interactions of two molecules by fixing one of the molecules on a thin metal film and keeping the other one mobile (Figure 10). Interaction of the mobile molecule to the immobilized molecule alters the refractive index of the film [65]. To detect the binding of an analyte to a receptor, the analyte is injected through the flow cell, while the receptor is immobilized on to the surface of the sensor. A prism is used to direct polarised light to the surface of the metal film. This generates surface plasmons at a critical angle of the reflected light. The reduction in the intensity of the reflected light shows the absorption of light. The real-time measurement using SPR is usually shown as a sensogram (Figure 11). The interaction between the analyte and the receptor molecule triggers a change in the refractive index of the metal surface. This change is seen as an increase in the intensity of the signal and this increase is described using resonance or response units (RU). Factors such as optical property, binding affinity of the analyte and surface coverage of the receptor affects the lowest detectable concentration in an SPR study [66].

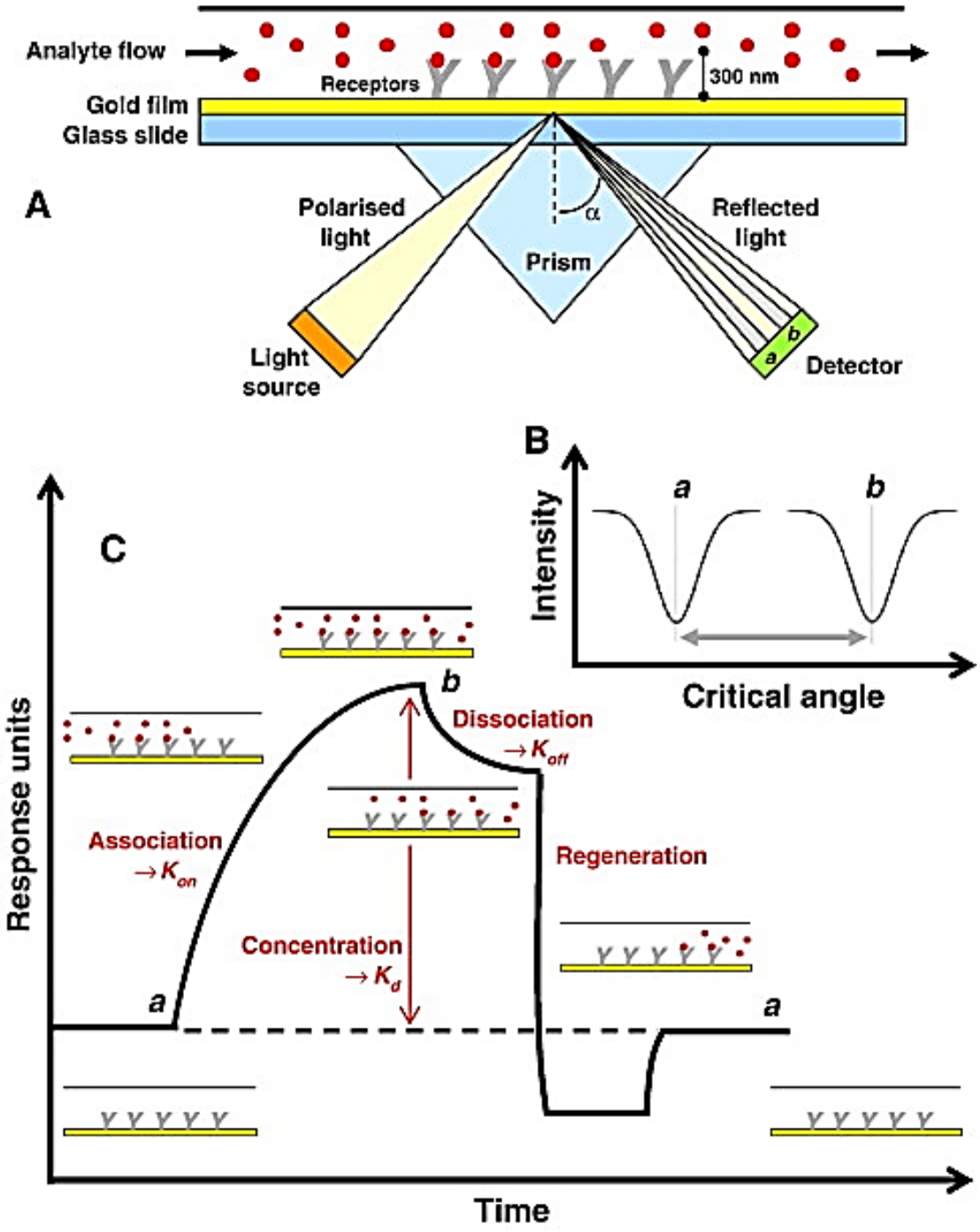

Figure 11: Schematic illustration of the SPR set up

This SPR set up can be used for measuring the interaction of an analyte to a receptor [66].

5.4.2. Isothermal titration calorimetry (ITC):

ITC is a technique that measures the thermodynamic parameters related to complex-formation or ligand-binding. It measures the heat exchange associated with molecular interactions at a fixed temperature. ITC gives an entire thermodynamic profile in a single experiment that includes binding affinity constant (K_a), changes in enthalpy (ΔH) and

stoichiometry (n), which in turn allows for the calculation of the Gibbs free energy, ΔG, and entropy, ΔS, changes. These parameters are associated to the binding mechanism of a biomolecule and therefore, this technique is routinely used to measure the thermodynamics of ligand binding [67,68,69].

An ITC instrument consists of two cells: a reference cell and a sample cell (Figure 12). These cells are made of efficient thermal conducting material. The sample cell contains the biomolecule and the ligand is titrated in to the sample cell using a syringe. The temperature changes between the cells are detected by sensitive thermocouple circuits, while maintaining the isothermal conditions between the cells. The heat change in the sample cell is monitored during the titration process and the power needed to maintain the isothermal conditions within the cells is detected by a calorimeter. Power is plotted against time to determine the peaks of heat flow and the area under these peaks gives the enthalpy of binding. The molar ratio of the ligand can be plotted against the heat formation to calculate the binding isotherm. This gives the information about binding affinity constant (K_a), enthalpy (ΔH) and stoichiometry (n) that can be used to determine the Gibbs free energy (ΔG) and changes in entropy (ΔS) [69,70].

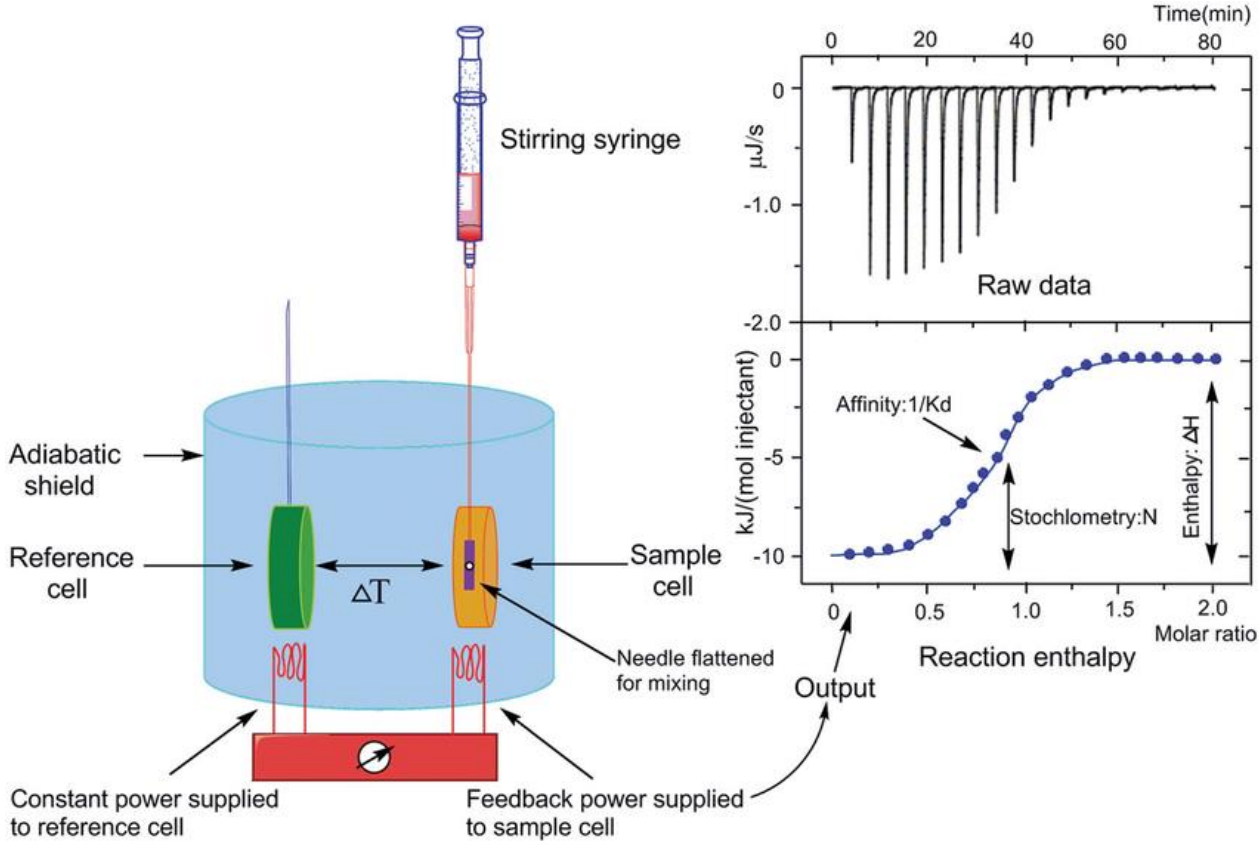

Figure 12: Schematic illustration of the ITC set up [71]

5.5. Methods to detect drug-protein interactions in cells

The thermal shift assays and the other techniques discussed above require high-quality purified protein samples for measurements. However, the study of protein-ligand interactions using purified proteins does not necessarily translate into binding of the protein to the ligand in living systems. Therefore, it is desirable to determine the ligand binding to a protein in complex mixtures such as lysates or intact cells. This helps, for example, to understand the efficiency of drugs by monitoring target engagement in the early stages of drug discovery. It has, however, been challenging to measure drug target engagement directly in cells and therefore, researchers have instead depended on monitoring downstream cellular responses as secondary readouts of drug target engagement. Several methodologies have been developed in the recent years that enable the detection of target engagement in cells and tissues. Some of these methodologies need the alteration of the biologically active compound, while other techniques adapt label-free approach for measurements [72]. The different methods to study drug-target interaction in cells are described in the following section.

5.5.1. Techniques that require the alteration of both the target protein and the biological molecule

Fluorescence or bioluminescence resonance energy transfer measurements (FRET and BRET) can be used to understand the interaction between a ligand and its target protein.

FRET: A donor fluorophore upon excitation transfers the energy to an acceptor fluorophore that is in proximity (Figure 13A). This transfer of energy occurs if three conditions are satisfied and they are: strong overlap between the emission spectrum of the donor and the absorption spectrum of the acceptor, right distance between the donor and the acceptor and proper orientation of donor and the acceptor. Fluorescence lifetime imaging microscopy (FLIM) can be used to monitor the change in fluorescence lifetime of the donor [73]. FRET-FLIM monitors target engagement in intact cells by studying the temporal and spatial distribution of the ligand-protein complex. For this, the target protein is expressed in the cells labelled to a suitable fluorescent protein and the ligand is fused to a fluorophore at a site that does not interfere with the binding. The fluorescent labelled ligand is added to the cells that express the target protein linked to a fluorescent protein. The donor fluorophore's lifetime distribution within the cells is then determined, which shows the interaction-sites of the ligand in cells. The FRET technique can be used to study proteins that can be linked to a fluorescent protein [72,73].

BRET: This is a natural process that happens in marine organisms where energy is transferred between a luminescent donor and a fluorescent acceptor. The enzymatic action of a luciferase enzyme is responsible for this chemical reaction that produces resonance energy. The oxidation of the substrate by this enzyme produces light at 480 nm, which is called bioluminescence. If an acceptor is present in proximity (distance within 10 nm), the resonance energy gets transferred to the acceptor and upon excitation, the acceptor produces light of a longer wavelength (Figure 13B) [72]. For the BRET measurements, the ligand is labelled with a fluorophore and the target protein is expressed in cells linked to a luciferase. The fluorescence from the acceptor molecule is detected as a readout using a plate reader. The phenomena such as photobleaching and background fluorescence do not take place in BRET measurements as no optical excitation of the donor molecule is needed. This technique allows the study of ligand-protein interactions in cells by means of kinetic measurements [72].

5.5.2. Technique that requires the alteration of the biological molecule

Affinity-based chemical proteomics for ligand that covalently bind to the protein: This technique can be used to study target engagement of ligands that can be made to act by covalent modifications of the target protein [74]. The ligand molecules are altered with chemical handles such as an azide or alkyne group. The cells are treated with this probe where it interacts with the protein target and covalently links to it. The chemical handles are probed with biotin that enables the affinity purification of the covalently bound target proteins using streptavidin beads. The proteins are then identified by LC-MS technique (Figure 13C).

5.5.3. Technique that requires the alteration of the protein

Enzyme Fragment Complementation: Ligand interaction with the target protein can change the stability of the protein in the cells. This change in the cellular protein stability is determined to study ligand-protein interaction. An enzyme fragment complementation assay (EFC) was recently developed by the company DiscoveRX to monitor ligand interactions in cells (Figure 13D) [72]. For this study, the protein b-galactosidase (b-gal) was cut in to two fragments: the enzyme acceptor (EA) and the enhanced pro-label (ePL). These fragments do not possess b-gal activity independently but when combined demonstrates enzyme activity. The target protein of interest was

linked to the ePL and expressed in the cells. The cells underwent lysis upon ligand treatment in the presence of EA and the target protein level was determined as a measure of the restoration of b-gal activity. This method can be used for all enzymes that can be tagged [72].

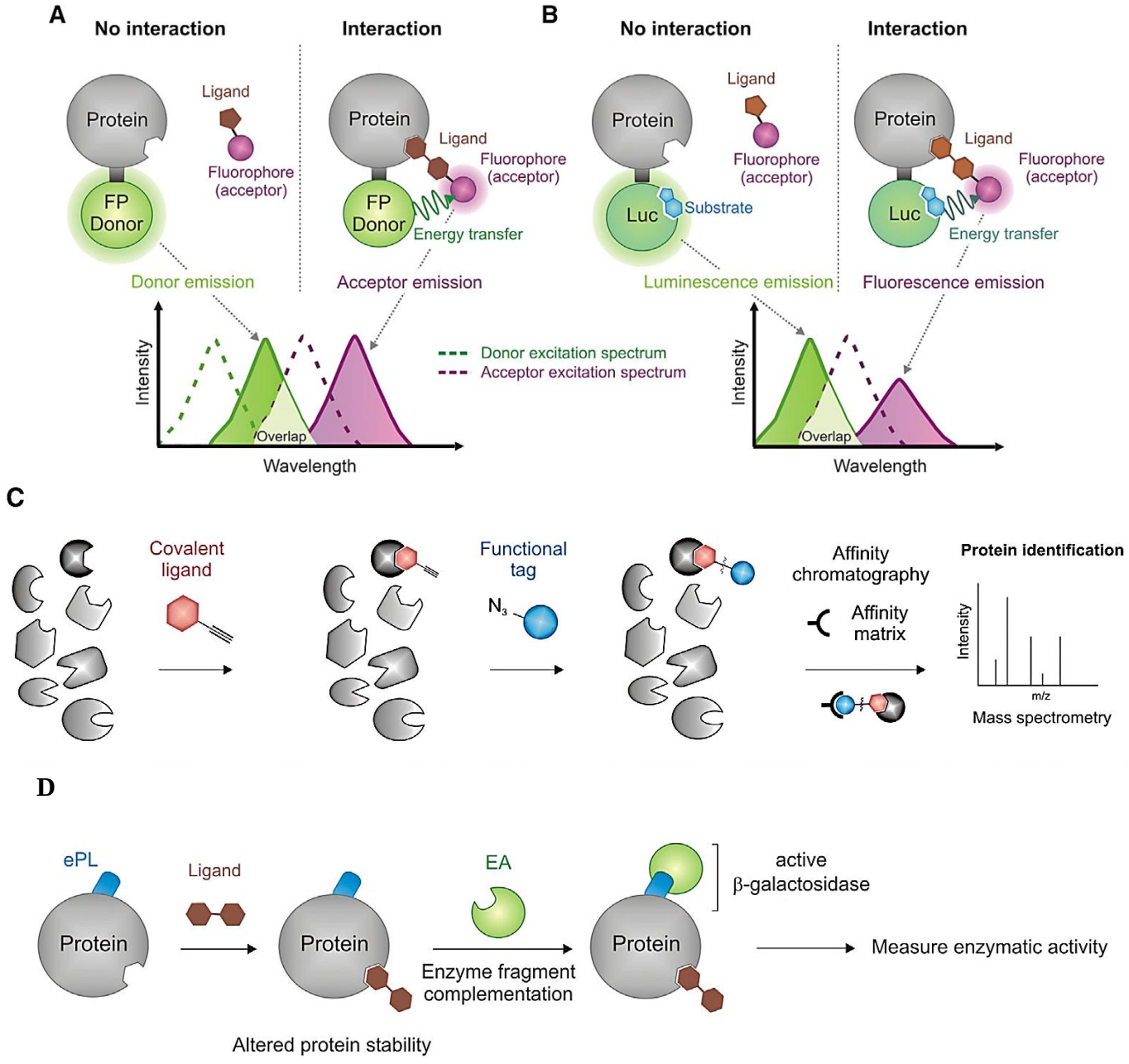

Figure 13: Methods to detect drug-protein interactions in cells

FRET (A), BRET (B), affinity-based chemical proteomics for ligand that covalently bind to the protein (C) and enzyme fragment complementation (D) [72].

We have developed a technique called cellular thermal shift assay (CETSA) to study drug target engagement in complex mixtures such as lysates or cells [75].

6. Cellular Thermal Shift Assay (CETSA)

Monitoring drug-target engagement in cells and tissues is very important in the field of drug discovery, to determine the efficiency of novel drugs [75]. As discussed above, it is often quite challenging, as there in many cases has been no applicable methods to directly measure drug binding in cells. This has led to failure of several drugs in advanced clinical trials, as the drugs were later found to not bind the anticipated target protein within cells [76].

CETSA is a novel strategy to determine drug target engagement in cells and tissues developed by our group. CETSA is based on the biophysical principle of ligand-induced thermal stabilization of the target proteins discussed above [75]. Figure 14 shows a schematic illustration of the CETSA experimental set up. In this method, cells or cell lysates are aliquoted and heated at different temperatures. After heating, the samples are cooled and the soluble protein fraction is separated from the precipitated protein fraction. The target protein in the soluble fraction can subsequently be quantified by an immune assay such as western blot or by quantitative mass spectrometry [75]. Thus, CETSA measures the remaining native non-precipitated protein fraction after heat challenge in contrast to the thermal shift assays such as DSF and DSLS, which in different ways observe the denatured/precipitated fraction.

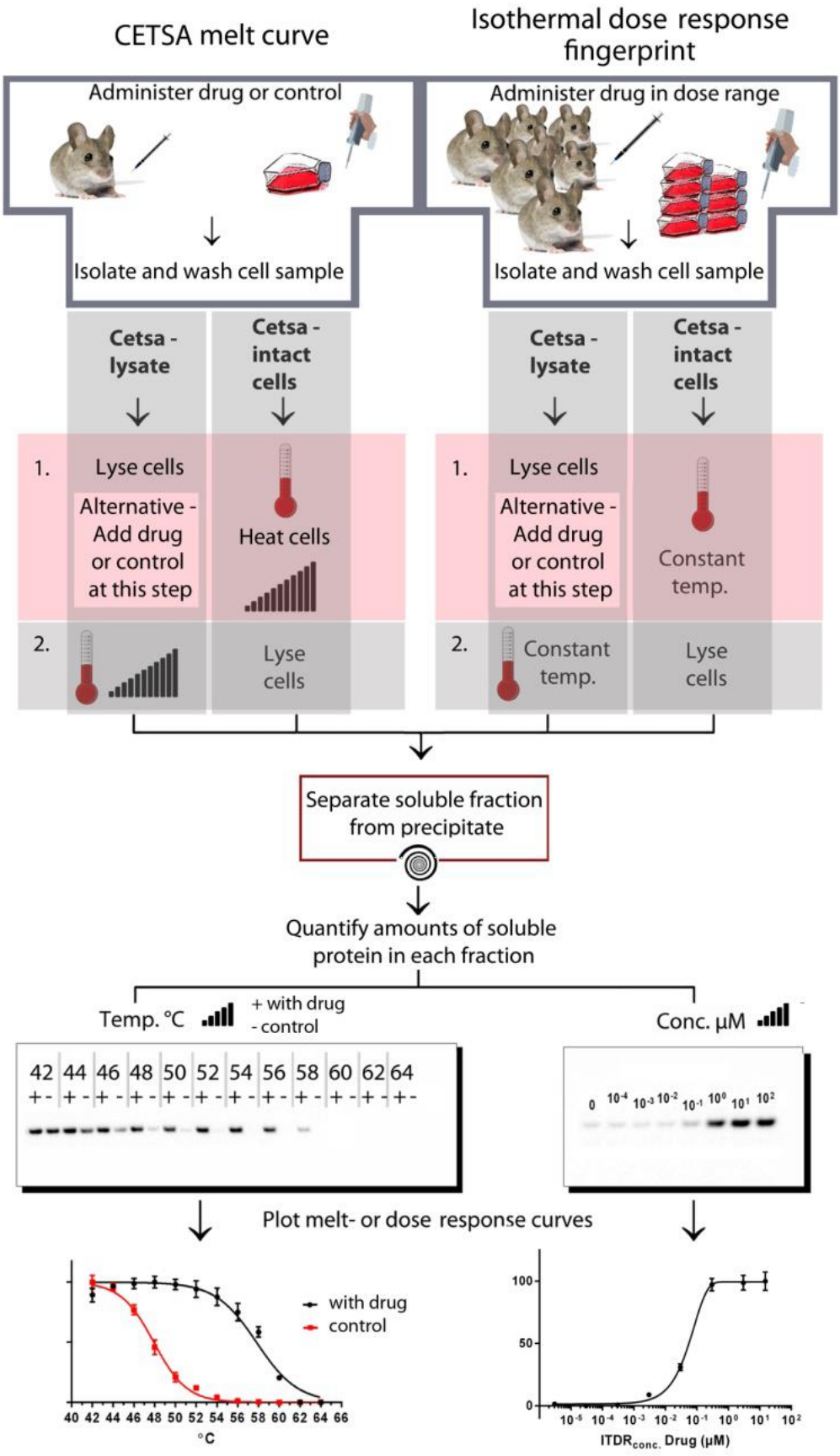

Figure 14: Schematic illustration of CETSA melt curve and ITDR$_{CETSA}$ experimental set up [75].

In our first CETSA paper CETSA was used to evaluate the thermal melting profile of different clinically relevant drug targets in cell lysate [75]. The targets tested included CDK2, CDK6 and MetAP2. All the proteins showed well-defined melting profiles and upon addition of the known inhibitors of these proteins to the lysate, evident shifts were observed in the melt curves (Figure 15A and 15B). To determine the concentration effects of drugs an isothermal dose-response procedure ($ITDR_{CETSA}$) was established, which gives a fingerprint of the target engagement. In this method, the lysate aliquots were treated with different concentration of the inhibitors and were then subjected to heating at a constant temperature (Figure 15C and 15D).

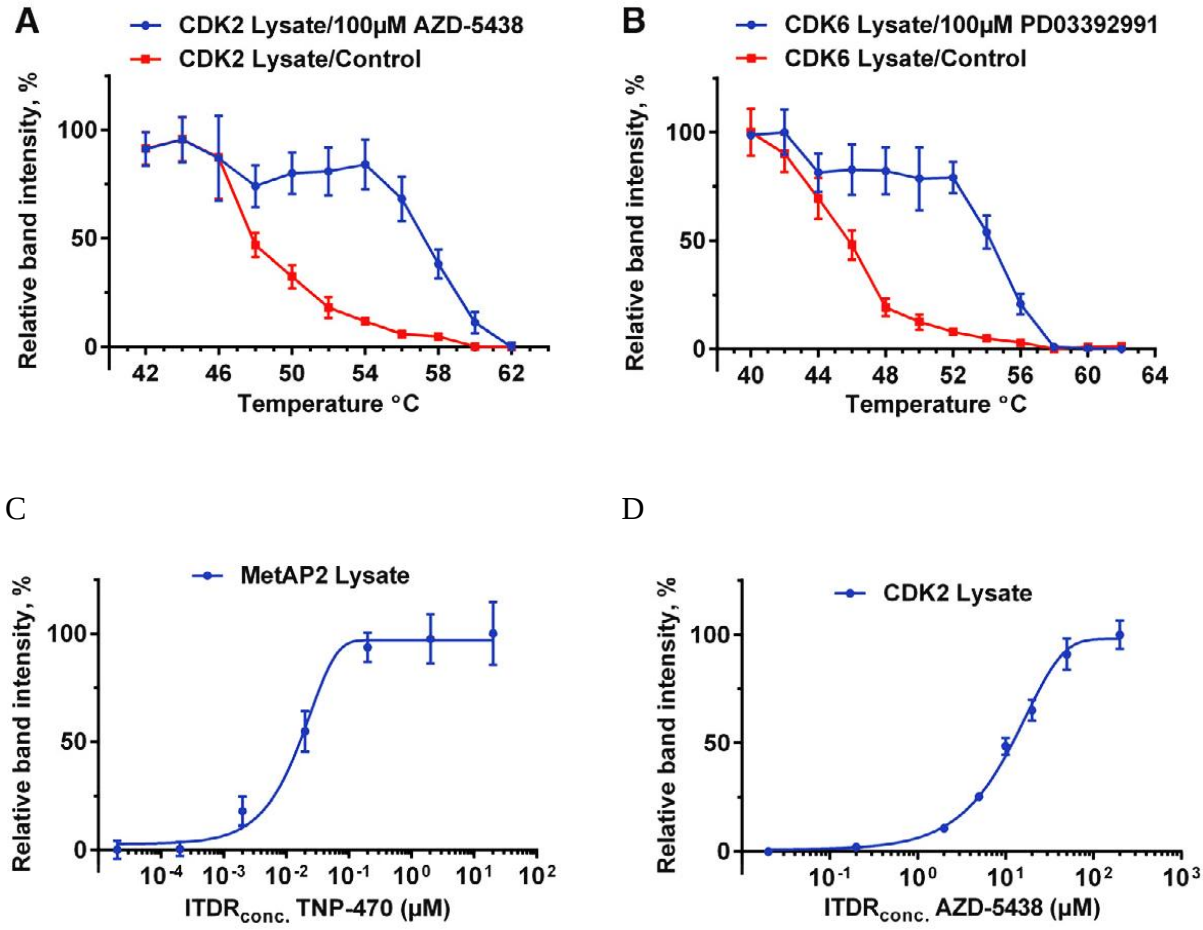

Figure 15: Evaluation of clinically relevant drug targets using CETSA

CETSA melt curves of CDK2 (A) and CDK6 (B) with the corresponding inhibitors. $ITDR_{CETSA}$ of MetAP2 withTNP-470 at 72^0C (C) and CDK2 with AZD-5438 at 52^0C (D) [75].

The changes in drug transport and activation in cells can lead to resistance to drugs such as the anti-metabolites folate or nucleoside analogues. To study this, isothermal dose-response procedure was used. In the methotrexate experiment, effects of suramin, an inhibitor of the enzyme polyglutamate synthase (FPGS) that activates the drug was also studied. The cells were exposed to different concentrations of methotrexate followed by lysis and heating at a constant temperature to give a $ITDR_{CETSA}$ [75]. It was subsequently shown that inhibition of the enzyme FPGS by suramin compromised drug activation in the cells (Figure 16A and 16B).

It was also demonstrated in this study that CETSA can yield data on target engagement in animal tissues. TNP-470, the inhibitor of methionine aminopeptidase-2 (MetAP2) was used for the mice experiments. Mice were treated with TNP-570 and compared with mice in non-treated control group. The harvested organs were frozen and lysates were prepared before the heating step to ensure reproducibility. When this is a covalent drug, target engagement was still retained. It was observed that the CETSA melt curve of METAP2 in mouse liver samples showed significant stabilization when treated with TNP-470 (Figure 17A). Dose response behaviour of the drug was examined after administering six different doses of the compound to the mice. The $ITDR_{CETSA}$ of MetAP2 in liver samples demonstrated a 50-fold difference relative to MetAP2 in the kidney sample (Figure 17B).

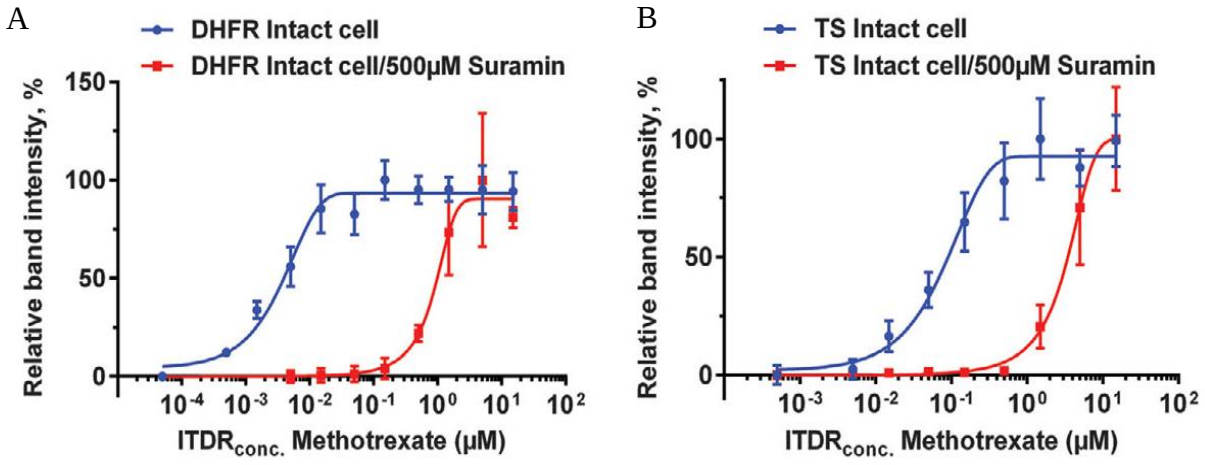

Figure 16: CETSA to study antifolate drug transport and activation in cells

$ITDRF_{CETSA}$ of DHFR (A) and TS (B) in intact cells after inhibition of methotrexate activation by blocking FPGS with suramin [75].

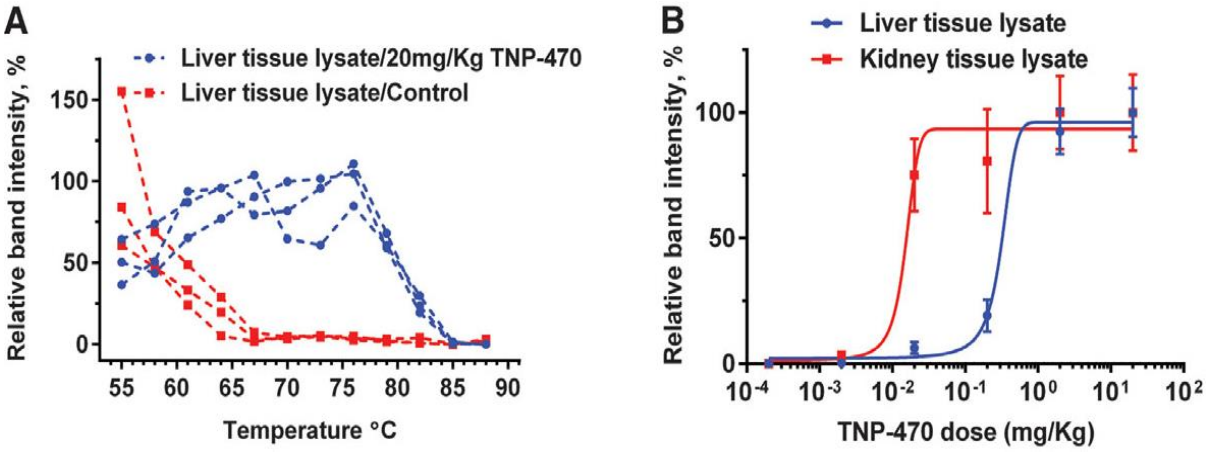

Figure 17: CETSA to study drug target engagement in animal tissues

CETSA melt curves of MetAP2 in mouse liver lysates with and without TNP-470 treatment (A). $ITDRF_{CETSA}$ of MetAP2 in liver and kidney at six different TNP-470 dosage levels (B) [75].

6.1. Thermal proteome profiling using CETSA combined with mass spectrometry

The CETSA studies discussed above used western blot for detecting the drug target engagement using protein-specific antibodies. A study by M. M. Savitski *et al.* showed that a combination of CETSA with quantitative mass spectrometry (MS) enables the proteome-wide determination of protein thermal stability in cell lysates and intact cells (Figure 18) [77]. This MS-CETSA approach, also termed the thermal proteome profiling (TPP), extended CETSA principle to address two important problems in drug discovery, which are identification of molecular biomarkers and off-target effects. It was shown in this study that determining the protein thermal stability across the proteome under different conditions enables the recognition of direct as well as downstream effects.

The neutron-encoded isobaric mass tagging reagents (TMT10) were used with mass spectrometry in this study, to determine the protein thermal stability across ten different temperatures. In a melt curve experiment, the cells were grown under different conditions and then divided in to ten aliquots. Each of the aliquots was then heated at different temperatures followed by cell lysis. The sample extracted from lysis was trypsinated and labelled with different TMT10 tags and subsequently combined and examined using LC-MS. The melting temperature of each protein was calculated by fitting the reporter ion intensities obtained from the MS spectra. The melting curves of proteins after drug treatment was then compared to that of the vehicle treatment. The proteins with melt curves showing significant stabilization upon

drug treatment were identified for further analysis. The thermal profiling data was collected from cell lysates and intact cells. From the experiment on intact K562 cells, data from 5299 proteins was acquired. The proteins showing stabilizations in their melt curves were checked for dose dependent stabilization effects using $ITDR_{CETSA}$ experiment combined with MS detection [77].

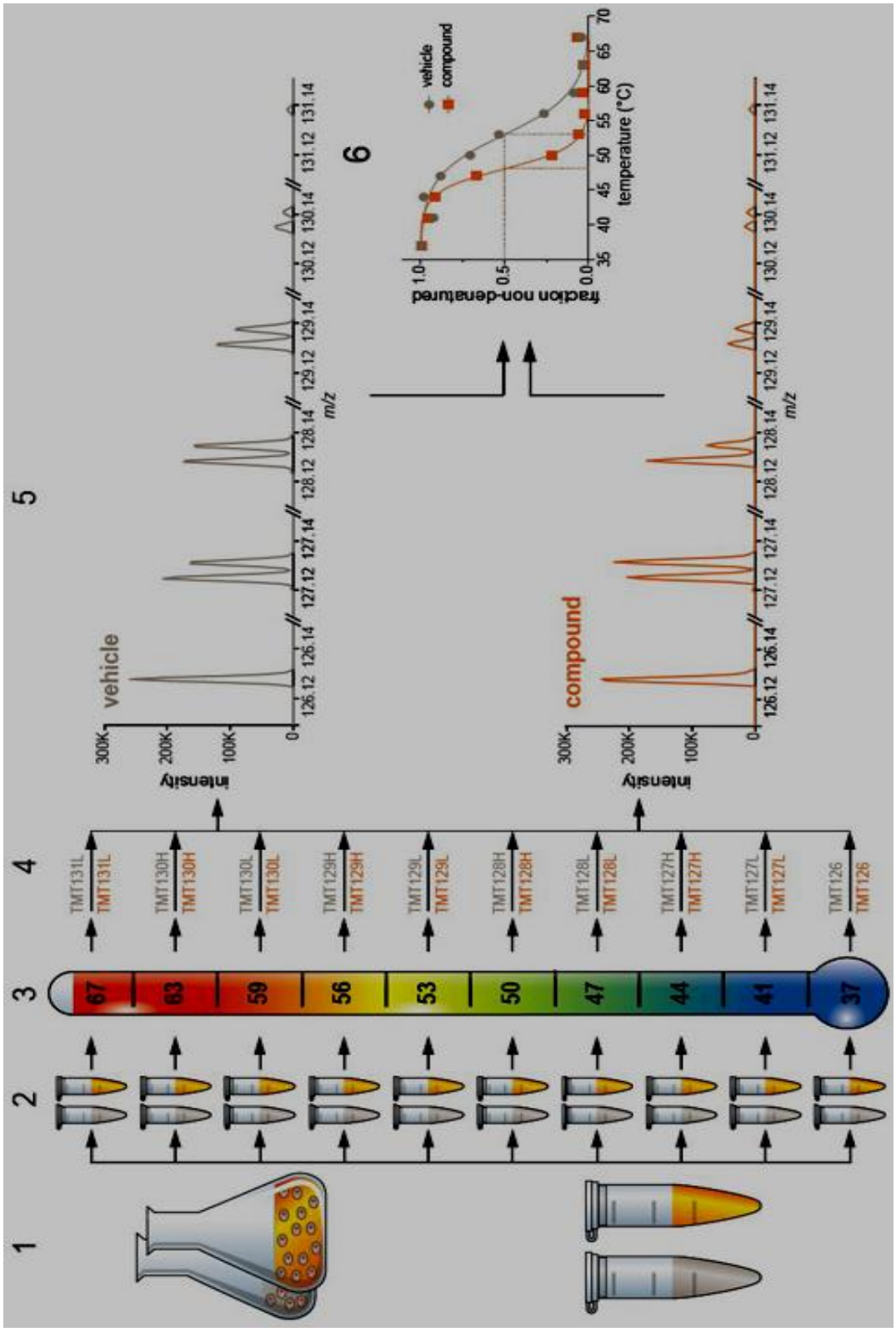

Figure 18: Thermal proteome profiling using CETSA set up combined with quantitative mass spectrometry [77]

6.2. CETSA to study crizotinib resistance in ALK-expressing human cancers

In a recent study by Alshareef, A., *et al.*, CETSA was used to understand crizotinib resistance in ALK-expressing human cancer cell lines [78]. They showed by correlating CETSA shifts with inhibition of cell proliferation of a set of ALK sensitive cell lines that the interaction between crizotinib and ALK is an important factor that determines crizotinib sensitivity in these cells. They conclude that compared to other techniques used to study drug resistance such as detecting ATP binding by recombinant proteins, CETSA is beneficial as it can assess drug-target interactions in a cellular context. They also proposed that after performing studies with clinical samples, CETSA could be used in clinical settings to understand drug sensitivity. [78]. This study gave novel insights in to mechanisms causing crizotinib resistance in ALK+ cancer cells.

6.3. The use of CETSA to perform screening for target engagement

In the original CETSA publication western blot was used to detect the stabilized protein from the soluble fraction in the samples [75]. Western blot detection is relatively simple to perform if a good antibody against the target protein is available. However, in circumstances such as high-throughput screening where multiple samples should be analysed, western blot is not a good detection strategy. Such cases require CETSA to be used with a microplate based detection strategy so that the treatment steps can be done using an automated liquid handling equipment. This assay should minimize the number of steps to increase the assay throughput and also to reduce well to well variability across the samples. Techniques such as enzyme-linked immunosorbent assay (ELISA), dot blots and proximity ligation assays can be used in a microplate format but the throughput is compromised due to the need of wash and separation steps before detection. The detection method should instead allow the measurement of soluble protein fraction without the need of wash and separation steps in between. AlphaScreen (amplified luminescent proximity homogeneous screen) is a well-studied homogeneous detection method that uses antibodies to detect folded protein in cell lysates.

In a study by Axelsson H**.** *et al.*, the different steps involved in the development of an alphascreen based CETSA assay for HTS is described [79]. The protein Thymidylate Synthase (TS) was used as an example to demonstrate the steps involved assay development and the efficiency of HTS CETSA for identifying hit compounds from a large library.

Alphascreen is a bead based proximity assay that uses a donor bead and an acceptor bead for detection. Both the beads have a large surface area for the binding of the biomolecules. The donor bead upon excitation generates singlet oxygen molecules that travels in solution and reaches the acceptor bead. This results in the excitation of the acceptor bead that emits light if the donor and acceptor are in close proximity, which happens due to complex formation (Figure 19).

The first step in the assay development is the identification of a suitable antibody pair with good selectivity and affinity for the target protein. These antibodies should be able to also detect soluble protein from a background of aggregated proteins. If several antibodies are available that satisfy these conditions the various antibody combinations should be tested. An important limiting factor in the antibody selection is the quenching of the signal due to the ligand-induced suppression of the antibody identification. This can happen because of the conformational changes in the target protein due to ligand binding [79]. The assay validation is critical to overcome the risk of false negatives [79,80]. Therefore, known inhibitors from different structural classes should be included during the process of assay development.

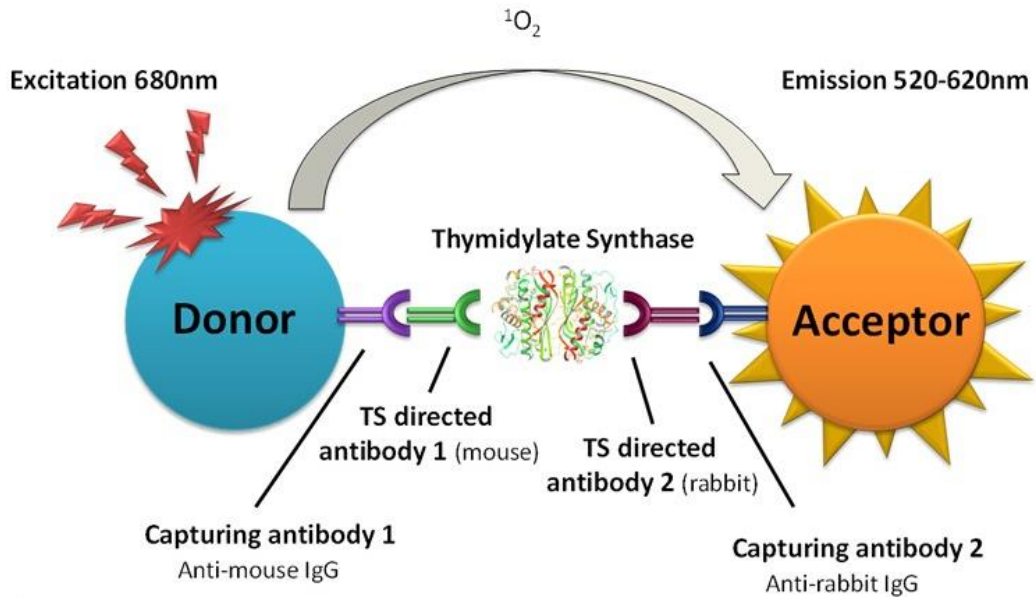

Figure 19: Schematic illustration of alphascreen detection

Alphascreen set up to detect TS using donor and acceptor beads containing capturing antibodies (anti-mouse IgG and anti-rabbit IgG) detecting anti-TS antibodies (from rabbit and mouse) [79].

6.4. The identification of known and novel thymidylate synthase inhibitors and slow intracellular activation of 5-fluorouracil by CETSA

In the work by *Almqvist* H. *et al.,* CETSA was implemented to establish the first compound library screen for thymidylate synthase ligands in cells [81]. A library consisting of 10,928 compounds that includes nucleosides, known drugs and lead-like compounds were screened against TS to identify stabilizations (Figure 20D). The screen apparently identified all known drugs that was known or anticipated to inhibit TS in the library. It also discovered compounds with novel chemistry and drugs that were not previously known to inhibit TS. Large scale screening was enabled by establishing a no-wash assay for TS, using the alphascreen technique in 384-well plates. In this study, K562 cells were pre-incubated with the compounds or controls to permit cellular uptake and binding to TS. The treated cells were then heated using a PCR machine. The cells were then cooled to room temperature and lysed after which the stabilized level of the protein was measured. The assay was validated by examining the behaviour of two drugs of TS: raltitrexed and floxuridine.

$ITDR_{CETSA}$ experiments were performed to study the response of these drugs. CETSA melt curves showed significant shifts in the melting profile of TS in the presence of these drugs (Figure 20A). Both the drugs demonstrated dose-dependent stabilization of TS when tested using $ITDR_{CETSA}$ studies (Figure 20B and 20C). The study also showed that the drug 5-fluorouracil undergoes slower activation in the cells as compared to the nucleoside based drugs such as floxuridine and 5-fluorouridine (Figure 20E) [81].

A

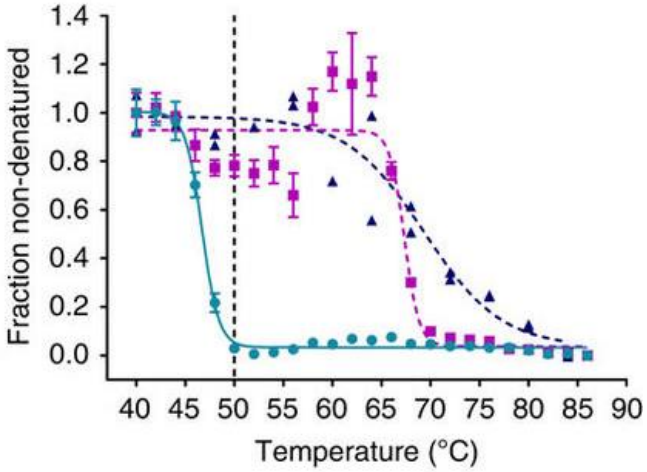

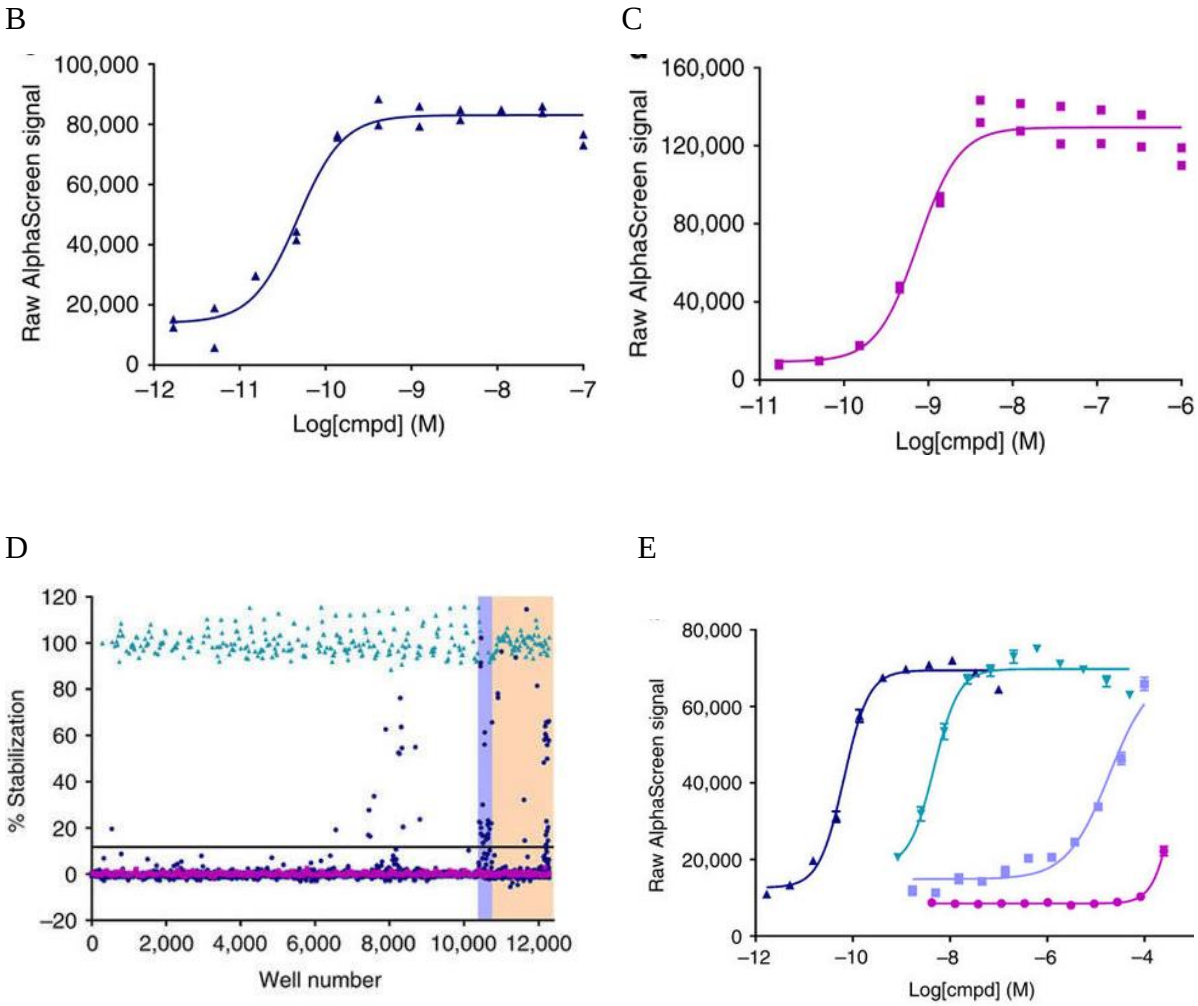

Figure 20: CETSA to identify known and novel TS inhibitors and slow intracellular activation of 5FU

CETSA melt curves of TS in K562 cells in the presence of DMSO (green circle), floxuridine (blue triangle) and raltitrexed (lavender square) (A). $ITDRF_{CETSA}$ of floxuridine at 50 °C in K562 cells (B). $ITDRF_{CETSA}$ of raltitrexed at 50 °C in K562 cells (C). Data from the compound library screening where 0% denotes the TS signal in the presence of DMSO (lavender square) and 100% denotes the TS signal in the presence of raltitrexed (green triangle) (D). $ITDRF_{CETSA}$ data of floxuridine (dark blue upward triangle), 5-fluorouridine (green downward triangle) 5-FU (light blue square) and a novel TS inhibitor CBK115334 (lavender circle) (E) [81].

7. Thymidylate synthase, a key target in chemotherapy

DNA synthesis is critical for cell proliferation and the generation of the pyrimidine nucleotide TMP from dUMP is an important step in the synthesis of DNA precursors. Thymidylate synthase (TS) is the enzyme that catalyzes this reaction using the folate substrate 5,10-methylene tetrahydrofolate (CH_2THF) - this is the only ab initio thymidylate production in cells [82].

TS uses dUMP and CH_2THF to carry out this reaction and it forms a ternary complex with these substrates to perform the reductive methylation of dUMP to TMP [83]. During this conversion, the tetrahydrofolate gets converted to dihydrofolate. The enzyme dihydrofolate reductase (DHFR) regenerates the tetrahydrofolates from dihydrofolates produced from the reaction (Figure 21).

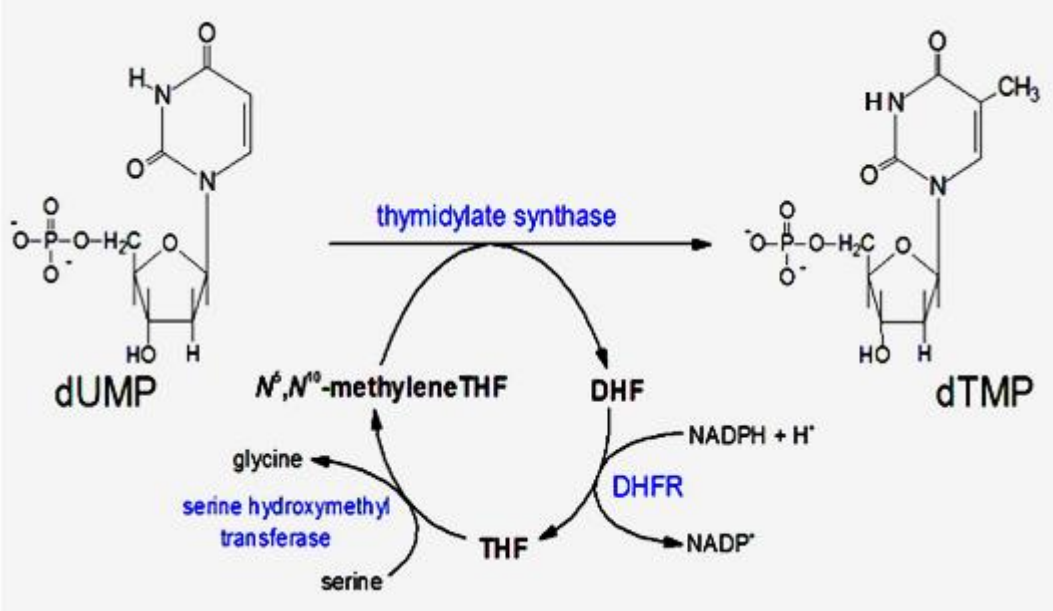

Figure 21: Function of thymidylate synthase

TS catalysing the reductive methylation of dUMP to dTMP to produce thymidylate in cells (Proteopedia.org).

It is also possible for the mammalian cells to import thymidine from extracellular sources to generate dTMP. Circulating thymidine is therefore a source of dTMP that might assist cancer cells to grow in in vivo.

TS is an mRNA binding protein and it can bind to its own mRNA. This inhibits translation, which suggests an autoregulatory feedback mechanism (Figure 22) [84,85]. This interaction was found to be specific and the other unrelated mRNAs were unaffected by the TS protein

[84]. The inclusion of the TS substrates or inhibitors completely restores the TS mRNA translation, which suggests that a specific conformational state is required for the TS protein for interacting with its own mRNA. When TS protein without catalytic activity was made to interact with the TS mRNA, it was observed that the interaction does not take place. This shows that the protein should be in biologically active state for this interaction to happen [84].

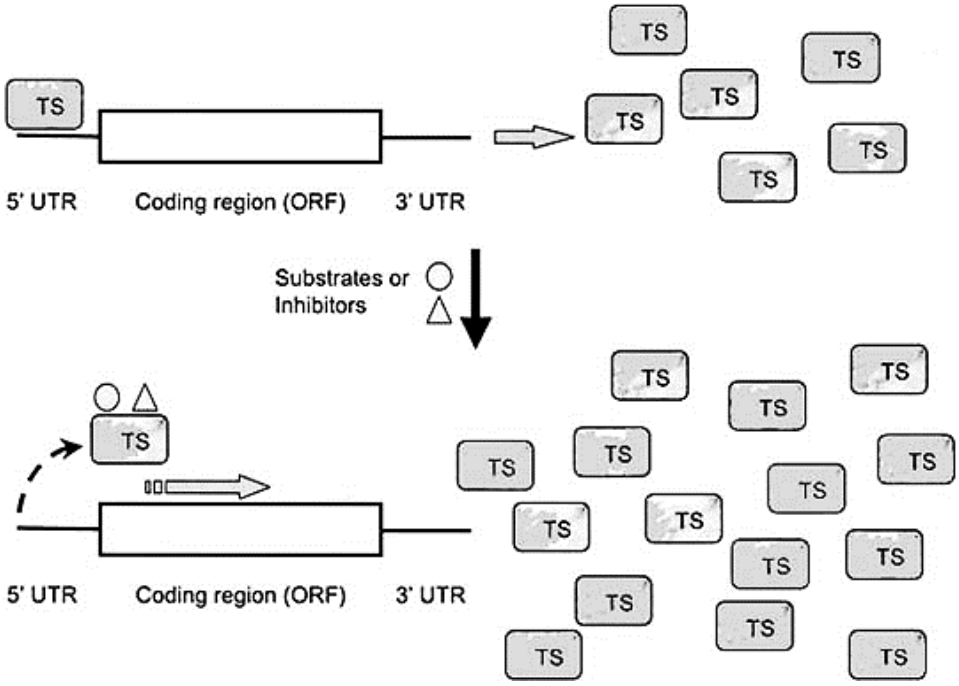

Figure 22: The autoregulatory feedback mechanism of TS

The binding of TS to the 5'-untranslated region (UTR) leads to the inhibition of TS mRNA translation. The binding of TS substrates and inhibitors to the protein relieves this repression that allows translation and this results in an increase in the levels of TS protein [83].

7.1. TS inhibitors

Due to the important function of TS in the production of thymidylate, DNA synthesis and cell proliferation, this enzyme has been a critical target for cancer treatment for many years [83]. Both the nucleotide binding site and folate binding site of TS are targeted and major classes of TS inhibitors are the antifolates and the fluoropyrimidines (Figure 23).

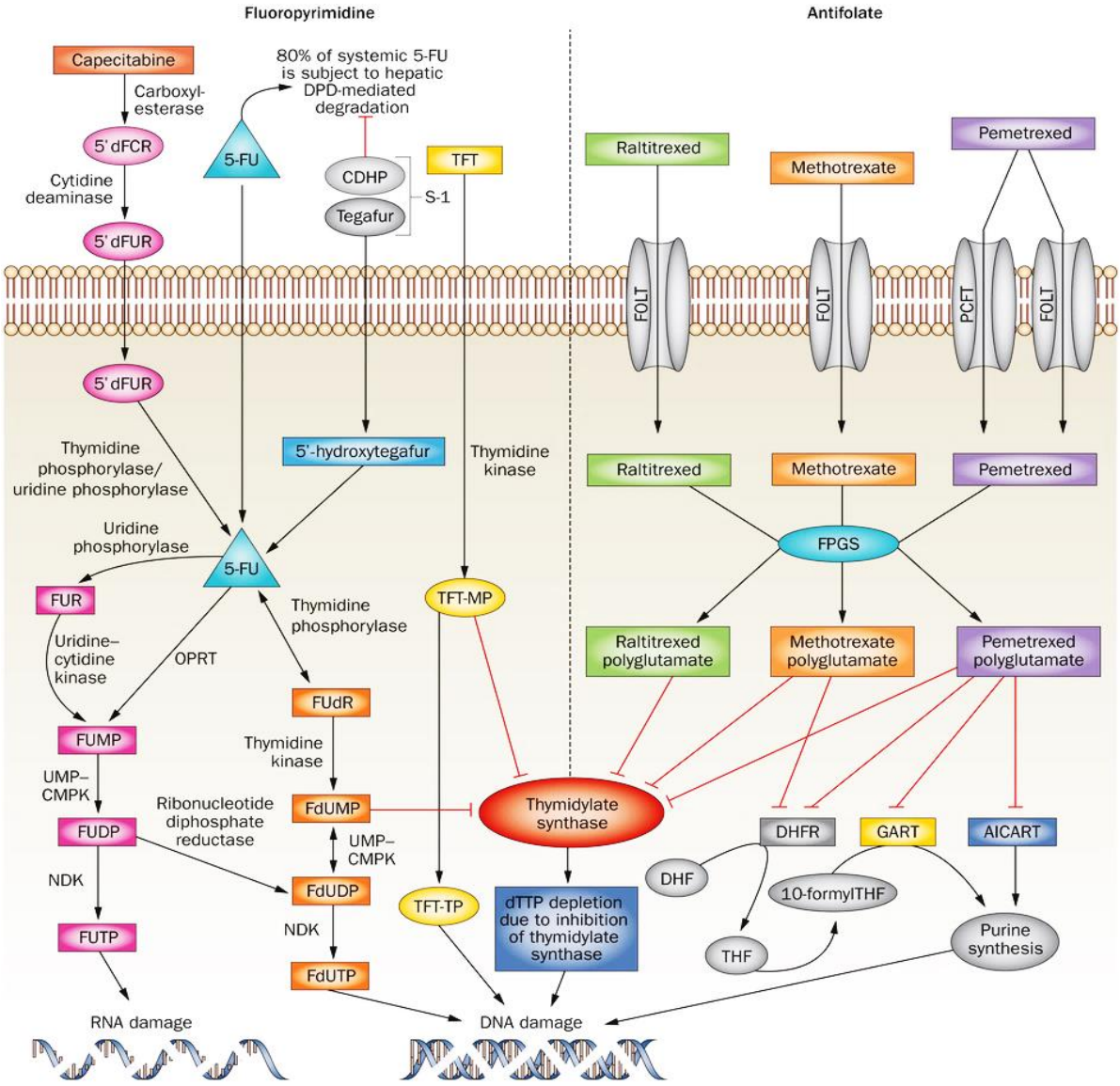

Figure 23: Major classes of TS inhibitors

The antifolate and fluoropyrimidine classes of TS inhibitors and their mechanism of action. [86]

7.1.1. Antifolates

In the 1940s, it was found that the antifolates are successful in treating childhood leukemia due to the important role of folates in the biosynthesis of thymidylate [87]. Many new generation antifolates were designed and developed decades after this discovery. These antifolates were developed aiming at inhibiting the important folate dependent proteins that leads to the inhibition of nucleotide biosynthesis followed by cell death [88]. Antifolate drugs are classified mainly in to two classes: polyglutamatable and non-polyglutamatable antifolates. The polyglutamatable antifolates are generally hydrophilic and contain a glutamic acid residue that undergoes polyglutamation in the cells. On the other hand, the non-

polyglutamatable antifolates are lipophilic and lack the glutamic acid residue and therefore do not undergo polyglutamation [89].

The major antifolate drugs used for cancer therapy are described below:

Raltitrexed (RX):

Raltitrexed is a potent drug developed by the company AstraZeneca, that inhibits TS (Ki=62nM) and belongs to the aqueous-soluble antifolate class of inhibitors (Figure 24). It is transported by reduced folate carrier protein (RFC) to enter the cells. Inside the cells, RX undergoes polyglutamation by enzyme folyl polyglutamate synthetase (FPGS), this polyglutamated form of the drug is retained in the cells and causes prolonged inhibition of TS [90]. The process of polyglutamation increases the inhibitory potency of RX to TS by 100-fold compared to the parent form [90,91]. RX is used for treating advanced colorectal cancer and is commonly used to treat patients showing intolerance to the fluoropyrimidine drug 5-fluorouracil (5FU). It was also found in a phase III clinical trial that RX in combination with cisplatin improves the overall survival in malignant pleural mesothelioma (MPM) [92].

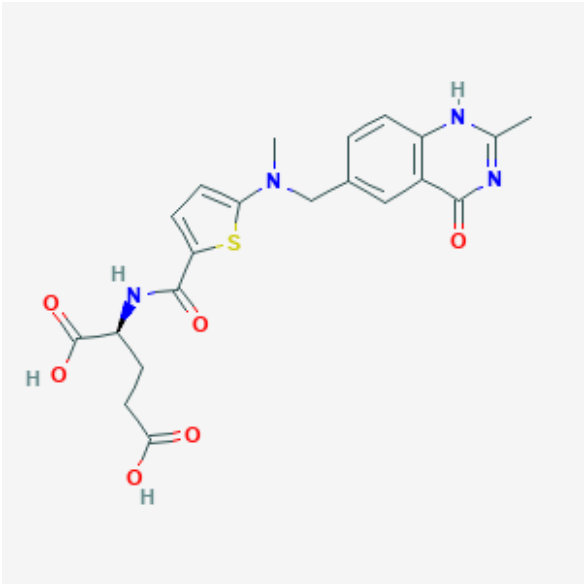

Figure 24: Structure of raltitrexed

Methotrexate (MX):

Methotrexate is an old antifolate drug introduced into the clinic in 1948 and it inhibits the enzymes DHFR and TS (Figure 25). Currently, MX is used for treating several forms of malignancies such as breast cancer, head and neck cancer, bladder cancer and

osteocarcoma [93]. It is also used in the treatment of immune disorders such as psoriasis and rheumatoid arthritis. MX also involves a carrier mediated transport by RFC and it gets polyglutamated in the cells. DHFR inhibition by MX is not affected by its polyglutamation but the polyglutamated forms gets retained in the cells and becomes a potent inhibitor of TS [93].

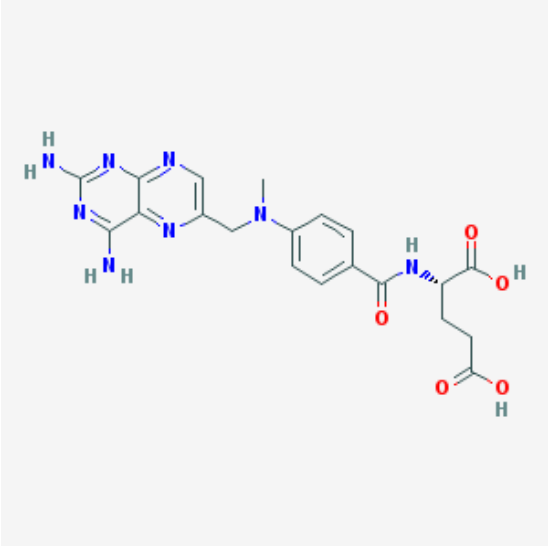

Figure 25: Structure of methotrexate

Pemetrexed (PX):

Pemetrexed is a multitargeted antifolate drug that targets TS, DHFR and GARFT, TS being the primary target (Figure 26) [94]. PX is taken up by the cancer cells by RFC and proton coupled folate transporter (PCFT) and it undergoes fast and efficient polyglutamation. An important factor that makes PX superior to MX is that PX can undergo rapid polyglutamation even at low intracellular levels. This is because PX is a superior FPGS substrate and its Km to FPGS is 100-fold less than that of MX. The polyglutamation of PX improves the inhibitory potency of the drug to 84-fold towards TS as compared to the monoglutamate form [94,95]. The inhibitory potency of PX to GARFT and DHFR also increases significantly upon polyglutamation.

It was also demonstrated that PX has inhibitory activity towards the enzyme AICARFT, involved in the purine biosynthesis [94,95]. The intracellular levels of folates decrease the cytotoxicity of PX because the cellular folates compete with the drug for target binding and polyglutamation. When the cellular folate levels are high,

there is a decrease in the polyglutamation of PX, which reduces the inhibitory potential of this drug [94,95].

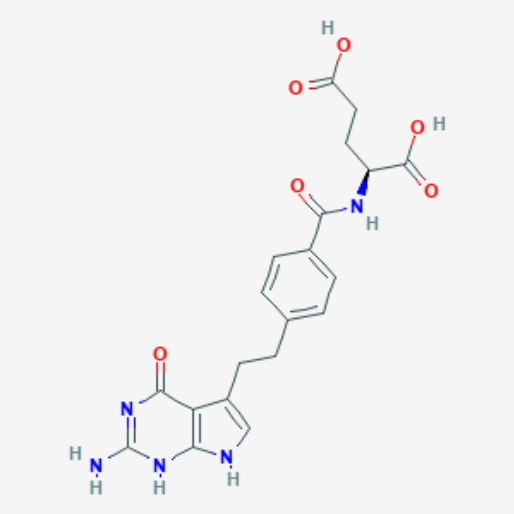

Figure 26: Structure of pemetrexed

Nolatrexed (NX):

Nolatrexed is a nonclassical antifolate drug that inhibits TS (Figure 27). This is a lipophilic, non-polyglutamatable form of drug developed to block the folate binding site of TS. NX enters the cells by passive diffusion and as it does not contain a glutamate moiety, NX does not undergo polyglutamation. Therefore, NX is not affected by the classical resistance mechanisms associated with antifolates that includes defective cellular transport mechanism and polyglutamation [96].

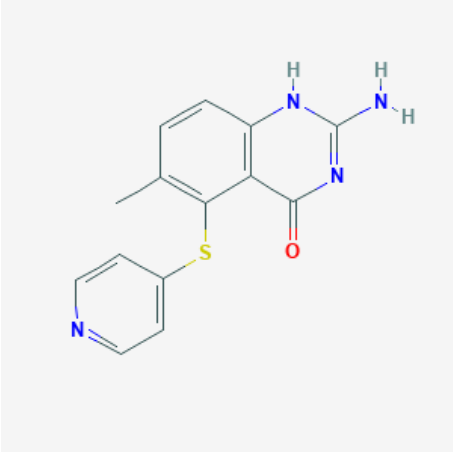

Figure 27: Structure of nolatrexed

7.1.2. Fluoropyrimidines

These are the nucleotide analogues targeting the dUMP binding site of TS. 5-fluorouracil (5FU), the fluoropyrimidine drug has been used over many years for cancer treatment is a key component in e.g. the first line treatment colorectal cancer (Figure 28A). 5FU not only has direct effects on TS but also causes damage due to mis-incorporation in to RNA and DNA and imbalance in dTTP/dUTP pools. Inside the cells, 5FU gets metabolized in to the active metabolite 5-FdUMP, which forms a covalent complex with TS and CH2-THF (Figure 28B) [97].

A

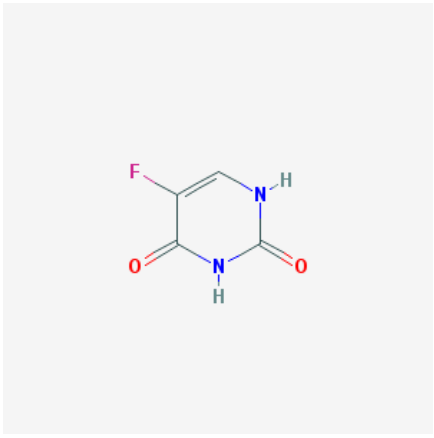

B

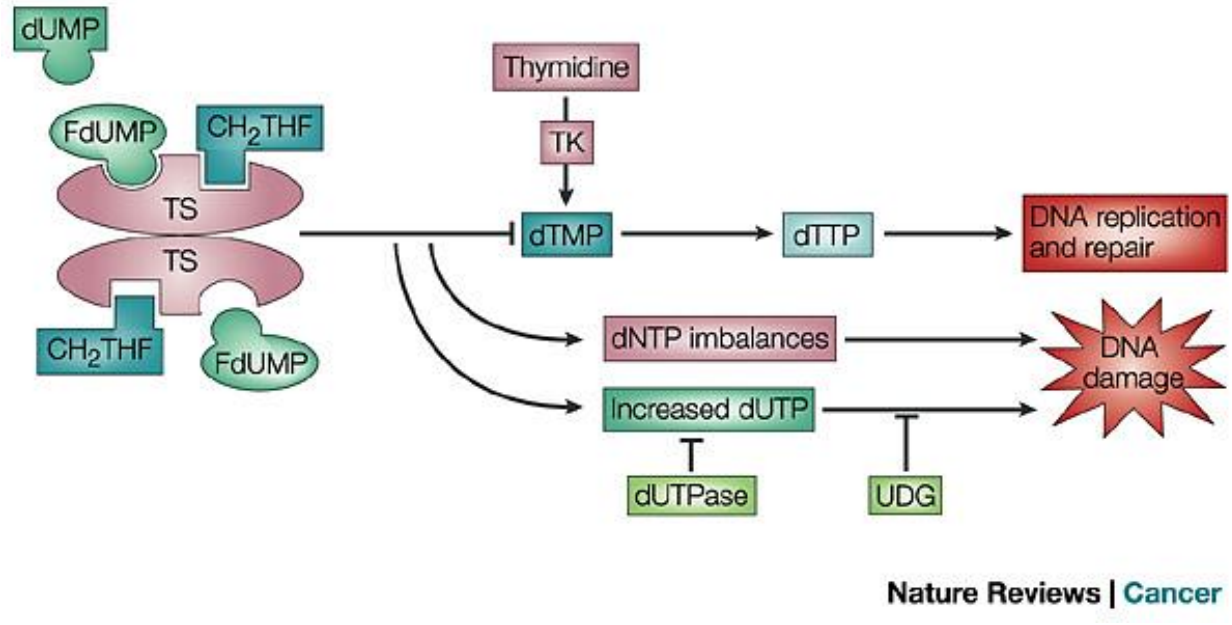

Figure 28: The structure (A) and mechanism of action of 5FU (B) [97]

8. Drug resistance

Drug resistance is a critical problem that leads to failure of cancer treatments. Even though many patients respond to drug treatment, over time drug resistance often develop. This is often due to mutations in DNA and metabolic changes in the cancer cells that decreases the drug efficiency [98].

Drug resistance to chemotherapeutic drugs can develop during chemotherapy, so called acquired resistance, or can be present in the cells already before treatment, innate resistance [99]. In the last few decades, many studies have been performed to address the mechanisms causing drug resistance and few of the important mechanisms are described below (Figure 29).

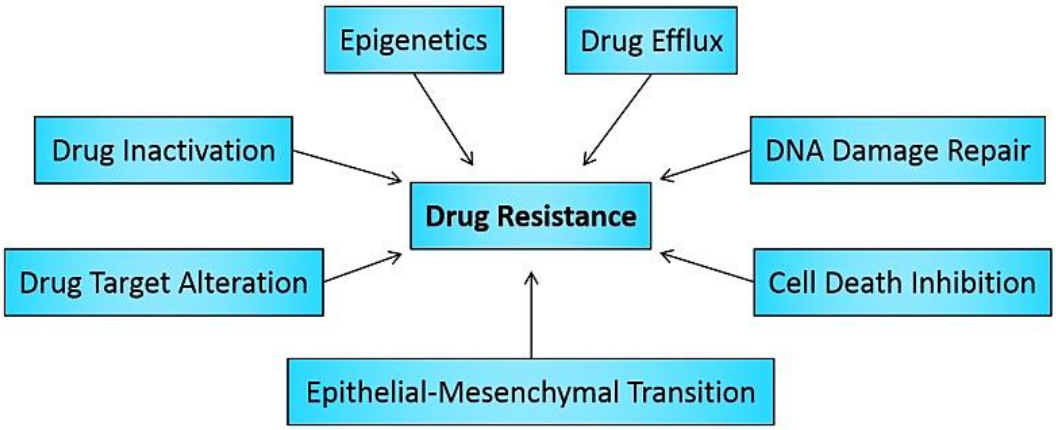

Figure 29: Mechanisms causing drug resistance development during cancer treatment [98]

8.1. Mechanisms causing drug resistance during cancer therapy

8.1.1. Defective transport mechanisms:

The classical antifolates are imported in to the cells by the transport proteins such as the reduced folate carrier (RFC), folate receptor (FR) and proton coupled folate transporter (PCFT). Antifolate resistance can develop due to the loss of function of these transporters that includes inactivating mutations, decreased expression levels or silencing because of the loss of function of transcription factors.

For example, studies show that malignancies undergoing antifolate drug treatment can have decreased RFC levels that causes resistance to these drugs [100,101]. No resistance mechanisms related to the loss of function of PCFT are reported. But it is possible that in conditions where RFC is inactive or less active, PCFT becomes the

primary transporter, which gives rise to resistance mechanisms associated with PCFT. There is not enough data to suggest that changes in the FR could lead to antifolate resistance. However, in cancers with increased levels of FR such as in nasopharyngeal epidermoidcarcinoma (KB) cells, MX treatment can result in down regulation of FR protein leading to drug resistance [99,102]. Studies show that the alterations in the transcription factors also cause antifolate resistance as it regulates the expression of RFC. Also, variations in post-translational modifications results in a marked decrease in the mRNA levels of RFC, thereby leading to antifolate resistance [103,104].

Mutations in the RFC protein can change the transport activity of antifolate drugs. Several mutations such as point and inactivating mutations in the RFC coding region results in reduced transport affinity to antifolates drugs. This finally causes reduced transport of the drugs and antifolate resistance. However, these cells retain adequate cellular folate transport, which is essential for DNA synthesis and cell proliferation [89].

8.1.2. Loss of FPGS activity:

Polyglutamation is the process of attaching multiple glutamate moieties to a molecule by an enzymatic process. This process increases the retention of antifolate drugs in cells. FPGS is the protein responsible for polyglutamating the antifolate drugs and therefore loss of FPGS activity can develop resistance to classical antifolate drugs. From many studies, it was found that reduced FPGS activity leads to reduced intracellular levels of MX and RX polyglutamates [105,106,107]. For MX, polyglutamation is important for cellular retention but it has non-significant effect on the drug affinity to the target enzyme DHFR. For RX and PX, polyglutamation is crucial in enhancing their binding affinity to the primary target proteins [108]. In a study by Liani et al., 2003, fourteen antifolate resistant sublines of human leukemia cell lines (CCRF-CEM) were exposed to high dose pulses of polyglutamatable antifolates. The antifolate drugs tested were MX, aminopterin, edatrexate, RX, GW1843, lometrexol and PX. Out of the fourteen sublines tested, eleven showed antifolate resistance due to defect in the activity of FPGS, with a loss of FPGS activity more than 90%. One of these resistant sublines showed a Cys346Phe inactivating mutation at the active site of FPGS, suggesting an intervention in its catalytic activity. This resistant subline with the mutation showed a 23-fold decrease in affinity towards L-glutamate. Decrease in the FPGS mRNA levels was observed in four other sublines,

which lead to antifolate resistance. This implies the presence of post transcriptional mechanisms or mutations associated with the FPGS regulation and activity. Impaired post-transcriptional modification causing splicing of FPGS, leads to loss of FPGS activity in MX resistant leukaemia cells and in leukaemia patients [109]. Therefore, the loss of FPGS function due to decreased mRNA levels, mutations and/or post-transcriptional modifications can result in resistance to classical antifolates.

8.1.3. Overexpression of target enzymes:

Increase in the activity of the target enzymes due to gene amplification is a well-studied mechanism of antifolate and fluoropyrimidine drug resistance. For example, MX is a potent inhibitor of DHFR. The amount of MX required to inhibit DHFR activity is directly proportional to the quantity of DHFR in the cells. Studies have shown that human MX resistant cell lines contain increased DHFR levels due to gene amplification [110]. Therefore, higher concentration of drug is required to inhibit the enzyme completely. Reports show that gene amplification is a common mechanism associated with MX resistance when the cell lines are exposed to step wise increase of MX treatment [110]. Similarly, overexpression of TS is demonstrated in 5FU resistant subline, which interferes with the efficiency of drug treatment causing drug resistance. TS overexpression can happen also because of the autoregulatory feedback mechanism of TS, which is described in the previous section.

8.1.4. Mutations in the target enzymes:

A drug's efficiency is affected by its target enzyme and mutations in the enzyme can interfere with the drug interaction. If the target enzyme gets mutated in the active site, the drug won't be able to bind, which can lead to drug resistance. For example, DHFR mutations are common in MX resistant cell lines exposed to increasing drug doses. However, when patient samples were studied and the cDNA sequence of DHFR were analysed across eight patients, no evidence of DHFR mutations were found. Mutations in TS is a mechanism sometimes contributing to resistance in 5-fluorodeoxyuridine (5FdU) resistant cell lines.

It was shown in a study that that the resistant mutants possessed 1–5 amino acid substitutions along the entire length of the polypeptide [111,112]. The catalytically important Arg^{50} loop and the Cys^{195} near the active site were mutated frequently and many mutations were scattered throughout the cDNA [112].

8.1.5. Mutidrug resistance due to activation of drug efflux pumps:

Cancer cells exposed to a drug can develop clones resistant to the single drug or several antitumour drugs not belonging to the same class. This phenomenon of the cancer cells developing resistance to multiple drugs is termed as multi drug resistance (MDR). The proteins that belong to the ATP-binding cassette (ABC) transporter family causes this efflux and are crucial, well-studied regulators in healthy cells. These transporters are transmembrane proteins in human cells that transports several substances across cellular membranes [98]. The ABC family in humans consists of 49 members and they have two distinct domains- a variable transmembrane domain and a highly-conserved nucleotide binding domain. ATP hydrolysis at the nucleotide binding site takes place when a substrate binds to the transmembrane domain. This leads to a conformational change, which transports the substrate out of the cell. This process of efflux plays a crucial role in counteracting the accumulation of toxic compounds in cells. Because of this, the ABC transporters are upregulated in the liver and intestine, where they pump out drugs and other toxic compounds into the bile duct and intestinal lumen to protect the body [113]. These transporters also play a major role in preserving the blood-brain barrier [114].

Drug efflux by ABC transporters is a common physiological process but it is also a well-studied drug resistance mechanism during cancer therapy. Three major transport proteins: multidrug resistance-associated protein 1 (MRP1), breast cancer resistance protein (BCRP) and multidrug resistance protein 1 (MDR1) are involved in the process of resistance development. They protect the cancer cells by pumping out various drugs such as taxanes, anthracyclines, kinase inhibitors and epipodophyllotoxins from the cells. [115]. This is believed to happen mainly because of the upregulation of P-glycoprotein, a cell membrane protein responsible for the transport of drugs and other physiological molecules from the cells to the extracellular space [116]. Because of such drug efflux, the drug concentration at the intracellular environment of the target decreases, which causes drug resistance.

8.1.6. DNA damage repair:

The DNA-damage repair has an important role in antitumor drug resistance. Drug-exposure often causes DNA damage directly or indirectly. The DNA damage response (DDR) can reverse the damage caused by drug treatment. Drugs such as cisplatin that contains platinum causes apoptosis by harmful DNA crosslinks and antifolates and

nucleotide analogs often leads to missincorporation of nucleotides into DNA [117]. The important DNA repair mechanisms such as homologous recombination and nucleotide excision repair causes resistance by reversing damage caused by such drugs [118]. Thus, the failure of the DDR mechanisms in cancer cells affects the efficiency of the DNA-damaging cytotoxic drugs. Cancer cells could be sensitized to chemotherapy if the DNA- damage repair pathways are inhibited [119].

8.1.7. Cell death inhibition:

Apoptosis is the most important mechanism for cell death and there are two basic pathways for apoptosis [98]. They are: the intrinsic pathway controlled by the mitochondria and which includes B-cell lymphoma 2 (BCL-2) family proteins, Akt, caspase-9 and; the extrinsic pathway that is initiated by apoptotic receptors on the cell surface. The activation of down-stream caspase-3 combines the intrinsic and extrinsic pathways that lead to apoptosis. The BCL-2 family apoptosis inhibitors and the down-stream transcription modulators such as NF-κB and STAT are highly active in several types of cancer that makes them potential targets for cancer therapy [98]. Several drugs inhibiting BCL-2 family proteins, kinases and caspase family proteases are showing promising results in recent clinical trials [120]. As an example, inhibitors targeting BCL-2 are efficient in causing apoptosis in tumour cells but prolonged use of these drugs can also lead to resistance development.

8.2 Methods to study drug resistance

MTT assay:

MTT assay is a colorimetric assay used to assess the metabolic activity of cells. The assay measures number of viable cells with the help of NAD(P)H-dependent cellular oxidoreductase enzymes. This enzyme reduces the tetrazolium dye MTT 3-(4,5-dimethylthiazol-2-yl)-2,5-diphenyltetrazolium bromide to insoluble formazan that has purple colour. This assay can be used throughout the time course of disease to monitor drug resistance development in fresh tumour samples of both solid and haematological malignancies [121]. Typically, cancer cells isolated from bone marrow or solid biopsies are exposed to drug for 48 to 96 hours and the cell viability is measured by MTT assay. A significant correlation was observed in the in vivo and in vitro studies for acute myeloid leukaemia (AML) and ovarian cancer. This study also correlated the

assay-results with the markers of drug resistance and showed that it is a suitable technique for screening for drug resistance. The development of drug resistance in cell line models was studied using this technique with a vision of its prevention [121]. Even though MTT assay is widely used to study the cytotoxicity of drugs, the compounds that alter the cell metabolism and reaction conditions can interfere with the assay. This interference can produce false screening results [122].

Cancer biomarker tests:

As discussed above here are several classes proteins that play potentials roles in cancer drug resistance. Immunochemistry can be used to determine the levels of such proteins in tumour samples. Techniques such as proteomics, genomics and transcriptomics also enables the study of biological molecules that are associated to drug toxicity and drug efficacy. The samples from patients with drug resistance can be compared with the material from patients without drug resistance, using mathematical and computing techniques [123,124,125]. Several studies describe the usage of sensitive analysis algorithms to identify new biomarkers [126]. However, the clinical importance of most of these biomarkers in drug resistance is yet to be proven.

Positron emission tomography tests (PET)

Positron emission tomography (PET) is a nuclear medicine method currently used for studying drug efficacy and resistance. This method allows for the detection of cancer localisation and to discover the metabolic activity of tumours. PET detects the dynamic uptake profiles of radiolabelled drugs after injection. The blood clearance value that gives information on kinetic modelling is determined from the blood pool forms in the images. Treatment response is determined by analysing PET scans before and after therapeutic intervention [126].

We showed that CETSA developed by us can monitor complex cellular processes like drug transport and activation in cells [75]. These processes are often involved in drug resistance development. Therefore, in this work we have explored the potential to use CETSA to study resistance development during chemotherapy.

CHAPTER 2: MATERIALS AND METHODS

1. Chemicals and buffers

6-(5H)-phenanthridinone (PARP1 inhibitor), raltitrexed, 5FU and 5FdU (TS inhibitors) were purchased from Sigma Aldrich. methotrexate (DHFR inhibitor), pemetrexed (TS inhibitor), olaparib and iniparib (PARP1 inhibitors) were purchased from Selleck chemicals. Nolatrexed (TS inhibitor) was purchased from Santa cruz Biotechnology. The inhibitors were dissolved using dimethyl sulfoxide (DMSO) (Sigma Aldrich) to make appropriate stock solutions.

Phosphate-buffered saline (PBS) was procured from Nascalai tesque. Kinase buffer (KB) was made with the following composition: 25 mM Tris (hydroxymethyl)- aminomethane hydrochloride (Tris-HCl, pH 7.5), 5 mM beta-glycerophosphate, 1 mM tris(2-carboxyethyl)phosphine (TCEP), 0.1 mM sodium vanadium oxide and 10 mM magnesium chloride. Tris-buffered saline with tween (TBST) (150 mM NaCl, 0.05% (v/v) tween-20, 50 mM Tris-HCl buffer (pH 7.6) was used as washing buffer in the TPA and western blot experiments. 3% bovine serum albumin (BSA) (Sigma Aldrich) diluted in TBST was used as blocking buffer. Complete (EDTA-free) protease inhibitor cocktail was purchased from Nascalai Tesque.

2. Heterologous protein expression and purification

The human PARP1 gene K662-T1011 was cloned into pNIC28-Bsa4 vector with an N-terminal hexahistidine tag and a TEV protease recognition site (GenBank™ accession number EF198106) for protein expression. T1 phage-resistant BL21 (DE3) *E. coli* strain (Merck) was used as the host strain for protein expression. The cells were grown at 37^0C in 0.75 L of Terrific Broth medium supplemented with 50 μg/mL Kanamycin, 34 μg/mL Chloramphenicol and 8 g/L glycerol, using a shaker incubator. The temperature was reduced to 18^0C when the culture reached an OD_{600} of about 2.0. After 30 minutes, 0.5 mm of isopropyl β-d-thiogalactopyranoside was added to induce the expression of the target protein and the cells were incubated for 20 hours. The cells were then harvested by centrifugation at 4500 x *g* for 15 min, resuspended in lysis buffer and then stored at -80^0C. The lysis buffer constituted of 100 mM HEPES, 500 mM NaCl, 10% (v/v) glycerol, 10 mM imidazole, 0.5 mM TCEP, pH 8.0 supplemented with 125 U/ml of benzonase (Merck) and protease Inhibitor Mixture Set III, EDTA free (Nascalai Tesque). The cells were sonicated on ice at 70% amplitude with 3 s on/off cycles for 3 min using Vibra-Cell processor (Sonics & Materials Inc., Newtown, CT, USA). The lysate was centrifuged at 47,000 × *g* for 25 min at 4^0C and the supernatant was

harvested and filtered through a syringe filter (1.2-µm). The protein was purified using an ÄKTAxpress automated purification system (GE Healthcare). The filtered protein was loaded onto the machine, which does the purification in two steps: Immobilized Metal Ion Affinity Chromatography (IMAC) followed by Size Exclusion Chromatography (also called as Gel Filtration or GF). The crude protein mixture was then loaded on to a Ni-NTA super flow column (Qiagen). The column was washed with 20 column volumes of the IMAC wash1 buffer comprising of 20mM HEPES, pH 7.5, 500mM NaCl, 10mM imidazole, 10% glycerol, 0.5mM TCEP. It was then washed with 15 column volumes of IMAC wash 2 buffer comprising of 20mM HEPES, pH 7.5, 500mM NaCl, 25mM imidazole, 10% glycerol, 0.5mM TCEP. Five column volumes of the IMAC elution buffer (20mM HEPES, pH 7.5, 500mM NaCl, 500mM imidazole, 10% glycerol, 0.5mM TCEP) was used to elute the desired protein. The eluate was used for further purification by loading it onto a superdex-75 or superdex-200 SEC column and then eluted using GF buffer (20mM HEPES, pH 7.5, 300mM NaCl, 10% glycerol, 0.5mM TCEP). The system collected 2ml protein fractions from the elution peaks, which were verified by SDS-PAGE. The protein bands with lowest amounts of contaminants were pooled and concentrated at 4^0C using vivaspin 20 filter concentrators (15-kDa MW cutoff) (GE Healthcare). The final protein concentration of PARP1 was 15.5 mg/mL with a yield of 9 mg. The protein batches were then aliquoted, frozen in liquid nitrogen, and stored at -80^0C.

The clone for protein tankyrase-2 (hTNKS2) (NP_079511) was obtained from *Structural Genomics Consortium*, Karolinska institute. The recombinant carbonic anhydrase-2 (hCA2) (NP_000058.1) with His tag was purchased from Sino Biological.

3. DSF and DSLS Experiments

The denaturation temperature of the purified protein variants was determined either by differential scanning fluorimetry or by differential static light scattering.

To perform DSF, the protein was diluted to 0.2mg/ml in 20 mM HEPES pH 7.5, 150 mM NaCl. A total volume of 25µl (with 0.2 mg/ml protein, compounds and 5 x sypro orange (Invitrogen)) was dispensed into a 96-well plate. In the control wells, the same amount of DMSO was added instead of the compounds. Microseal B adhesive sealer (Bio-Rad) was used to seal the plate and it was heated in the iCycler (Bio-Rad), from 25 to 80^0C (56 heating cycles in 28 min). The fluorescent filter was used for sypro orange with λexcitation = 492 nm and λemission = 610 nm. The mid-point of the curves (Tm) was calculated using software package XLfit (ID Business Solutions).

For DSLS experiments, the protein was diluted to 0.2mg/ml in 20 mM HEPES pH 7.5, 150 mM NaCl and dispensed in to the wells of 384-well optical bottom plates with black upper structure (Nunc). The samples were sealed with 50µL of mineral oil (Sigma-Aldrich) and centrifuged at 15°C for 3min at 3200xg. Static light scattering was monitored using a DSLS detection system (Stargazer, from Harbinger Biotechnology & Engineering), with a temperature range of 25^0C to 80^0C, with a gradual increase in temperature of 1^0C /min.
Graphical representations of the stability profiles obtained were generated using GraphPad Prism software. The melting temperatures and aggregation temperatures were determined by the software, using the Boltzmann equation.

4. TPA experiments

For the TPA experiments, purified protein (0.5 µg) was added to a 96-well PCR plate and buffer (20 mM Hepes pH 7.5, 150 mM Nacl) or *E.coli* lysate and ligands were added to adjust the volume to 25 µL. The samples were then subjected to thermal stress for the required time (20 minutes) and temperature using a veriti thermocycler (Applied Biosystems/ Life Technologies). The heated samples were centrifuged at 3000xg for 15 minutes and then filtered using a 0.65µm multiscreen HTS 96-well filter plate (Merck). The filtered sample was then dotted (3 µL) on to a nitrocellulose membrane for blotting.
HisProbe-HRP (Thermoscientific) was used as the probe for immunoblotting in the experiments with purified protein. In the experiments using *E.coli* lysate, primary antibody penta-His antibody BSA-free (Qiagen) and secondary goat-anti-mouse IgG/HRP conjugate (Santa Cruz) were used for immunoblotting. The membranes were blocked with 3% BSA and washed 3 times with the TBST buffer. The antibodies were diluted in the blocking buffer and supersignal west dura chemiluminescence kit (Thermoscientific) was utilized for developing the membranes. Fujifilm LAS-3000 imaging system (Fujifilm, Tokyo, Japan) was used to image and detect the chemiluminescence intensities of the dots and ImageJ software was used to process the raw dot blot images. The microarray profile plugin(http://image.bio.methods.free.fr/dotblot.html) was utilized to subtract the background from the raw images. GraphPad Prism software was used to plot the graphs and fitting of the curves was performed using the sigmoidal dose-response function (variable slope).

5. Isothermal fragment screening

The isothermal fragment screening for hPARP1, hTNKS2 and hCA2 was performed using our in-house fragment library (Maybridge) comprising of 500 fragments in seven 96-well

plates. Purified protein (0.5 µg) was added to the wells of a PCR plate and the volume adjusted to 25 µL by addition of buffer (20 mM Hepes pH 7.5, 150 mM Nacl,) or *E.coli* cell lysate and ligands (1mM) depending on the experimental setup. The plates were then heated for 20 minutes in a water bath at 51 degrees, followed by centrifugation, filtration and immunoblotting steps. The initial hits were internally validated, by checking for dose response behavior.

6. Cell culture

Human cancer cell lines HeLa (ATCC No. CCL-2) and K562 (ATCC No.CCL-243) were cultured in DMEM (Gibco/ Life-technologies) and RPMI-1640 medium (Gibco/ Life-technologies) respectively. All culture media were supplemented with 10 % fetal bovine serum (FBS, Gibco/Life technologies), 1X Penicillin-Streptomycin-Neomycin (PSN) Antibiotic Mixture (Gibco/Life-technologies), 1X MEM Non-Essential Amino Acids Solution (Gibco/ Life-technologies). The HeLa and K562 cell lines were used for the TS experiments. Equal numbers of cells (1 X 10^6 cells per data point) were seeded in T-25 cell culture flasks (BD Biosciences) in appropriate volumes of culture medium and exposed to drug for 1 hour in the 37^0C incubator (with 5% CO2). Control flasks were incubated with equal volume of diluent for the corresponding drug. Following the incubation, the cells were harvested (either directly or detached from surface using trypsin/EDTA solution (Sigma-Aldrich)) and washed with PBS in order to remove the excess drug. Equal amounts of cell suspensions (50 µl each) were aliquoted into 96-well PCR plate for heating on the PCR machine.

7. CETSA Experiments

For the cell lysate CETSA experiments, cultured HeLa and K562 cells were harvested and washed with phosphate buffered saline (PBS). The cells were diluted with the kinase buffer supplemented with complete protease inhibitor cocktail. The cell suspensions were freeze-thawed three times using liquid nitrogen and passed through 21G needle five times. The soluble fraction (lysate) was separated from the cell debris by centrifugation at 15,000xg for 20 minutes at 4^0C. The cell lysates were diluted with appropriate buffer and divided into two aliquots, with one aliquot being treated with drug and the other aliquot with the diluent of the inhibitor (control). After incubation at room temperature for 30 minutes, the respective lysates were divided into smaller (50µL) aliquots and heated individually at different temperatures

for 3 minutes (Veriti thermal cycler, Applied Biosystems/Life Technologies) followed by cooling for 3 minutes at room temperature. The appropriate temperatures were determined in preliminary CETSA experiments. The heated lysates were centrifuged at 20,000xg for 20 minutes at 4^0C to separate the soluble fractions from precipitates. The supernatants were transferred to new microtubes and analyzed by sodium dodecyl sulfate polyacrylamide gel electrophoresis (SDS-PAGE) followed by western blot analysis.

For the intact cell experiments, the drug-treated cells from the *in vitro* experiments above were heated as previously described followed by addition of kinase buffer (30µL) and lysed using 3 cycles of freeze-thawing with liquid nitrogen and mechanical shearing. The soluble fractions were harvested and analyzed by western blot as described earlier.

8. SDS-PAGE and western blot.

The proteins in the samples were resolved using NuPage® Novex Bis-Tris 4-12% polyacrylamide gels with NuPAGE® MES SDS running buffer (Life Technologies). The iBlot® blotting system (Life Technologies) was used to transfer the proteins on to nitrocellulose membranes. Primary anti-dihydrofolate reductase, anti- thymidylate synthase antibodies as well as the secondary goat anti-mouse HRP-IgG and bovine anti-rabbit HRP-IgG antibodies were purchased from Santa Cruz Biotechnology. All membranes were blocked with blocking buffer (3% BSA). Supersignal west dura chemiluminescence kit (Thermo Scientific) was used to develop the dot-blot images. Fujifilm LAS-3000 imaging system (Fujifilm, Tokyo, Japan) was utilized to detect the chemiluminescence intensities of the dots and ImageJ software was used to process the raw dot blot images. The microarray profile (http://image.bio.methods.free.fr/dotblot.html) plugin was utilized to subtract the background from the raw images. GraphPad Prism software was used to plot the graphs and fitting of the curves was performed using sigmoidal dose-response (variable slope).

9. Growing the drug resistant cell lines

The 100nM raltitrexed resistant K562 cell line (RX_step) was developed using the step wise increment strategy. The K562 cells were seeded on to a T75 flask and grown in complete RPMI media supplemented with 10% FBS, 100 units/mL penicillin, streptomycin and neomycin and non-essential amino acids. When the cells were about 20% confluent, they were treated with 10-20% IC_{50} of the drug. For the RX resistant cells, the treatment was started at a dose of 5nM and the dose was increased at every passage. The increase in dose was generally two-fold at each step. The cell viability was checked at each passage. If the cells were

susceptible to the drug (lot of dead cells floating, unhealthy morphology), they were put in drug-free media for recovery up to 2 weeks before the next treatment. The dose of RX was increased up to 100nM in a period of 9 months. The cell viability and growth curve experiments confirmed that the cells are resistant to 100nM RX.

The 1µM and 5 µM Raltitrexed resistant cells (RX_pulse (low) and RX_pulse (high) respectively and the 50 µM nolatrexed resistant cells were developed using the pulse strategy. The K562 cells were grown in a T75 flask in complete RPMI media supplemented with 10% FBS, 100 units/mL penicillin, streptomycin and neomycin and non-essential amino acids. When the cells were 50% confluent, they were treated with the corresponding drug at the specific concentration for 4 hours. After the drug pulse, the cells were washed thoroughly with PBS and grown in drug free media for a week. Growing the cells in complete media after drug treatment is termed as recovery. After 1 week recovery, the process of giving drug treatment/pulse and recovery in drug free media was repeated. The cell viability was measured before and after the drug pulse. After 6 months of this process, it was noticed that the cells became resistant to the particular drug dose used for pulse treatment.

10. Growth curve

The growth curve experiments were done on all the parent and resistant cell line pairs. For suspension cell lines (K562), the growth curve was studied by measuring the cell viability in the absence and presence of corresponding drugs, using a haemocytometer. For the adherent cell lines (HCC1806, HCT15), CellTiter-Blue® Cell Viability Assay (Promega) was used for determining the growth curve in the presence and absence of the respective drugs. The cells were grown at 37^0C in the presence/absence of the drug in a 96-well plate, at a final concentration of 1000 cells in 100 µl per well. 20µl of Celltiter-blue® reagent was added to each well and the plate was incubated again at 37^0C for 4 hours. The fluorescence values were measured using a plate reader (Tecan) at 560/590nm. The cell viability was measured from day1 to day 7 and the growth curve was plotted using the GraphPad Prism software.

11. CETSA experiments on the drug resistant cell lines

The following cell lines were obtained from the Resistant Cancer Cell Line (RCCL) collection (University of Kent): HCC1806 parent and 225nM Methotrexate resistant cell lines, HCT15 parent and 5FU resistant cell lines, A549 parent and Pemetrexed resistant cell lines.

The Methotrexate resistant cell lines were maintained in complete RPMI media containing 225nM Methotrexate. After confirming resistance by the growth curve, CETSA was

performed on these cell lines. The parent and resistant cells were treated with 225nM methotrexate/DMSO (diluent)/ 225nM folate for 1 hour and the melting profile of thymidylate synthase was compared across the cell lines. The $ITDR_{CETSA}$ of Methotrexate was studied at 50^0C for a concentration range of 50µM to 0µM (2- fold dilution) with a treatment time of 1 hour.

The RX_step cell line was maintained in 100nM Raltitrexed containing RPMI media. The RX_pulse (low) and RX_pulse (high) cell lines were treated once every week with raltitrexed doses 1 µM and 5 µM respectively. The CETSA melt curves of TS were studied in the resistant cells, at different stages of recovery in drug free media. The $ITDR_{CETSA}$ of Raltitrexed was measured in the resistant cells at different stages of recovery, at 50^0C for a concentration range of 50µM to 0µM (2- fold dilution) with a treatment time of 1 hour.

The 5FU resistant cell lines were maintained in complete RPMI media containing 16 µM 5FU. The CETSA melt curves of TS were studied in the resistant cells, at different stages of recovery in drug free media. The $ITDR_{CETSA}$ of 5FdU (the nucleoside version of 5FU) was measured in the resistant cells at different stages of recovery, at 50^0C for a concentration range of 0.5µM to 0µM (2- fold dilution) after 1 hour treatment.

12. Measurement of protein abundance levels using MS

The proteome profiling of the parent and resistant cells was done using mass spectrometry to compare the protein expression levels. 10 million cells from each condition were used for lysis. Kinase buffer was added and the cells were subjected to 3 freeze-thaw cycles using liquid nitrogen and mechanical shearing. Supernatant was harvested after centrifugation and the protein concentrations were estimated using BCA assay. 100µg of protein was taken from each set of cell lines for mass spectrometry. Sample preparation was done using the protocol described in the section ‘sample preparation for mass spectrometry’.

The peptide identification and intensities of the reporter ions for each peptide-spectrum match were taken from the MS/MS scans in to Proteome Discoverer 2.0. For the data normalization, the sum of protein abundance values across each channel, and mean of the sums were calculated. A scaling factor was generated for each channel using the following formula:

Scaling factor = (Mean of sums)/(Sum of abundance across each channel).

The abundance values in each channel was multiplied by the scaling factor. The ratio of abundance of each protein in the resistant cells relative to the parent cells was calculated to determine the fold change in expression levels.

13. Alphascreen detection of thymidylate synthase

Alphascreen detection was used to detect TS in the following cell lines:

- HCC1806 parent and MX resistant cell lines
- K562 parent, RX_pulse (low) and RX_pulse (high) cell lines
- HCT15 parent and 5FU resistant cell lines
- K562 parent and NX resistant cell lines
- A549 parent and PX resistant cell lines

The cells were harvested, washed twice with PBS and then re-suspended in PBS at a concentration of 10 million cells/ml. The compounds or diluents (5 µl) was added in to the wells of a 96-well PCR plate at the desired concentrations. 5µl (about 50,000 cells) was added to the PCR wells containing the compound or diluent and mixed well. The cells and compound/diluent were incubated at 37^0C for 60 to 90 minutes. The samples were heated at 50^0C using a Veriti thermal cycler (Applied Biosystems/Life Technologies) for 3 minutes and then cooled for 3 minutes at room temperature. The samples were lysed by adding 10µl alphascreen surefire lysis buffer (2.5X) (PerkinElmer) and pipetting up and down. The lysate was mixed thoroughly and 3µl was transferred to a 384 proxiplate (PerkinElmer). A reagent mix was prepared in 5X immunoassay buffer (PerkinElmer) with the antibodies, donor and acceptor beads. The 1.5X reagent mix contained 0.6nM of Santa Cruz mouse monoclonal anti-TS IgG, 1.5nM of Proteintech - rabbit polyclonal anti-TS IgG (15047-1-AP), 60 µg/ml anti-mouse IgG alpha donor beads (PerkinELmer) and 15 µg/ml of anti-rabbit IgG alphalisa acceptor beads (PerkinElmer). 6µl of reagent mix was added to the samples and the plate was incubated in the dark overnight. The alphascreen readings were taken using an Envision plate reader (PerkinElmer) and the curves were plotted using the GraphPad Prism software and fitted using the sigmoidal dose-response function (variable slope).

14. Reagents and cell culture for the thermal proteome profiling studies

The reagents were purchased from Sigma Aldrich unless otherwise stated. K562 cells obtained from ATCC were grown in RPMI medium (Invitrogen) supplemented with 10% FBS, 100 units/mL penicillin and streptomycin, non-essential amino acids, and 0.3g/L L-glutamine. The cells were expanded to 1 x 10^6 cells/ml before the experiments were performed.

15. Lysate-CETSA meltcurve/ITDR

The cells were harvested and washed with PBS and then re-suspended in 1X kinase buffer. The cell suspension was lysed as described earlier and the lysed sample was centrifuged at 4^0C at at 20,000xg for 20 min. For the lysate CETSA experiment, the metabolites or PBS (control) were added to the lysate to a final concentration of 1mM and the samples were incubated for 3 minutes at room temperature. The sample was aliquoted in to 10 parts for a 3-minute heat treatment at the desired temperature range. The samples were heated using a 96-well thermocycler and then cooled for 3 minutes at 4^0C. The heated and cooled samples were centrifuged at 4^0C for 20 minutes at 20,000xg and the supernatant was harvested and transferred in to fresh tubes for analysis using mass spectrometry or western blot. For the lysate $ITDR_{CETSA}$ experiments, a serial dilution of the metabolites was done in PBS before the addition of lysate. The samples were then aliquoted in to 10 parts for a 3-minute heat treatment at 52^0C using a 96-well thermocycler. The samples were then cooled for 3 minutes at 4^0C, centrifuged and the supernatant was extracted for further analysis using the above-mentioned techniques.

16. In-cell-$ITDR_{CETSA}$ experiments

The K562 cells were re-suspended in complete RPMI media and treated with a four-fold dilution range of dU, dC and dT with 20mM being the highest concentration of treatment. The treated cells were washed with PBS and heated for 3 minutes at 52^0C using a 96-well thermocycler. The cells were then cooled for 3 minutes at 4^0C and lysed using the above-mentioned procedure.

17. Sample preparation for mass spectrometry

BCA assay kit (Thermo Scientific) was used to determine the protein concentration in the supernatant after lysis. At least 100µg of the protein was used for further steps. The protein was reduced using 20mM TCEP and denaturated with 0.01% (w/v) rapigest (w/v) at 55^0C for 20 minutes. The protein was then alkylated with 55mM CAA for 30 minutes at room temperature (in the dark). The samples were incubated for 3 hours with LysC followed by trypsin digestion overnight at 37^0C. Rapigest was hydrolyzed after the digestion step using 1% TFA at 37°C for 45 min. The samples were centrifuged at 4^0C for 10 minutes at 20,000xg, the supernatant was taken in to new tubes and dried using a centrifugal vacuum evaporator. The samples were then solubilized at a concentration of 1µg/µl using 100mM TEAB. Tandem Mass Tags -10plexTMT, (Pierce) was used to label 25µg of the protein. High pH conditions

were maintained during the labeling with 100mM TEAB and the labeling was carried out for 1 hour at room temperature. After labeling, the samples were quenched with 1M Tris, pH 7.4. Desalting of the labeled samples was performed using a C18 Sep-Pak (Waters) cartridge. The desalted samples were then pre-fractionated using a High pH reverse phase Zorbax 300 Extend C-18 4.6 mm x2 50mm (Agilent) column and liquid chromatography AKTA Micro (GE) system in to 96 fractions. These were then pooled into 20 fractions.

18. LC-MS analysis

After the pre-fractionation step, the samples were dried using a centrifugal vacuum evaporator. The 20 pooled fractions from each experiment were used for MS-analysis using reverse phase liquid chromatography Dionex 3000 UHPLC system along with Q Exactive mass spectrometer (Thermo Scientific). A 50cm x 0.75mm Easy Spray column (Thermo Scientific) was used to separate each fraction at an 80 minute-gradient 0.5% CH3COOH in water (solvent A) and 80% MeCN, 0.5% CH3COOH in water (solvent B). The data acquisition parameters used were data dependent acquisition (DDA) with survey scan of 70.000 and AGC target of 3e6, isolation window of 1.6 m/z, AGC target of 1e5 and Top12 MS/MS 35000. Proteome Discoverer 2.0 software (Thermo Scientific), Sequest HT (Thermo Scientific) and Mascot 2.5.1 (Matrix Science), along with HHV4 Uniprot database (88559 entries) were used to generate the peak lists of subsequent searches. The search parameters used were: MS/MS 0.06 Da, 3 missed cleavages, MS precursor mass tolerance 30ppm; Variable modifications: Oxidation (M), Acetyl N-terminal protein, Deamidation (NQ); Static modifications: Carboamidomethyl (C). The false discovery rate was estimated in two levels: medium= FDR 5% and strict = FDR.

19. Quantification of protein and CETSA data processing

The peptide identification and intensities of the reporter ions for each peptide-spectrum match were taken from the MS/MS scans in to Proteome Discoverer 2.0. The protein abundance quantification was performed by using only unique peptides. An in-house R script (https://www.r-project.org/) was developed by our CETSA team for processing the data. The protein groups with the quantification information were exported into the R script for the extraction of data, data cleanup, normalization, curve fitting and plotting.

For the CETSA melt curves, the lowest temperature condition (37^0C) was used as a reference with a constant value of 1. The protein fold changes across the heating temperature range were quantified using this reference point. The normalization of the data was performed by

including the proteins commonly identified in the control and compound-treated datasets. These proteins contributed to the calculation of the global mean.

For normalizing the data, a fitting factor was calculated from each dataset. The median fold changes of all proteins were calculated at each of the ten temperatures. The overall melting profile of the whole proteome was represented by fitting all these median values into a sigmoidal curve. The ratio of the fitted median value to the original median value at each of the ten temperatures was calculated to determine the ten-element fitting factor. A four-parameter log-logistic nonlinear regression model was used for curve fitting utilizing the LL.4() function from the R package 'drc':

$$f(T) = c + \frac{d - c}{1 + e^{b(\log(T) - \log(e))}}$$

Where, T= temperature, f(T) = fold change value, b, c, d and e = constants that represents slope, lower limit, upper limit, and Tm value, respectively.

A scaling factor was calculated to adjust the differences in the baselines between the experimental conditions. The scaling factor was defined as the factor that should be multiplied with the fitted median value at the lowest temperature point, to obtain a constant value of 1. The ten-element vector of normalization factors were generated by multiplying this scaling factor to each element in the vector of fitting factors. The respective normalization factors were applied to the protein fold change values at each temperature to achieve data normalization. LL.4() function was used to fit the CETSA melt curves of the proteins and the curves were plotted in a multiplot style for simple inspection.

20. Dose response curve fitting and analysis of the ITDR$_{CETSA}$ experiments

The fold changes in the proteins across the different doses of treating compound were determined by using the sample treated with the lowest dose (0 mM) as reference. The fold-change value of a protein in each condition was divided by the median fold-change values of all proteins in that condition, to achieve the global normalization of the data. The change in the protein stability due to compound treatment is represented by the fold change in an ITDR$_{CETSA}$ experiment. The baseline variance from each experiment was determined to understand the fold-change cut-off for the selection of hits. The baseline variance was estimated by applying the median absolute deviation (MAD) scheme on the lowest three concentrations of all the proteins that are quantified. The protein fold-change value at the

highest dose sample was required to be at least 30% different from the lowest dose point, for any proteins to be validated as hits with stabilization or destabilization. Also, it was essential for the sigmoidal curve fitting to possess an R^2 of at least 0.8 and the protein identified to have more than three peptide spectrum matches (PSMs).

21. Euclidean distance-based scoring strategy to prioritize potential targets

A Euclidean distance (ED) score was generated for each protein in the dataset to quantify the thermal shift and the reproducibility of the replicates. The following formula was used to calculate the ED between two CETSA melt curves.

$$ED = \sqrt{\sum_{i=1}^{10} \left(f_1(T_i) - f_2(T_i)\right)^2}$$

Where, f_1T_i and f_2T_i are the protein fold-change values of melt curves 1 and 2 respectively, both at temperature T_i.

The shift between the compound-treated protein melt curve and the vehicle-treated melt curve is indicated by the sum of inter-treatment Euclidean distance (EDinter−treatment). The reproducibility of the melt curves in the replicate runs is indicated by the sum of inter-replicate Euclidean distance (EDinter−replicate). The reproducible shifts of the melt curves in replicates was determined by calculating the EDS using the following formula.

$$EDS = \frac{\sum ED_{inter-treatment}}{10^{\sum ED_{inter-replicate}}}$$

Larger EDS denotes proteins demonstrating reproducible shifts in the melt curves relative to the control. These proteins are considered as potential hits targeted by the compound.

CHAPTER 3: RESULTS

The aim of this work is to explore the potential of CETSA for different applications mainly, studying drug resistance development during cancer treatment, for high throughput fragment screening (using TPA) and to study the interactions of metabolites with the human proteome. The results from these studies are presented in this section.

1. Thermal precipitation Assay - a method derived from CETSA for fragment screening

Fragment-based drug design is an effective technique for the identification of lead compounds in drug discovery. The fragment-based drug design starts with the identification of highly soluble fragments, which are low molecular weight compounds that generally bind with weak affinity to the target of interest. Still, fragments often form high quality interactions and can in subsequent steps be optimized to lead compounds with high affinity and selectivity. Despite the big potentials of the technology, experimental methods for fragment screening often suffer several challenges such as low throughput, high cost of instruments and experiments, high protein and fragment concentration requirements.

Based on the principle of CETSA, we have introduced the thermal precipitation assay (TPA) as a highly sensitive screening assay for high throughput fragment screening, at a very low protein concentration, using simple and inexpensive equipment. For TPA, as well as other biophysical assays detecting protein-ligand interactions (discussed in the Introduction) purified proteins are used.

The proteins are produced in recombinant expression systems with the addition of a purification tag, for example the His-tag. TPA uses tag specific probes or antibodies for the detection of the protein of interest, hence can be used to detect large number of proteins. An advantage is that due to its high sensitivity, TPA screening can be done at a very low protein concentration (0.01 mg/ml), as compared to DSF and DSLS (0.2 mg/ml in both the cases) (Table 1) (Figure 30). TPA is derived from CETSA and this similarity makes it very easy to screen the TPA hits in a cellular context, using CETSA.

Table 1: Comparison of TPA, DSF and DSLS

Method	Protein concentration (mg/ml)	Reaction Volume (µl)
TPA	0.01	25
DSF	0.2	25
DSLS	0.2	45

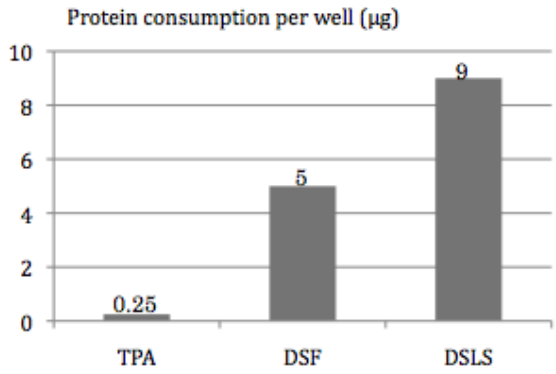

Figure 30: Comparison between TPA, DSF and DSLS

Protein consumption per well for TPA is 20 times less than DSF and DSLS.

TPA is essentially a DSLS experiment inversed and is based on the principle that when a protein is subjected to thermal stress, it unfolds and aggregates (Figure 31). DSLS measures the protein that aggregates due to heating, while TPA quantifies the soluble fraction of protein that survives.

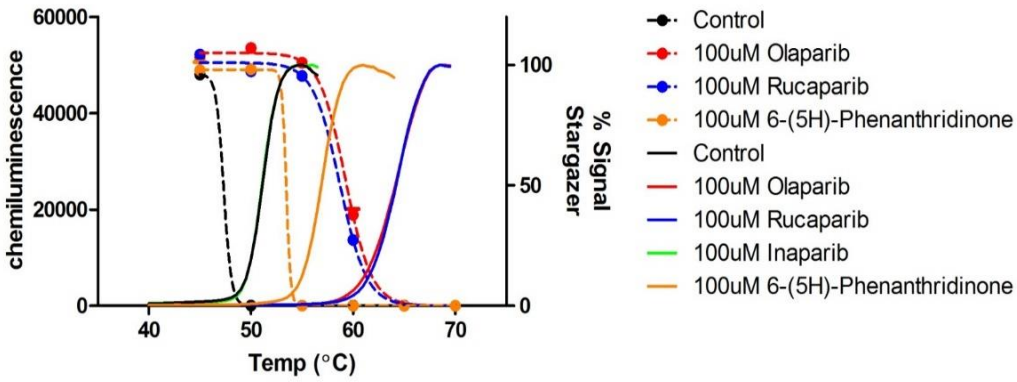

Figure 31: DSLS vs. TPA

Comparison of thermal shifts of purified hPARP-1, from the DSLS light scattering

experiment and the CETSA process. The top graph shows an overlay of melting curves of hPARP-1. Two experiments on purified protein were performed in the same buffer using DSLS (solid lines) and TPA experiment (symbols and dashed lines) with a set of PARP-1 inhibitors.

This data showed that the drop-in signal in the TPA experiment follows the increase of DSLS signal (which monitors the light scattering of the aggregates formed upon precipitation)
The increase in the level of protein in the soluble fraction is an indication of the factors that are stabilizing the protein, for example: fragments binding to the protein, buffer and pH conditions. The initial fragment hits can then be validated by testing for its dose dependent binding to the target protein. This can be done by treating the target protein with different doses of the hit compound and subjecting it to isothermal stress.
We used TPA for the following applications.

Table 2: Summary of targets screened using TPA

Protein	Experiment	Detection	Matrix
IDH1	metal ion effect on isocitrate recognition.	His probe	Buffer
***h*CA 2**	Fragment screen	His probe	Buffer
***h*TNKS 2**	Fragment screen	His probe	Buffer
***h*PARP1**	Fragment screen	His probe	Buffer
***h*PARP1**	Fragment screen	Bradford	Buffer
***h*PARP1**	Fragment screen	His AB	Cell lysate

1.1 Fragment screening of hPARP1 using TPA

The protein poly ADP-ribose polymerase 1 (PARP1) is an important cancer therapy target. PARP1 initiates single stranded DNA breakage in cancer cells and thus lead to the cancer cell survival. PARP1 inhibitors are considered as treatment for several forms of cancers (Figure 32).

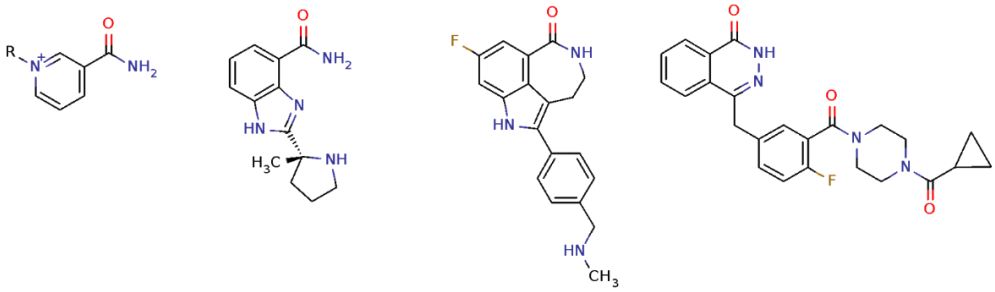

Figure 32: Known binders of PARP1

Nicotinamide moiety in NAD+, ABT-888, Rucaparib and Olaparib.

The different steps involved in the fragment screening of hPARP1 using TPA are described below.

1.1.1 Determining the melting temperature of hPARP1:

The first step was to determine the melting temperature of the protein when subjected to thermal stress. We used 6-(5H)-phenanthridinone (100 µM), the known hPARP1 inhibitor as a tool compound, to observe thermal stabilization. The protein was heated with and without the presence of phenanthridinone, over a temperature range of 40^0C to 65^0C for 20 minutes. We observed that the protein aggregates around 50^0C in the untreated sample. The melt curve showed 5-degree stabilization upon treatment with 6-(5H)-phenanthridinone (Figure 33).

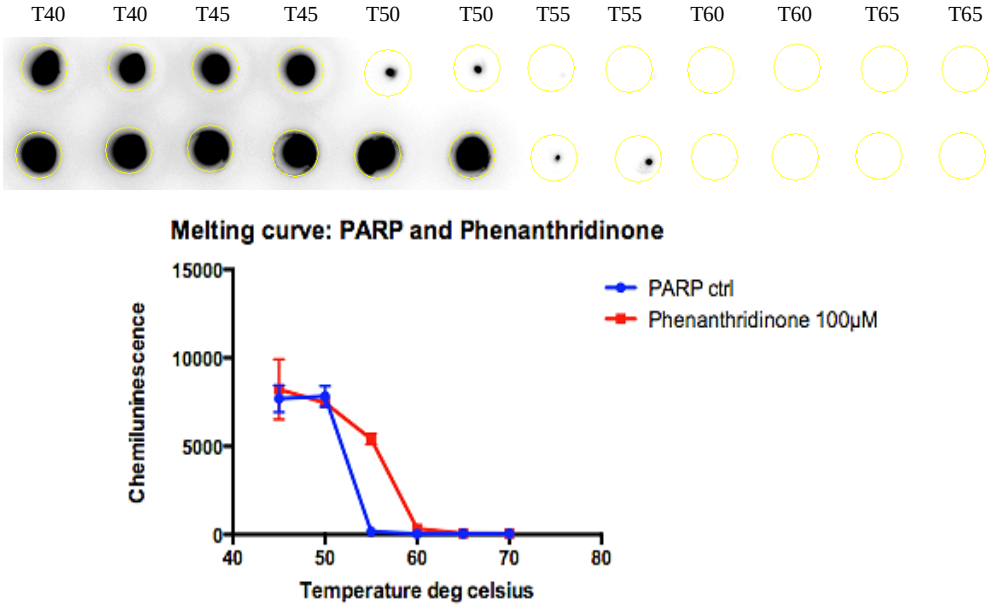

Figure 33: PARP1 melt curve

Melting curve of PARP1 in the absence and presence of tool compound 6-(5H)-phenanthridinone (100 µM). Data is representative of two technical replicates from single experiment.

1.1.2. Isothermal denaturation:

The selection of screening temperature is very important to acquire meaningful data because proteins have distinct melting temperatures. The assay becomes insensitive for weakly stabilizing compounds at high temperature, as only strongly stabilizing compounds can rescue any protein from unfolding. The assay becomes noisy when the temperature is set low as even weakly stabilizing compounds will rescue nearly 100% of the protein. Optimization should therefore be done prior to screening to find the suitable temperature. The dose dependent titrations of a positive control can be performed at different temperatures, to establish good experimental conditions. From this data, it is easy to judge the best condition for sensitivity (where the lowest concentration can be detected) and dynamic range. The dose response of phenenthridinone at six different temperatures showed that 51^0C is a good temperature for screening (Figure 34).

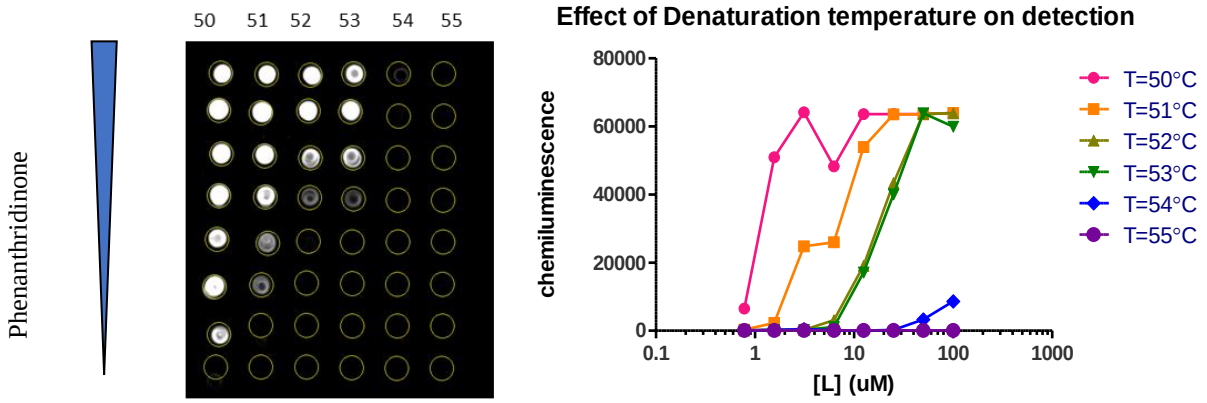

Figure 34: Dose response titrations of 6-(5H)-Phenanthridinone

Dose response of positive control compound 6-(5H)-Phenanthridinone, at six different temperature points.

1.1.3. Isothermal fragment screening and validation of hits:

We performed isothermal fragment screening of hPARP1 at 51^0C. The in-house fragment library, comprising 500 compounds was screened at 1 mM, to determine the hits stabilizing hPARP1. The format of screening was 80 compounds and 16 controls per screening plate and 7 plates were screened in total. We used the dose response titration of 6-(5H)-phenanthridinone in the first and last columns of the screening plate as the control (Figure 35).

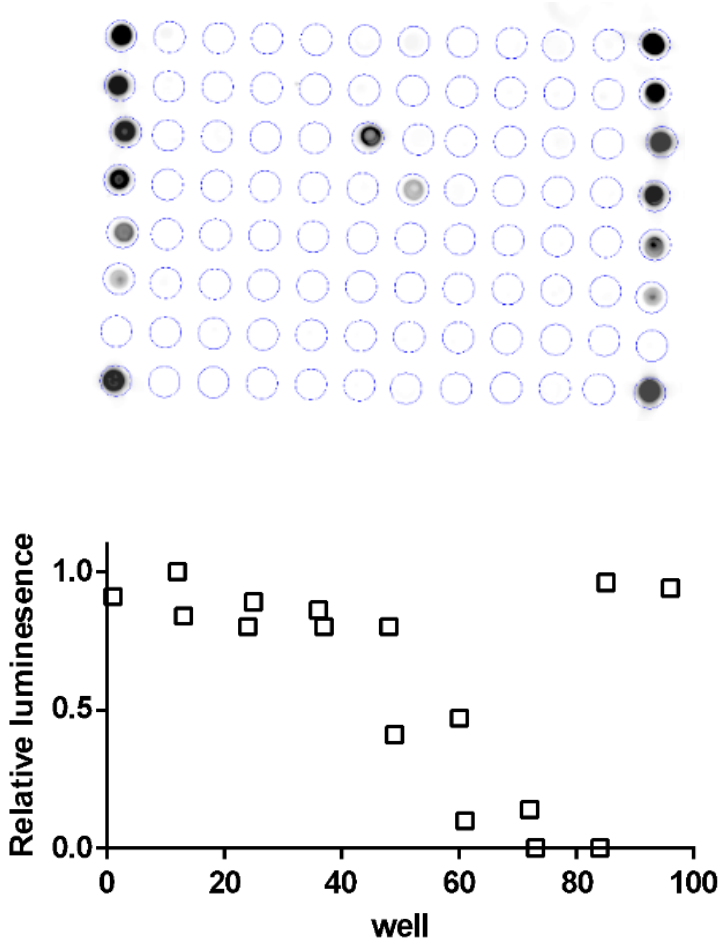

Figure 35: Format of fragment screening

Dose response of 6-(5H)-phenanthridinone used as control, with the highest dose in the corner wells of the plate. Hits picked by visual inspection for further validation.

The first-round positives can be chosen from the screen by visual inspection, for further validations. We used imageJ software to quantify the dot blots in cases where numerical analysis was required.

The isothermal fragment screening of hPARP1 was performed in two different matrices: hPARP1 in buffer and with recombinant protein added to *E. coli* lysate and the hits identified were compared. A high overlap was observed for the hits in the two screens. This overlap shows that TPA can be used for screening purified proteins as well as over-expressed, unpurified proteins in lysates, which enables it to screen low expressing targets that are hard to purify. The positives from the primary screens were subsequently validated internally by checking the dose dependent stabilization effects (Figure 36).

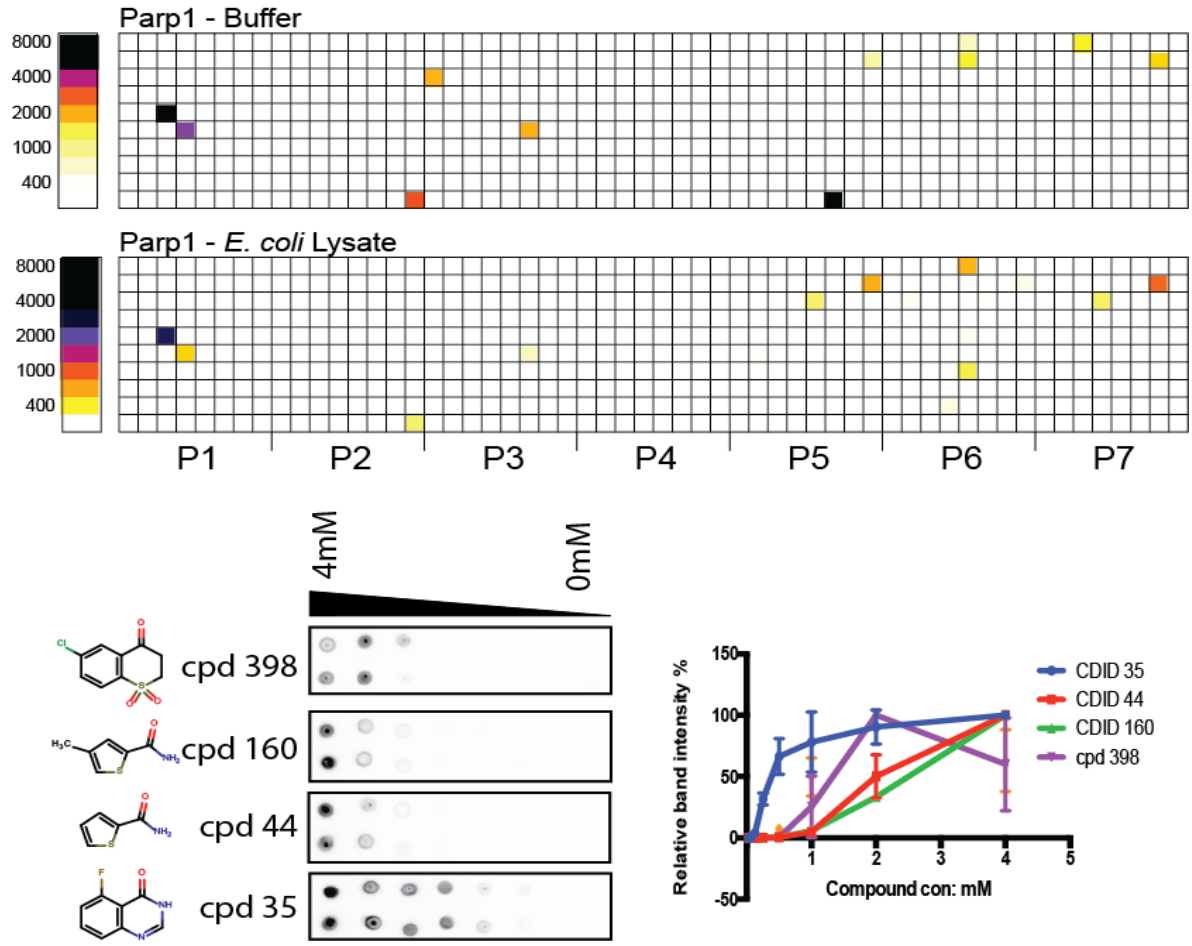

Figure 36: Isothermal fragment screening of hPARP1

Fragment screening of hPARP1, in buffer and *E. coli* lysate at 51^0C. Hits validated internally by checking for dose dependent stabilization effects. The dose response data is representative of two technical replicates from single experiment.

1.1.4. CETSA on the TPA hits from PARP1 screen:

The two prominent hits obtained from the fragment screen of PARP1 using TPA are the compounds 35 and 44. We wanted to understand if these compounds could show target engagement of PARP1 in cell lysate. For this, we carried out a CETSA melt curve experiment in HeLa lysate and looked at protein PARP1 using western blot detection (Figure 37). Both the compounds showed stabilization in the protein melting temperature.

Compound 35

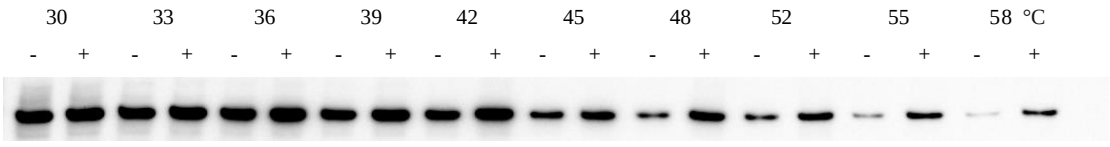

Compound 44

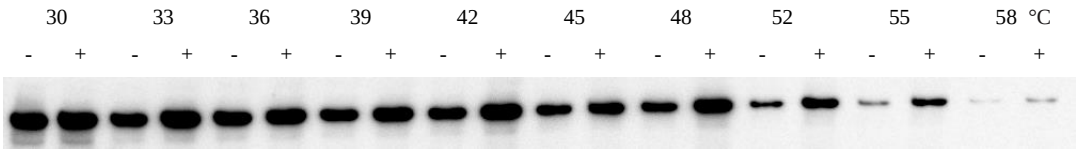

Figure 37: PARP1 melt curve in HeLa cell lysate

Melt curve of PARP1 in HeLa cell lysate in the absence and presence of treatment with compounds 35 and 44.

1.1.5. CETSA to validate PARP1 and inhibitors:

CETSA is an effective tool to validate clinical drug targets before performing clinical trials. To demonstrate this, we used the protein Poly ADP-ribose polymerase (PARP1) and inhibitors olaparib and iniparib. Iniparib, the proposed PARP1 inhibitor got in to phase III clinical trials and it was found inactive against PARP-1 in cells [75]. The CETSA results showed that olaparib, the well-validated PARP-1 inhibitor, showed stabilization in the protein-melting curve, while iniparib failed to induce a shift (Figure 38A). The $ITDRF_{CETSA}$ result for both the compounds supported the results, olaparib showed dose dependent behavior while iniparib did not (Figure 38B).

A B

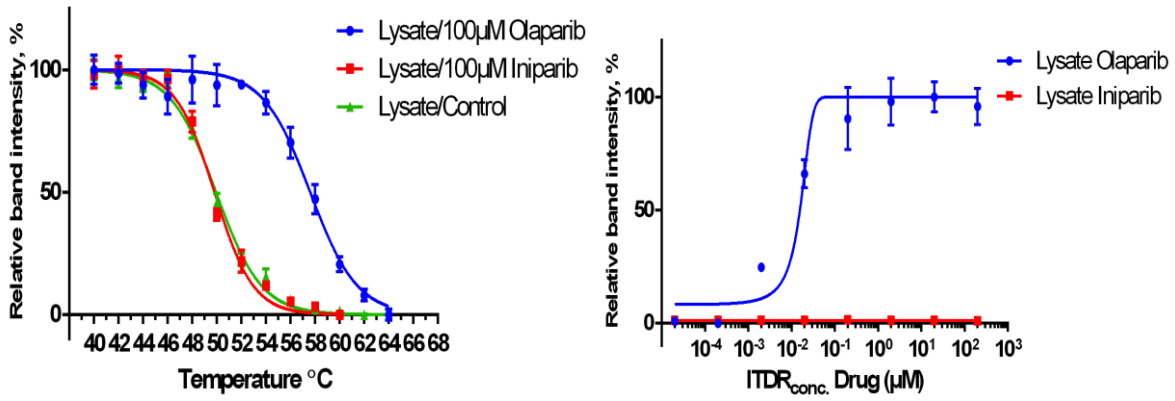

Figure 38: PARP1 CETSA melt curves in lysates

Melt curves of PARP1 with the inhibitors olaparib and iniparib (A) and the corresponding $ITDRF_{CETSA}$ at 50°C (B) [75]. The data is representative of three technical replicates from single experiment.

1.2 Fragment screening of hTNKS2 using TPA

We used TPA to screen Tankyrase 2 (hTNKS2) (Figure 39). hTNKS2 is a target that has been screened before using DSF [127]. The two compounds 12 and 495 were validated using dose response and compound 495 eventually evolved in to a 12nM inhibitor of hTNKS2. Both these compounds were detected in the TPA screening, in addition, two more compounds 149 and 489 emerged as hits which were validated using TPA.

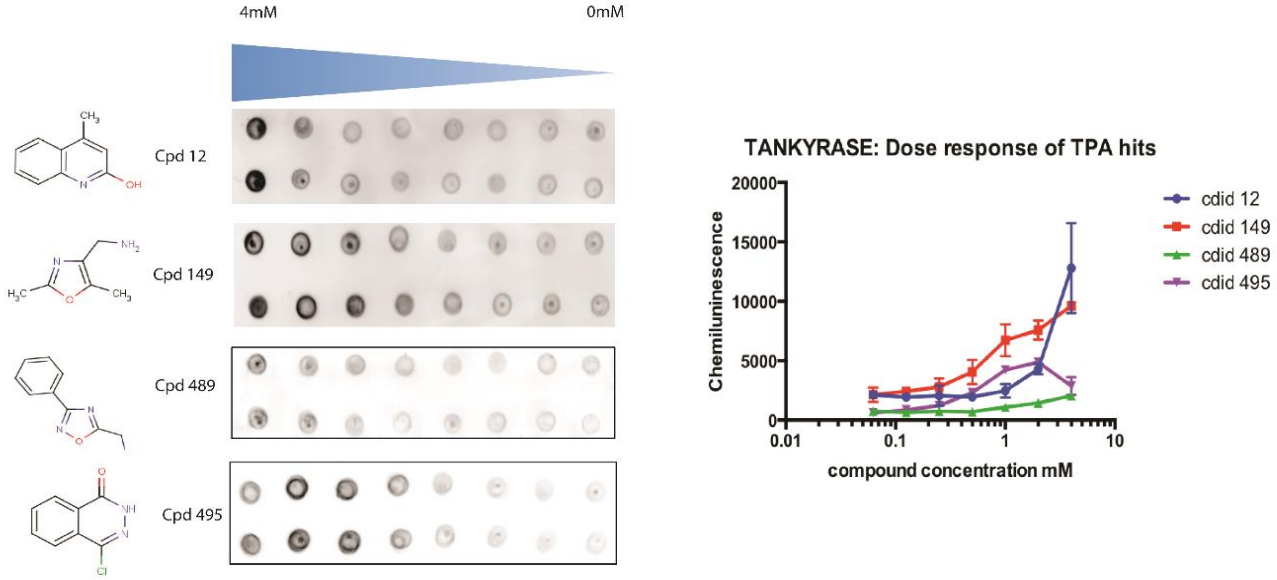

Figure 39: Validation of TPA hits from hTNKS2 screen

Hits from the screen showed dose dependent stabilization effects upon testing by TPA. The dose response data is representative of two technical replicates from single experiment.

1.3 Fragment screening of hCA2 using TPA

Carbonic anhydrase (hCA2) is an enzyme containing zinc that catalyzes the reversible hydration of carbon dioxide. This enzyme is the target for drugs, such as acetazolamide, methazolamide, and dichlorphenamide, which are used for the treatment of glaucoma. We screened hCA2 using TPA and validated the six hits from the screen by doing dose response experiments (Figure 40).

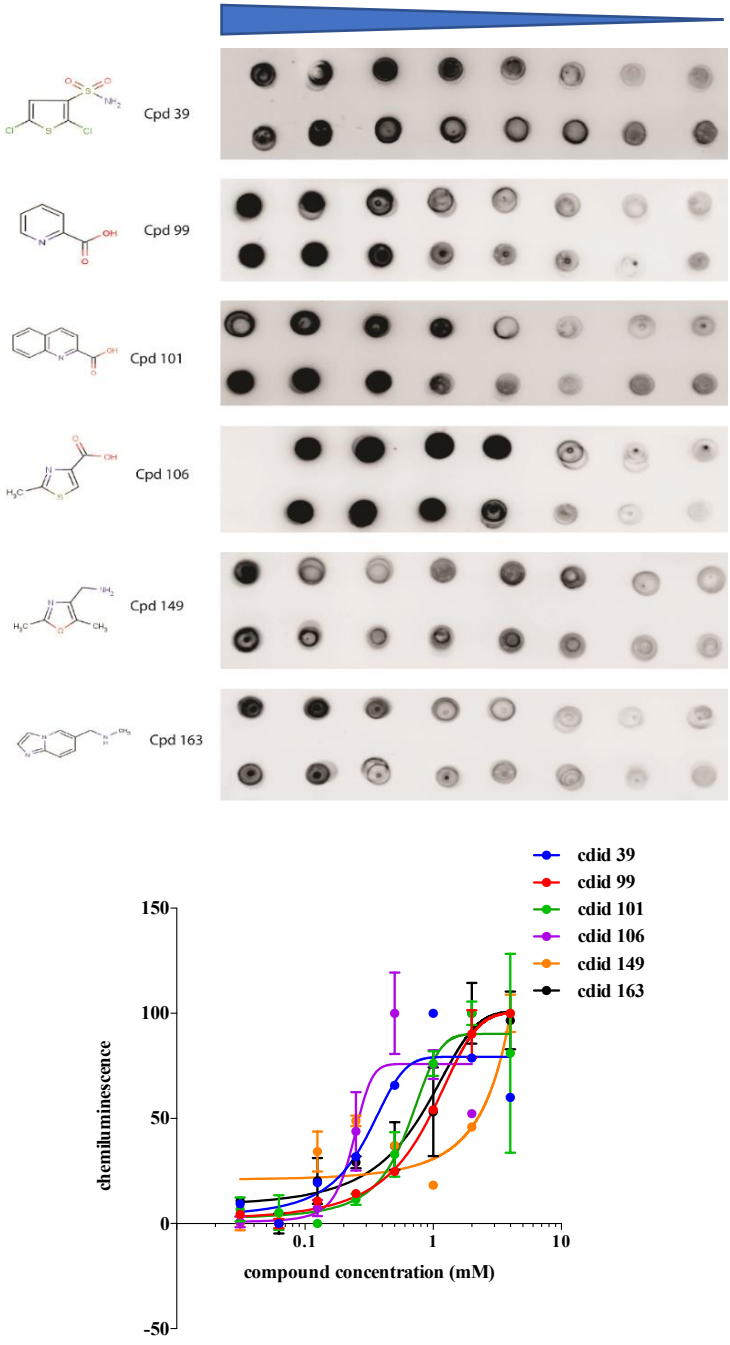

Figure 40: Validation of TPA hits from hCA2 screen

Hits from the screen showed dose dependent stabilization effects upon testing by TPA. The dose response data is representative of two technical replicates from single experiment.

1.4 Hits from TPA vs. DSF and DSLS

The hits found with TPA when compared to those found with DSF and DSLS showed a strong correlation. We used TPA to rescreen targets that were screened using DSF previously. The hit profiles were essentially identical for the stronger stabilizing hits with minor variation for the weaker ones closer to the detection threshold (i.e. ΔTm lower than 0.8^0C in DSF). For example, hTNKS2 gave 2 hits when screened previously using DSF. The same two compounds emerged as major stabilizers in the TPA screen as well. The hits from the TPA screen of hPARP1 when validated using DSF and DSLS, showed correlation (Figure 41).

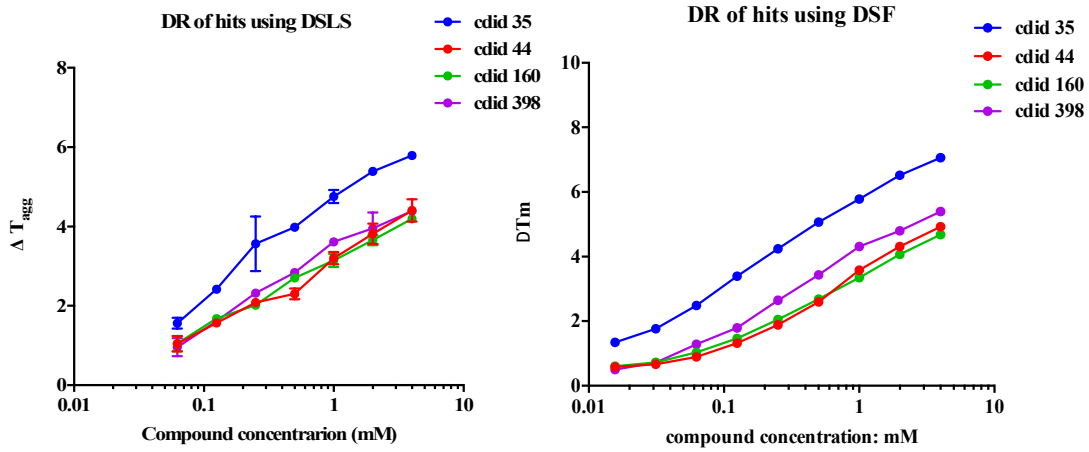

Figure 41: Dose response of the TPA hits of PARP1 using DSLS and DSF

All the 4 compounds showed dose response behavior upon screening by DSLS and DSF. The DSLS data is representative of two technical replicates from single experiment.

1.5 Melting curve of thymidylate synthase in different matrices

We used TPA to compare the melting profile of the protein thymidylate synthase in the presence of TS inhibitor raltitrexed (RX) in different conditions: buffer, *e-coli* lysate and mammalian cell lysate. The results showed good correlation to DSLS results. (Figure 42).

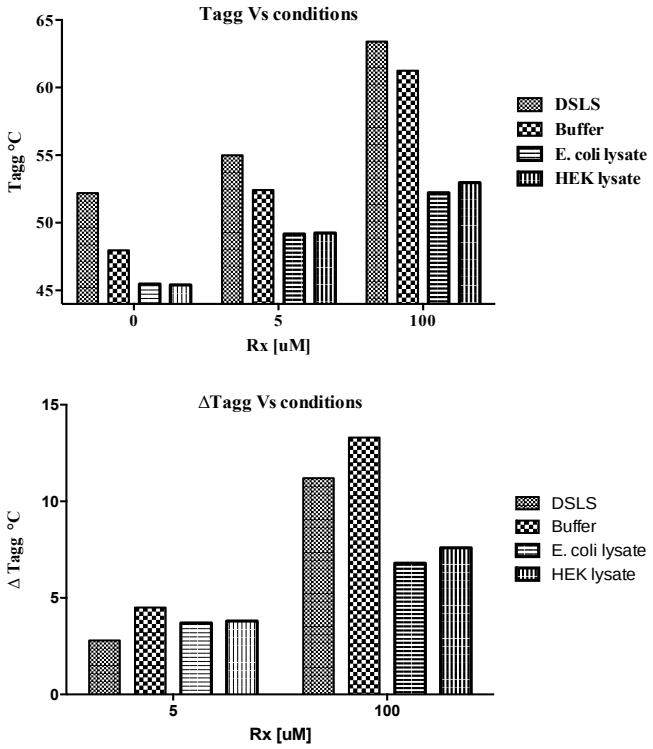

Figure 42: Tagg and ΔTagg of TS with and without raltitrexed in different conditions

Tagg of TS in buffer, e-coli lysate and mammalian cell lysate, when treated with different concentrations of RX (above). Shift in the Tagg of TS (represented as ΔTagg) when treated with different concentrations of RX (below). The results when compared to DSLS (stargazer) results, showed good correlation.

1.6 Assay dynamic range considerations and ligand depletion effects

Ligand depletion is an important factor to consider when performing measurements on interacting pairs with affinity close to the concentration of the protein. Ligand depletion refers to the bulk concentration of the added ligand changes upon equilibrium binding. The effect of ligand depletion happens in assays where the protein concentration is within an order of magnitude of Kd. To study the ligand depletion effect using TPA, we performed an experiment using hPARP1 at various concentrations and the drug olaparib (Kd 4nM) in dose response (Figure 43). We observed that to see binding at low concentrations of olaparib, correspondingly low concentration of PARP1 should be used. This comes at the expense of signal-to-noise but, it allows better ranking of high affinity compounds. Ligand depletion is important when observing high affinity interactions where the Kd of the compound is close to the protein concentration. In instances where Kd of the compounds is greater than the protein

concentration it is not a problem observing lower affinity interactions. Hence for fragment screening, normally perused at high compound concentration, ligand depletion is not an issue.

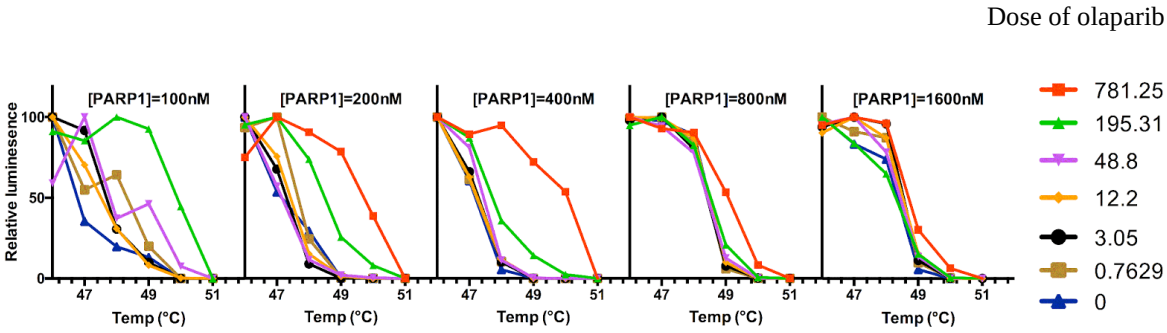

Figure 43: Study of ligand depletion effects by TPA

Ligand depletion effects in action and effect of protein concentration to observed thermal shifts showcased by melt curves of increasing concentrations of PARP1 (left to right) vs. dose response of olaparib (colors).

1.7 TPA to study the effect of metal ions on isocitrate recognition

Isocitrate dehydrogenases catalyze the oxidative decarboxylation of isocitrate to 2-oxoglutarate. We studied the effect of metal ions on the recognition of the substrate isocitrate by IDH1 using TPA (Figure 44). The metal ions Ca2+, Mg2+ and Mn2+ were tested. The metal ion concentration was kept constant at 2mM and a dose response of isocitrate was performed. We observed that in presence of the metal ions, the substrate recognition was better. Out of the three metal ions tested, Mn2+gave the isocitrate response even at much lower concentration.

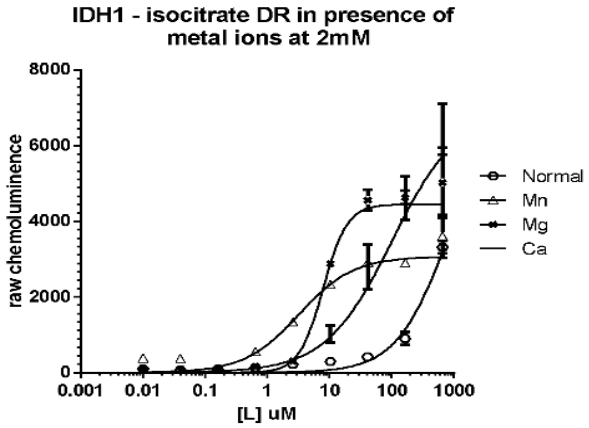

Figure 44: Effect of metal ions on isocitrate recognition

Mn2+ showed isocitrate response at a lower concentration as compared to the other metals. The data is representative of two technical replicates from single experiment.

1.8. Factors to consider while performing TPA

Heat challenge:

During the method set up and validation, heat challenge should be performed using a PCR machine to generate reproducible protein melt curves. The optimal protein concentration and temperature for isothermal fragment screening could be determined from the melt curves. A water bath could be used for heating the plates while doing isothermal fragment screening, which has the benefit of enabling parallel heating of many plates. The work and time required to screen one or multiple plates is the same if we use dot blot for detection. It is possible to screen six to eight plates per day with this approach and therefore, the method works well for high throughput screening applications.

Detection methods:

Quantification of proteins can be done in many ways (Table 3). We found that using antibodies or probes targeting the purification tags on the target is the effective way to get the best balance between sensitivity, quality, generic applicability and throughput. This does not require any expensive equipments or reagents and it also eliminates the need of expensive protein specific antibodies. Also, this produces little or no compound interference during screening.

Other detection assays such as bradford was tested and, it was found that this assay can be used for applications such as buffer screening and protein melting point determination. However, we observed that this assay when used for fragment screening interferes with the compounds, which makes it not suitable for screening applications. For example, bradford assay was used to screen hParp1 and the hit rate was significantly higher when compared to screening using western blot procedure. During further evaluation, we found that the new hits gave signal even without protein and this was due to the compound interaction with the Bradford reagents.

Table 3: Comparison of the different detection techniques used for TPA

Detection method	Compound screening	Matrix	Sensitivity	Speed[#]
Tag AB	Yes	Lysates, Buffer	++++	+
His Probe	Yes	Buffer	+++	++
Bradford	No	Buffer	++	+++

Ways to increase the throughput of screening:

The setup described above with 96-well filtration plates can be used to screen a fragment library consisting of 500 to 1500 compounds. This can be done in two to three days using very little protein. To increase the throughput of this biophysical assay, other techniques for performing filtration set up was investigated (Figure 45) (Table 4). One possible way of improving the throughput is to use the 384-well filter plate. Another way is to combine the filtration and blotting steps using sandwich blotting, by stacking a filter paper and membrane in a sandwich.

It was observed that if the sample is applied individually on the filter-membrane sandwich it worked well but, the usage of multichannel pipette for sample application gave inconsistent results due to small but significant variation of tip-length.

However, vacuum assisted filtration-blotting through sandwiched filter membrane using a commercial micro plate vacuum manifold worked well and allowed much smaller volumes to be used in comparison to the use of filter plates.

These are the significant improvements that can be made on the thermal precipitation assay.

Table 4: Comparison of different filtration methods

Filtration method	Requires plates	Multichannel	Volume
Filtration plate	Yes	Yes	15uL
Sandwich blot	No	No	2uL
Vacuum manifold	No	Yes	6uL

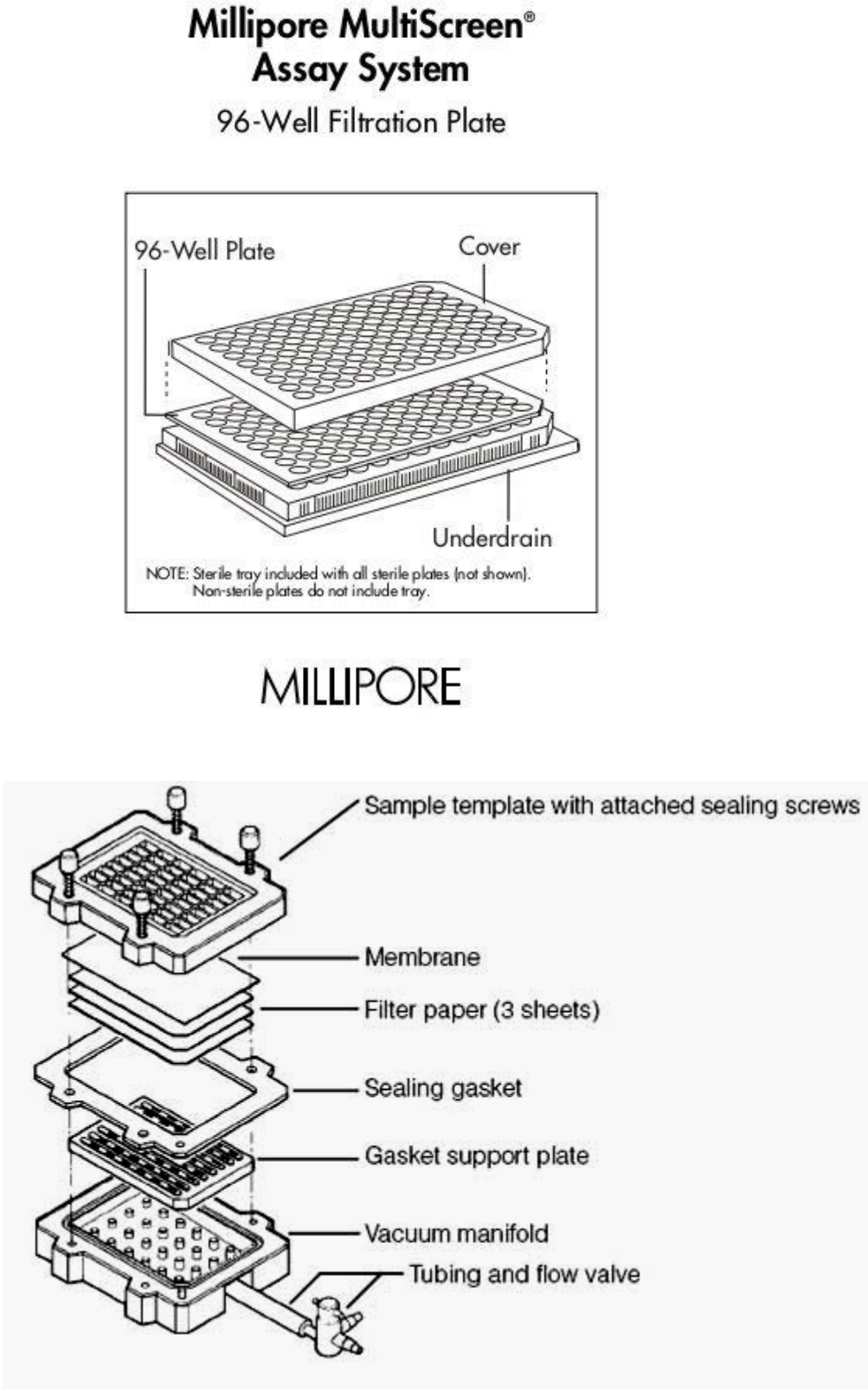

Figure 45: Different filtration methods

Filtration using 96 well filter plates (A) [www.millipore.com] and vacuum manifold (B) [www.bio-rad.com].

Problematic proteins:

It has been previously shown that DSF and DSLS work individually and to some degree complimentary for approximately 80% of tested proteins. Particularly problematic proteins for TPA and DSLS are proteins that are stable or meta-stable in solution even after unfolding (i.e. their unfolding is not immediately followed by aggregation and precipitation). Such samples are challenging to study using DSLS or TPA and can typically be identified by a strong protein concentration dependence of their Tagg.

2. CETSA to study drug resistance development during cancer therapy

Using cellular thermostability screening CETSA, protein stabilization in cell lysate, whole cells and tissues can be monitored. This enables monitoring of target engagement at a much earlier stage in drug discovery.

We studied the active transport of the antifolate drugs using CETSA. We compared the CETSA melt curve of TS with RX in K562 lysate and K562 whole cells (Figure 46). TS melt curve in the whole cells showed more stabilization upon RX-treatment, even though the concentration of RX used for treating the cells (10 μM) was much lower than that used for treating lysate (100 μM). This is due to the active transport and polyglutamation events of RX in the cells. We performed the same experiment using NX and the CETSA melt curve of TS with nolatrexed showed more stabilization in K562 lysate as compared to the whole cell (Figure 47). This demonstrates that no active transport is involved in the transport of nolatrexed in to the cells.

Thymidylate synthase and raltitrexed (RX)

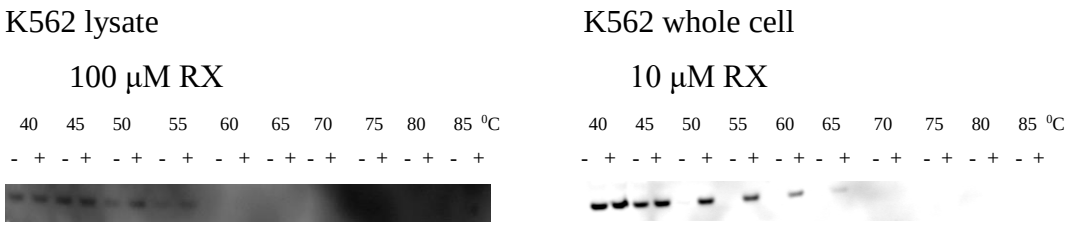

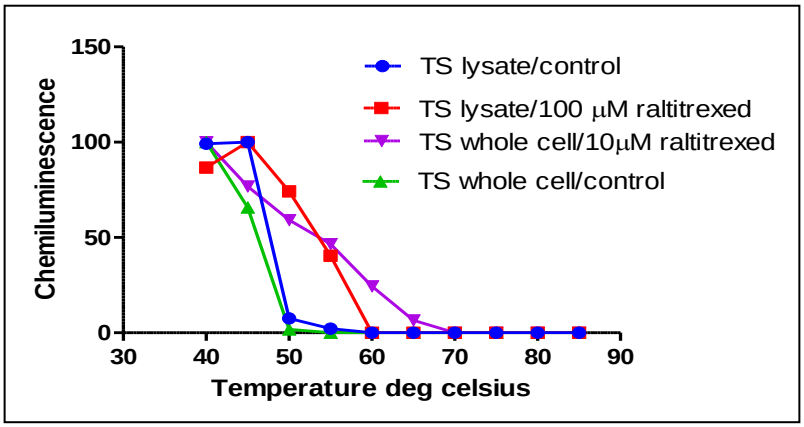

Figure 46: CETSA melt curve of thymidylate synthase with RX

Melt curve of TS in presence of inhibitor RX, in K562 lysate, K562 whole cell and comparison of the two melt curves.

Thymidylate synthase and nolatrexed (NX)

K562 lysate

100 μM NX

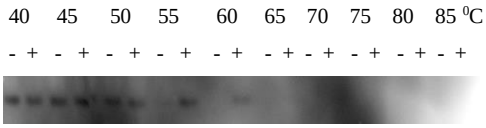

K562 whole cell

10 μM NX

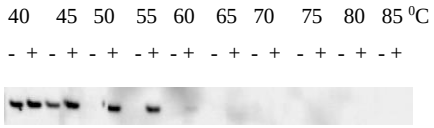

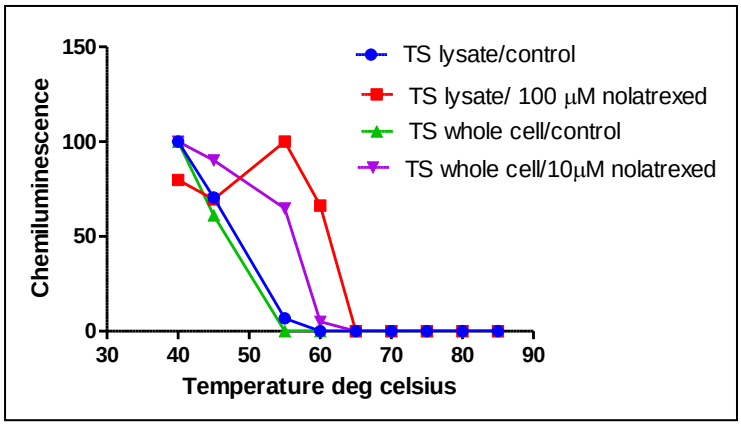

Figure 47: CETSA melt curve of thymidylate synthase with NX

Melt curves of TS with NX in K562 lysate, K562 whole cell and comparison of the two melt curves.

These processes of drug transport and activation are often involved in drug resistance development during chemotherapy. Therefore, these studies showed that CETSA can be used to study drug resistance development.

Drug resistance development is one of the major hindrances to successful cancer therapy. We have explored the potential of CETSA to study drug resistance development in cancer therapy. We developed drug resistant cell lines in the lab using step-wise drug concentration increment technique (called *step* in the following) and pulse strategy and also obtained some resistant cell lines from a cell repository. In the study, we compared parental and resistant cell lines for different antifolate and fluoropyrimidine cancer drugs. We applied CETSA on the drug-resistant cell lines and the corresponding parent cell lines to study whether CETSA can help in monitoring resistance development and eventually shed light on the processes responsible for resistance development.

The drug-resistant cell lines used for this project are given in the table 5.

Table 5: List of drug resistant cell lines

Serial No:	Name	Cell line	Drug	Concentration
1	MX resistant	HCC1806	Methotrexate	225 nM
2	RX_step	K562	Raltitrexed	100 nM
3	RX_pulse (low)	K562	Raltitrexed	1 μM
4	RX_pulse (high)	K562	Raltitrexed	5 μM
5	5FU Resistant	HCT15	5Fluorouracil	16 μM
6	NX Resistant	K562	Nolatrexed	50 μM

2.1 Growth curve

We performed a growth curve experiment after the parent and resistant cell line pair had been developed or obtained. For this, the parent and resistant cell lines were grown in normal cell culture media supplemented with FBS without the presence of drug and in media containing the dose of corresponding drug to which the cell lines are resistant to. The cell viability was then measured in the presence and absence of drug, using a hematocytometer (for suspension cell line such as K562) or fluorescence assay such as cell titer blue (for adherent cell lines such as HCC1806, HCT15 and A549).

The growth curves showed that the resistant cells survived and proliferated in the media containing the drug, while the parent cells did not grow in the presence of drug (Figure 48). The growth curve experiments were repeated and the results confirmed that these cell lines are resistant to the particular drug dose.

We noticed that the RX_step cells (Figure 48B) grow much slower than the parent cells whereas the proliferation rate of RX_pulse cells (Figure 48C and 48D) is similar to that of the

parent cells. The RX_step and the RX_pulse resistant cells were grown using two different strategies and therefore it is possible that the mechanisms contributing to RX resistance is different in these cell lines. The RX_pulse cells are resistant to a much higher drug dose (1µM and 5µM) as compared to the RX_step cells (100nM). Therefore in the pulsed cells there can be compensatory mechanisms activated that are absent in the RX_step cells, which enables it to proliferate in a similar rate as that of the parent cells.

A. Methotrexate resistance

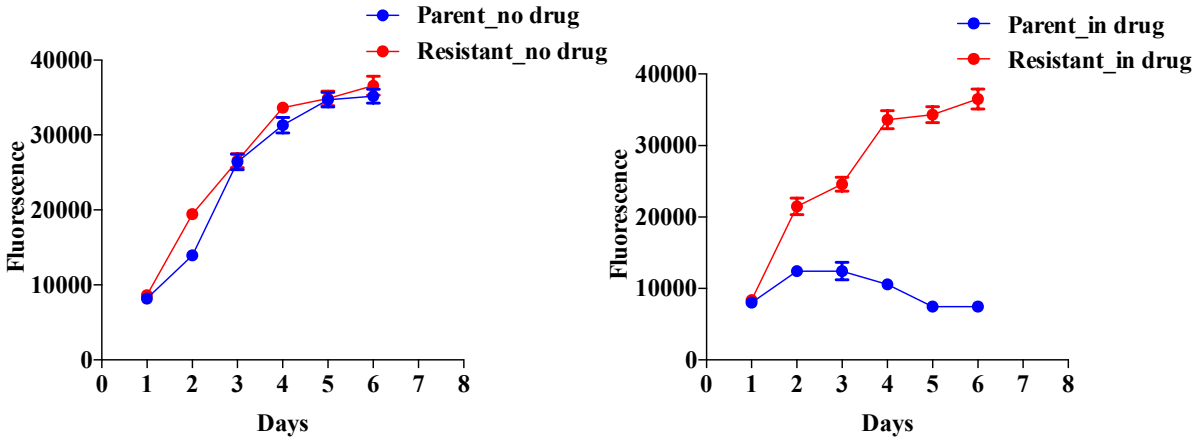

B. Raltitrexed resistance (RX_step)

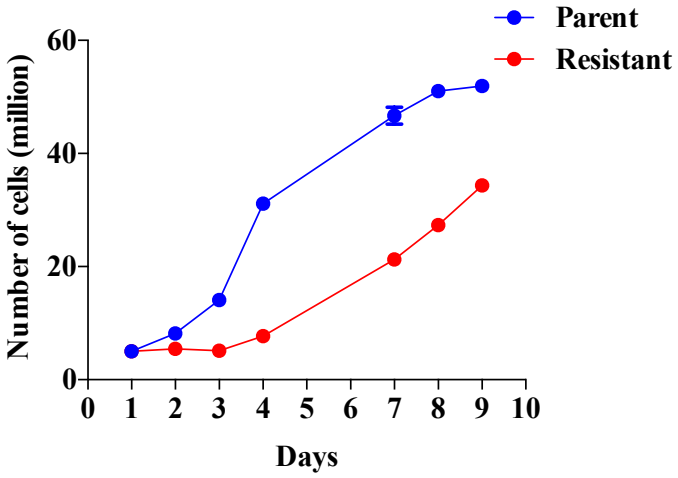

C. Raltitrexed resistance (RX_pulse (low))

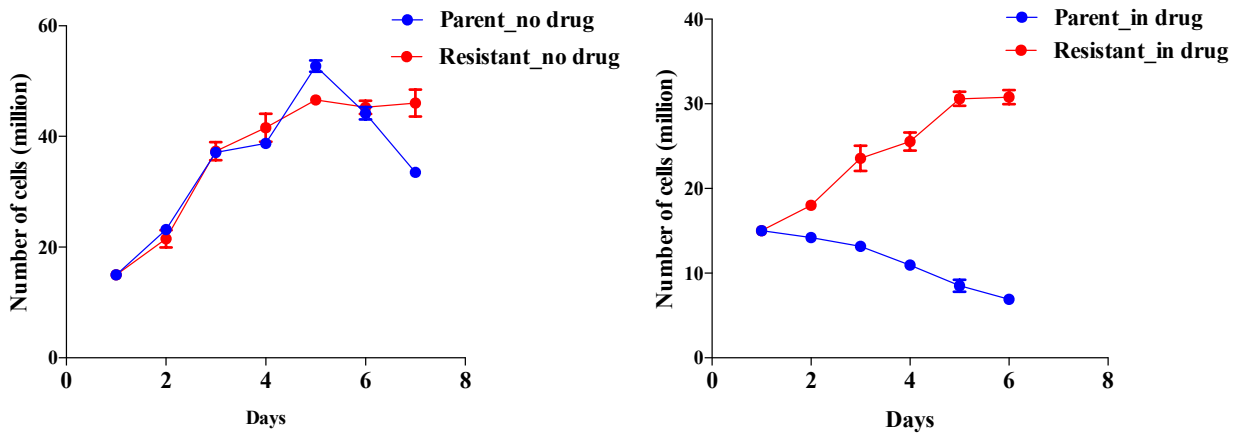

D. Raltitrexed resistance (RX_pulse (high))

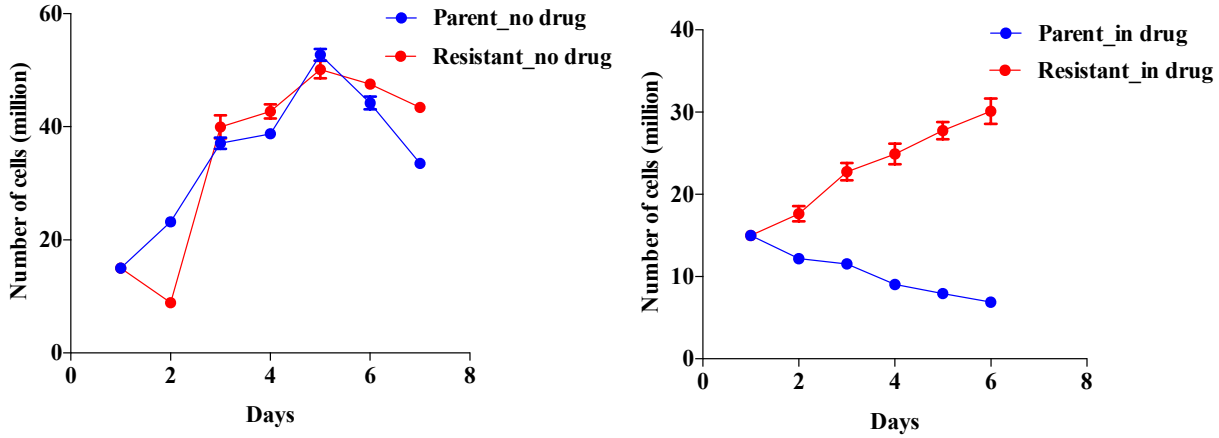

E. 5-Fluorouracil resistance

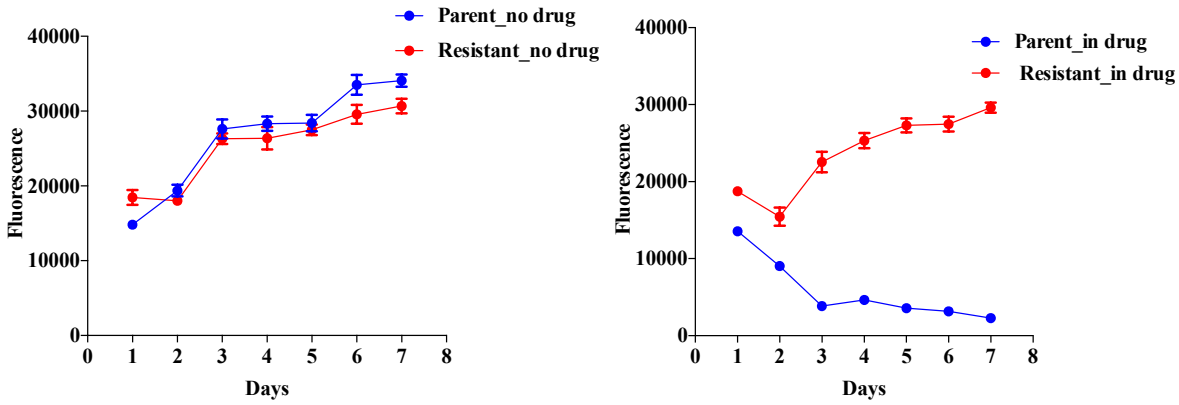

F. Nolatrexed resistance

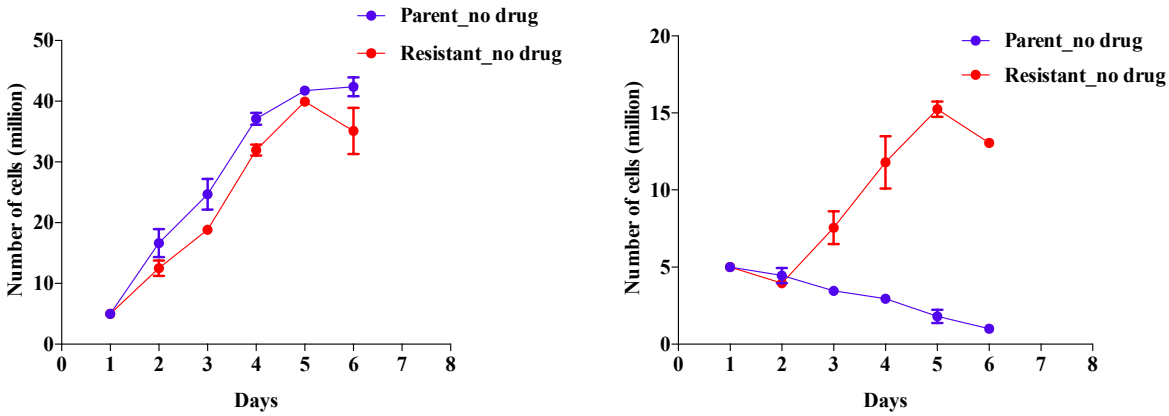

Figure 48: Growth curves of the parent and resistant cell lines

Growth curves of HCC1806 parent and MX resistant cells, in the absence and presence of 225nM MX respectively (A). Growth curves of K562 parent and RX_step resistant cells in the absence of 100nM RX (B). Growth curves of K562 parent and RX_pulse (low) resistant cells, in the absence and presence of 1µM RX respectively (C). Growth curves of K562 parent and RX_pulse (high) resistant cells, in the absence and presence of 5µM RX respectively (D). Growth curves of HCT15 parent and 5FU resistant cells, in the absence and presence of 16µM 5FU respectively (E). Growth curves of K562 parent and NX resistant cells, in the absence and presence of 50 µM NX respectively (F). The data is representative of two technical replicates from single experiment.

2.2 CETSA to study methotrexate resistance

Methotrexate is the antifolate drug that is used for treating acute lymphoblastic leukemia, osteosarcoma and lymphoma. It is a potent inhibitor of the enzymes dihydrofolate reductase (DHFR) and thymidylate synthase (TS). DHFR produces tetrahydrofolate from dihydrofolate, which is used by TS for thymidylate synthesis. Aforementioned, methotrexate is transported in to the cells by the reduced folate carrier protein (RFC), via active transport. In the cells the drug undergoes polyglutamation by the enzyme FPGS and it gets activated and retained in the cells.

The resistance mechanisms associated with methotrexate have been widely studied and the most common proposals are the following [128]:

1. Impaired drug transport that leads to decrease in the drug accumulation inside the cells.
2. Lack of polyglutamation that causes decrease in drug retention.
3. Increased levels of target enzymes
4. Mutations on the target enzymes.

All these mechanisms would lead to a lower target engagement and should therefore be possible to monitor with CETSA.

There are also other resistance mechanisms that would not lead to lower target engagement such as alterations downstream of the target protein that compensates for the target inhibition. In this way, regardless of the inhibition of the target protein by the drug, the signaling pathway is activated in parallel under the control of the newly activated or upregulated protein. For example, in $BRAF^{V600E}$ mutant lung adenocarcinoma resistance to Raf inhibitors occurs due to upregulation of EGF that activates EGFR and the downstream signaling pathway [129]. Resistance to inhibitors targeting several oncogenes happens due to activating mutations or upregulation of genes involved in the MAP kinase pathway. Resistance to EGFR inhibition occurs due to BRAF mutations, while resistance to ALK kinase inhibitor happens in EML4-ALK-drive lung cancer due to KRAS amplification [130,131].

To study methotrextae resistance using CETSA we used a 225nM methotrexate resistant HCC1806 cell line obtained from a cell repository. We confirmed resistance by doing growth curve and performed CETSA on this pair of cell lines.

CETSA melt curves of TS in the parent cells showed stabilization, when the cells were treated with 225nM MX and folates for 1 hour (Figure 49A). However, when the resistance cells were

given exactly the same treatment, TS melting temperature did not shift (Figure 49B). Then we looked at the isothermal dose response of MX in the parent and resistant cells after treating them with increasing MX-concentrations for one hour and then heating at 50^0C. We saw that in the resistant cells, a five times higher concentration of MX was required to produce maximum occupancy, relative to the parent cells (Figure 49C). The resistant cells showed higher MX dose threshold than the parent cells that means these cell lines have developed resistance with a mechanism that effect the target engagement of the drug.

After measuring resistance using CETSA, the next step was to shed light on the specific mechanism responsible for the resistance development. The CETSA melt curves showed that there is no target engagement in the resistant cells when treated with MX and folates. As discussed above this can happens due to several mechanisms; including impaired drug import, decreased polyglutamation, activation of drug efflux pumps or due to mutations in the target enzyme. We investigated the above-mentioned mechanisms to find the cause of resistance.

Reduced folate carrier protein (RFC) is responsible for importing methotrexate in to the cells and if this protein is downregulated in the resistant cells, it can lead to reduced or no drug import. We compared the basal levels of RFC in the parent and resistant cells by doing a western blot experiment (Figure 49D). The results showed that RFC is significantly downregulated in the resistant cells, which is the or one of the possible reasons for resistance development.

We did a proteome profiling of the parent and resistant cells using mass spectrometry, to compare the expression levels of other proteins. The aim was to select proteins with significant changes in their expression levels and investigate if this change is related to drug resistance development. Figure 50 shows the expression levels of TS, DHFR, FPGS and proteins related to drug efflux, in the cell line pair. We did not find any significant differences in the expression levels of these proteins across the cell lines.

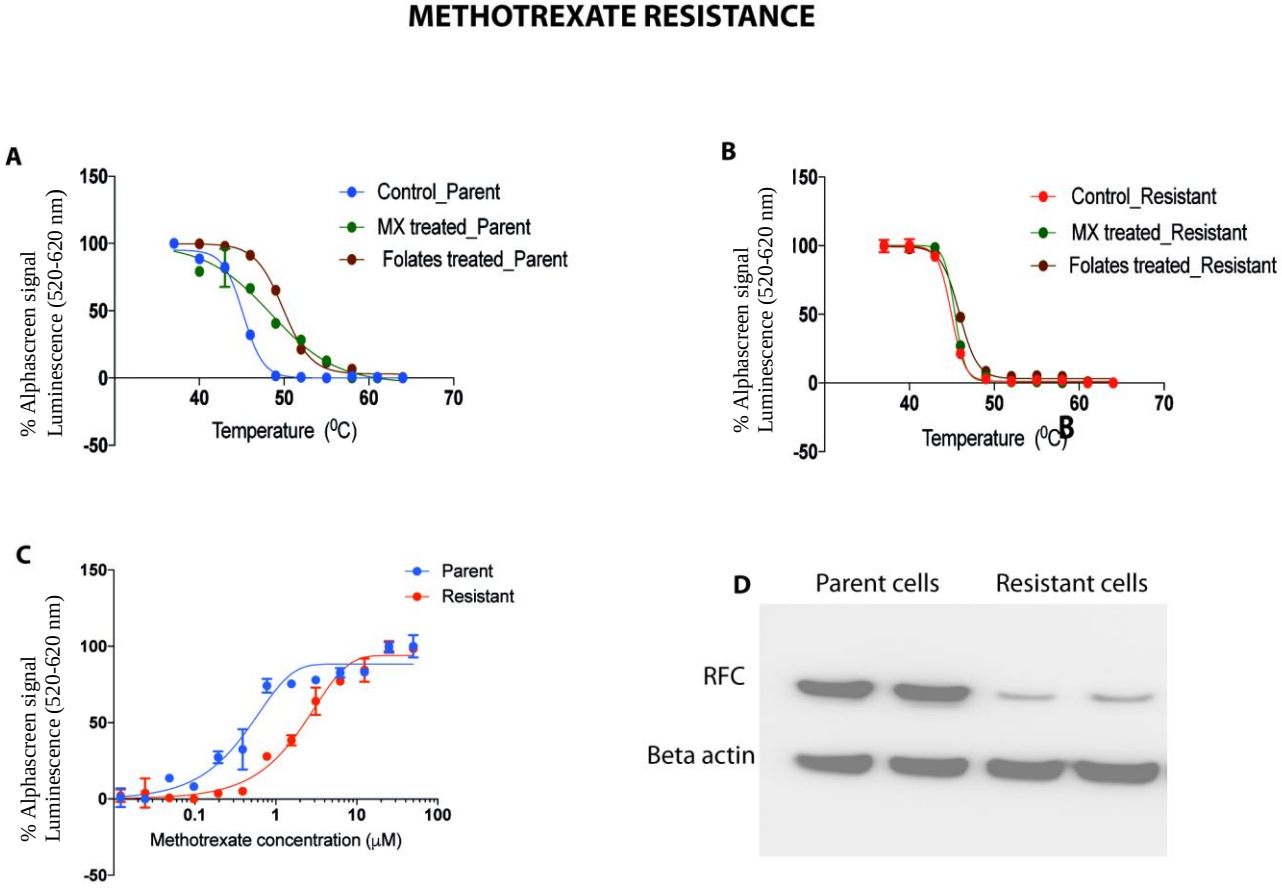

Figure 49: CETSA to study methotrexate resistance

CETSA melt curves of Thymidylate synthase in parent cells with methotrexate and folate (A). CETSA melt curves of Thymidylate synthase in MX resistant cells with methotrexate and folate (B). $ITDRF_{CETSA}$ of MX at 50^0C in parent and MX resistant cells (C). Reduced folate carrier protein (RFC) found to be down regulated in the MX (D). The melt curve data and $ITDRF_{CETSA}$ data are representative of two technical replicates from single experiment.

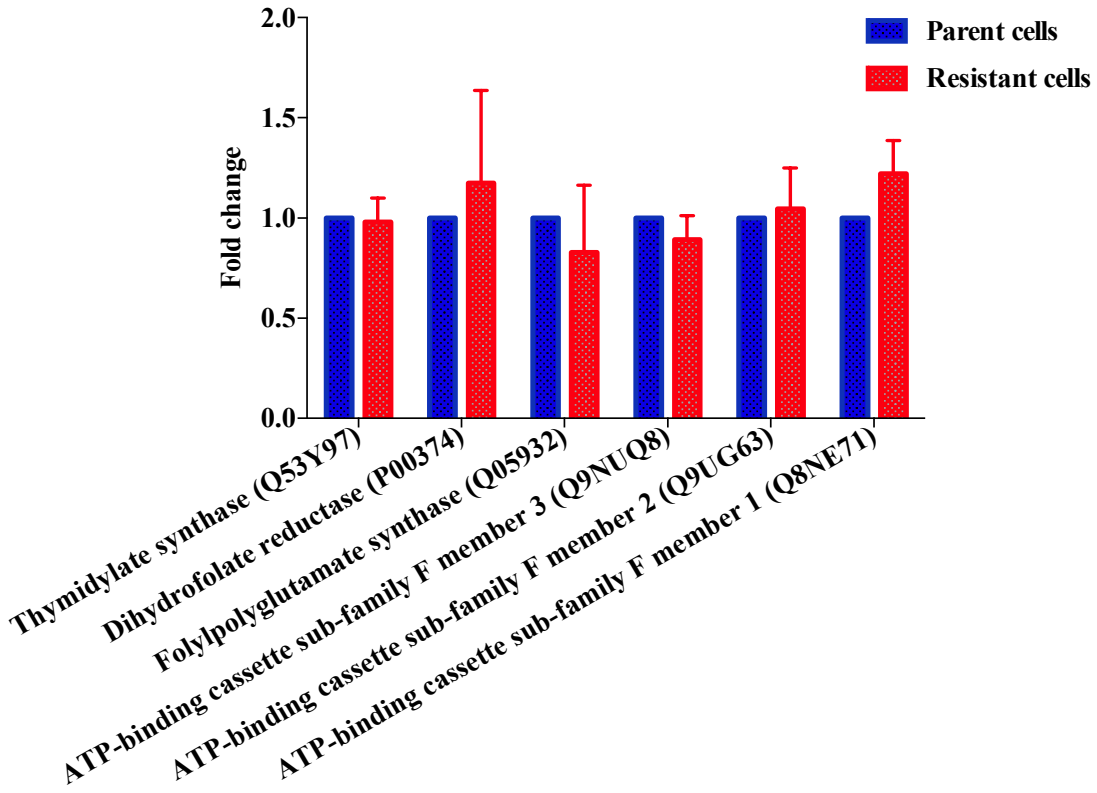

Figure 50: Proteome profiling of parent and MX resistant cells

Comparison of expression levels of selected proteins in the parent and resistant cell lines showing no significant difference in the expression levels. The data is representative of three biological replicates.

The reduced folate carrier protein (RFC) is responsible also for the transport of other antifolate drugs such as raltitrexed (RX) and pemetrexed (PX). Therefore, we examined the resistant cells to understand the effect of RFC downregulation on these drugs, by treating parent and resistant cells with increasing concentrations of RX, PX, NX and 5FdU (Figure 51). We performed the $ITDRF_{CETSA}$ experiment at 50^0C and observed that the methotrexate resistant cells have a higher drug dose threshold to other classical antifolates such as RX and PX. However, the drugs NX and 5FdU did not show any difference in drug threshold consistent with that they are not transported by the RFC.

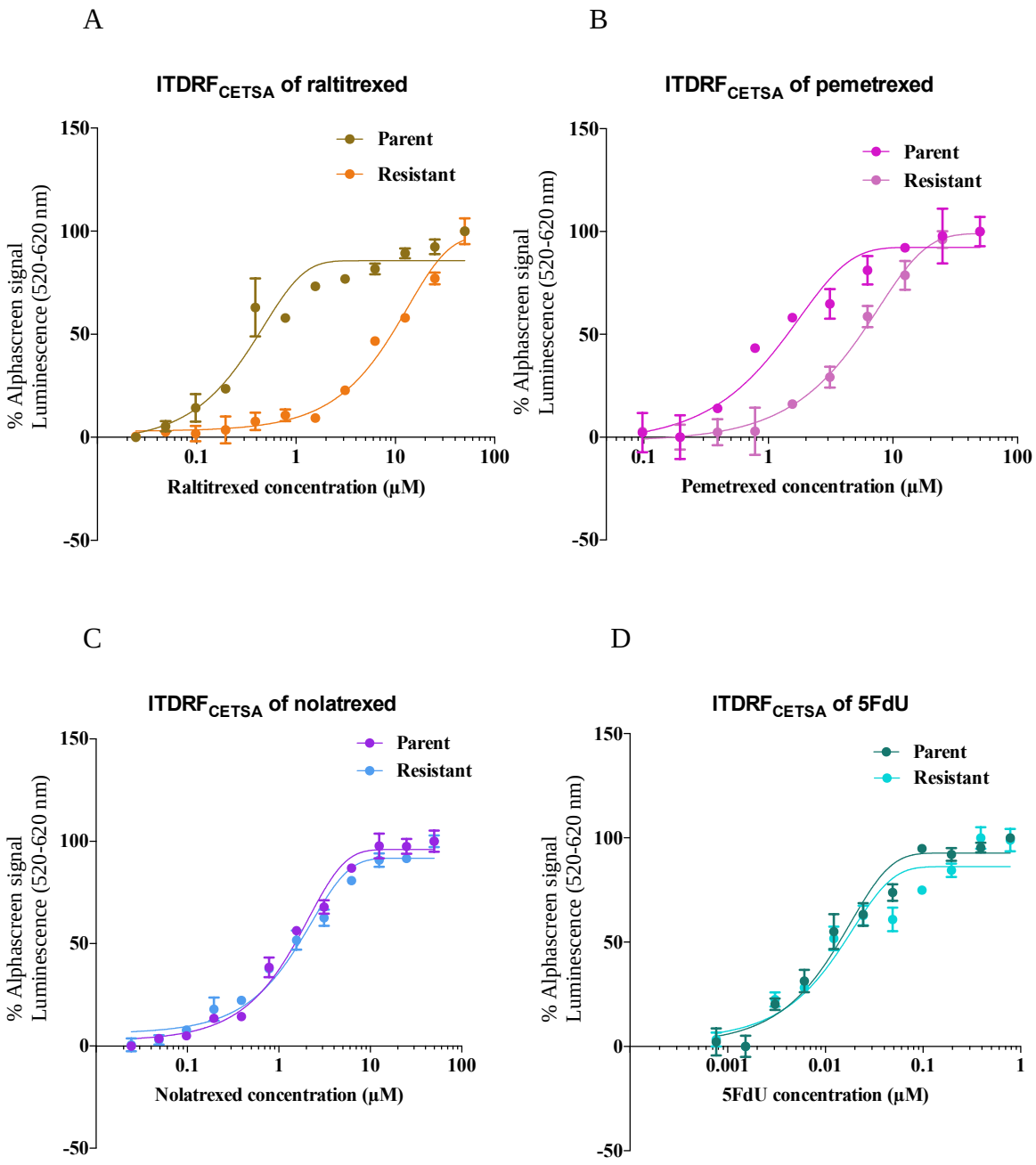

Figure 51: ITDRF$_{CETSA}$ of RX, PX, NX and 5FdU in HCC1806 parent and MX resistant cells:

Dose response of RX (A), PX (B), NX (C) and 5FdU (D) in the parent and resistant cells at 50^0C. The data is representative of two technical replicates from single experiment.

To confirm that the MX resistant cells are resistant to RX and PX as well, we generated the growth curves of parent and resistant cells in the presence of these drugs (Figure 52). The growth curves showed that the MX resistant cells survived and proliferated in the media containing RX and PX, while the parent cells died.

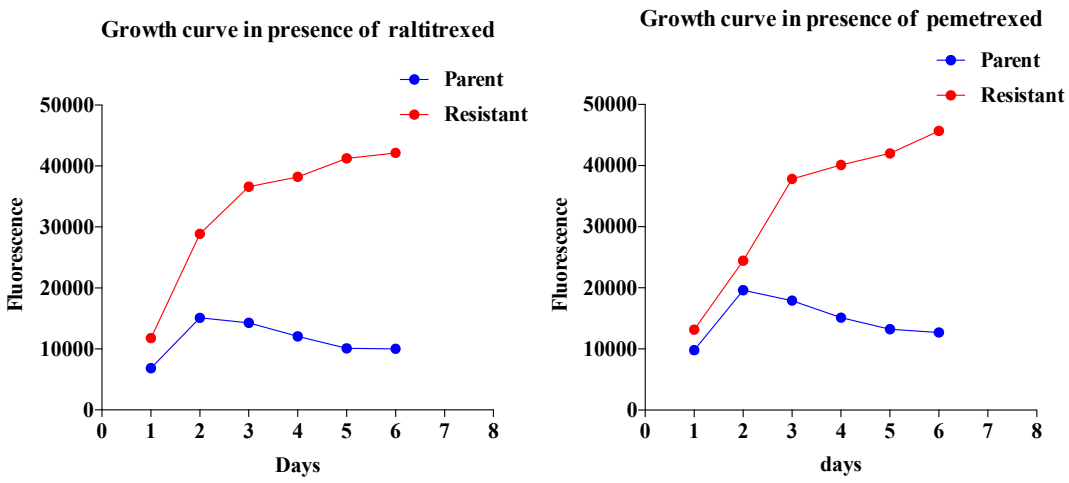

Figure 52: Growth curves with RX and PX

Growth curve of HCC1806 parent and methotrexate resistant cells in the presence of RX and PX respectively

The CETSA profiles and growth curves are therefore consistent with that the decreased RFC expression level is the major mechanism for resistance in this cell line. This supports that CETSA is an effective tool to understand the well reported mechanisms of resistance such as RFC downregulation that causes antifolate resistance.

2.3 CETSA to study raltitrexed resistance

Raltitrexed is a selective and potent inhibitor of thymidylate synthase (TS), which is used for treating advanced colorectal cancer. Raltitrexed enters the cell by RFC and then undergoes polyglutamation, with the polyglutamated form having hundred-fold greater inhibitory potency than the parent compound.

To study the polyglutamation property and the drug retention in the cells, we treated the parental K562 cells with 1μM raltitrexed for 4 hours and monitored the TS melt curve at different stages of recovery (Figure 53) (Note: Recovery refers to growing the cells after drug treatment in a complete media void of the drug but supplemented with FBS). We observed that even after 24 hours' recovery, TS did not melt at the given temperature range up to 64^0C, the maximum used when higher temperatures induce significant cell lysis. After 48 hours of recovery a small effect on target engagement was seen while after a week the melting curve had shifted very significantly supporting no or little target engagement remaining. Therefore, CETSA reveals that and active species of raltitrexed, which can engage TS is retained in the

cells for several days. This is likely a combined effect of polyglutamation, retaining the drug in the cell, and a high intracellular metabolic stability of the drug, which leads to its retention for days after the drug treatment.

The melt curves showed different alphascreen signal plateau levels with the signal being higher for melt curves with shorter recovery period. This difference is because the RX treatment causes change in the expression levels of the target protein TS. Raltitrexed stays in the cells for several days and therefore we observe changes in the expression levels of TS in the initial hours of recovery. The continuous exposure of RX can cause over expression of the protein, which can later contribute to resistance to the drug.

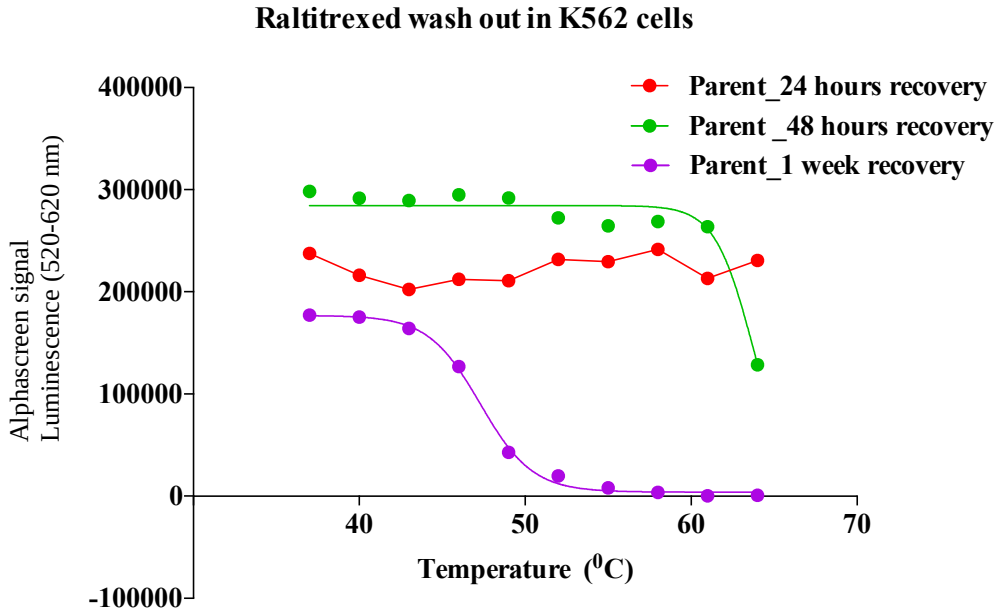

Figure 53: CETSA curves of TS in K562 parent cells

Melt curves of TS in parent cells, at different stages of recovery after RX treatment.

For this study, we developed raltitrexed resistant K562 cell lines in house using two different strategies, the stepwise drug increment technique and pulse strategy. The K562 cell line resistant to 100nM raltitrexed was generated using drug increment technique. For this, we seeded the K562 cells into a flask and, at 20% confluency, we treated them with 10-20% of the IC_{50} dose of the drug. The cells were then sub-cultured after it reached confluency. The concentration of the drug was doubled in each passage and the cells were monitored to find where they survive the drug treatment. For higher drug doses the cell growth slowed down and, they were recovered in drug free media for one passage if they did not withstand the increased drug dose.

We used pulse strategy to develop two cell lines, the 1µM and 5µM raltitrexed resistant cell lines termed as RX_pulse(low) and RX_pulse (high) respectively. In this method, the K562 cells were seeded on to a flask and treated with 1µM/5µM raltitrexed for four hours. After the treatment, the cells were recovered in drug free media for a week followed by the four-hour drug treatment. After the cells became resistant to the drug dose, we performed CETSA experiments on the K562 parent, RX_step, RX_pulse(low) and RX_pulse (high) resistant cells to study the effects on target engagement and to shed light on the mechanisms causing drug resistance.

Figure 54 shows the data from the parental and RX_step cell line. K562 parent cells upon treatment with 100nM raltitrexed for an hour showed more than 10-degree stabilization in the TS melt curve (Figure 54A). The TS control melt curves in the resistant cells at different stages of recovery were generated and compared with that of the parent cells (Figure 54B). TS in the parent cells melted at around 48^0C. In the resistant cells without recovery, we observed that there is a nearly 10-degree stabilization in the TS melt curve. As the recovery progressed from 5 hours up to 1 week, we found a gradual reversion of the TS melt curve back to the parental form. The washout was however slower in this cell lines as compared to the parental discussed above, when there was still remaining target engagement after 1 week in the resistant cells.

Next, we looked at the $ITDR_{CETSA}$ of raltitrexed at 50^0C in the parental cells and the resistant cells at different stages of recovery (Figure 54C). $ITDR_{CETSA}$ experiments at 0 and 1 hours showed high signals and no significant dose response supporting that target engagement was still close to 100% at these time points (data not shown). The resistant cells at 5 hours of recovery showed higher RX-dose threshold relative to the parent cells and we saw around 50-fold shift in the dose-response of the drug in the resistant cell lines. The curve gradually reverted to the parental form as the recovery progressed. The change in $ITDR_{CETSA}$ could be due to a reprogramming of the initially resistant cells but also that when grown without drugs, a small population of parental clones is taking over the culture in the later time points.

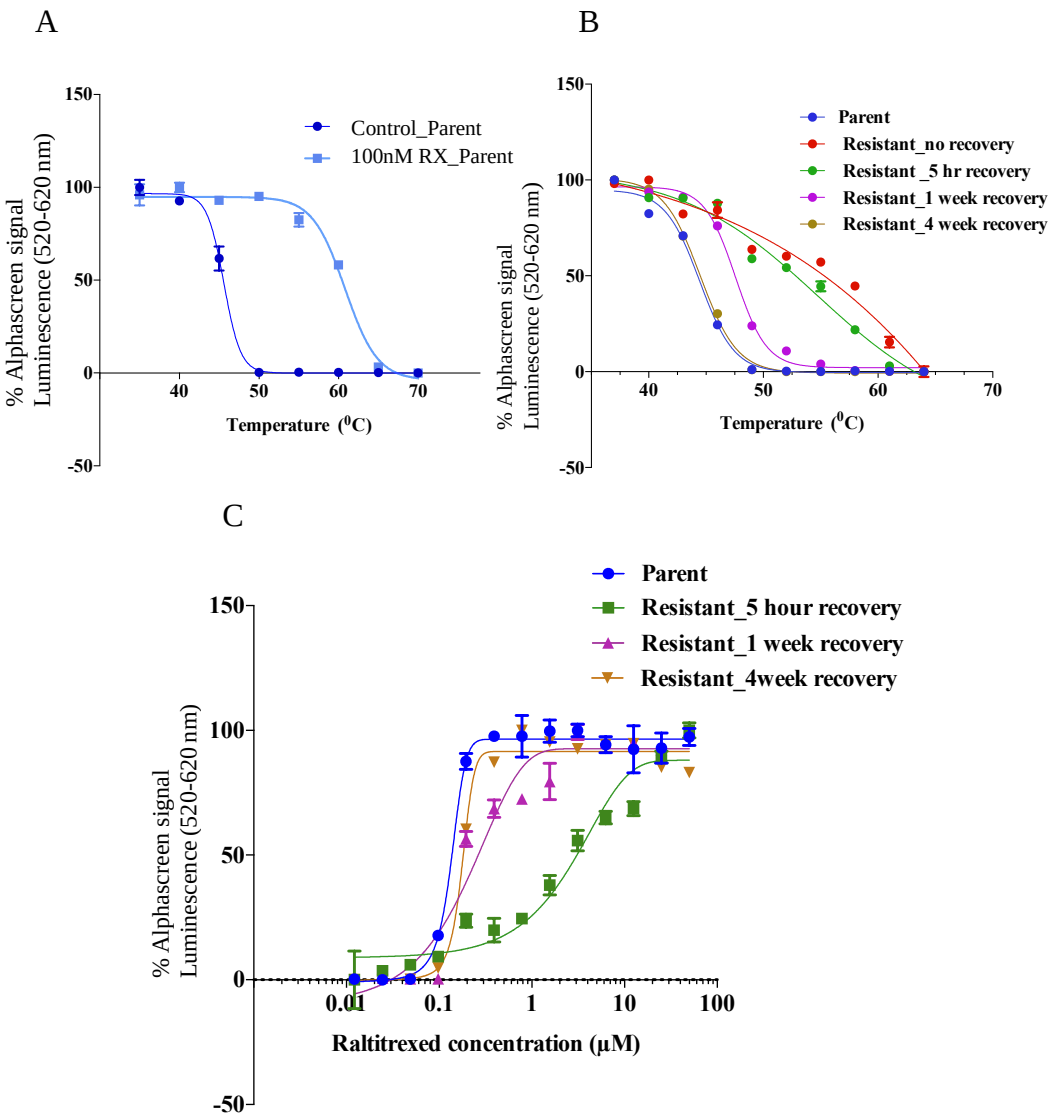

Figure 54: CETSA to study raltitrexed resistance in the RX_step cell line

TS melt cure in K562 parent cells with and without 100nM RX treatment (A), TS control melt curves in the parent cells and resistant cells (B), $ITDR_{CETSA}$ curves of raltitrexed at 50^0C in parent cells and resistant cells (C). The melt curve data and $ITDRF_{CETSA}$ data are representative of two technical replicates from single experiment.

We also characterized the RX_pulse(low) and RX_pulse (high) resistant cells using CETSA (Figure 55). The melt curves of TS in the resistant cells at different stages of recovery were compared with that of the parent cells (Figure 55A). The protein did not melt at the given temperature range when the resistant cells were not recovered. After 1 week of recovery, we observed some melting at the highest temperature still indicating a high level of target engagement. The melt curves reverted to the parental form upon the progress of recovery. The $ITDR_{CETSA}$ curves of RX at 50^0C, was measured and as for RX Step resistant cells, no response

could be measured at early time points supporting sustained target engagement. RX_pulse(low) and RX_pulse (high) $ITDR_{CETSA}$ could only be measured in a week's range and showed relative small shifts in the dose response (Figure 55B). The CETSA melt curves and the $ITDR_{CETSA}$ curves of the RX_pulse (high) resistant cells showed a similar trend (Figure 55C and 55D).

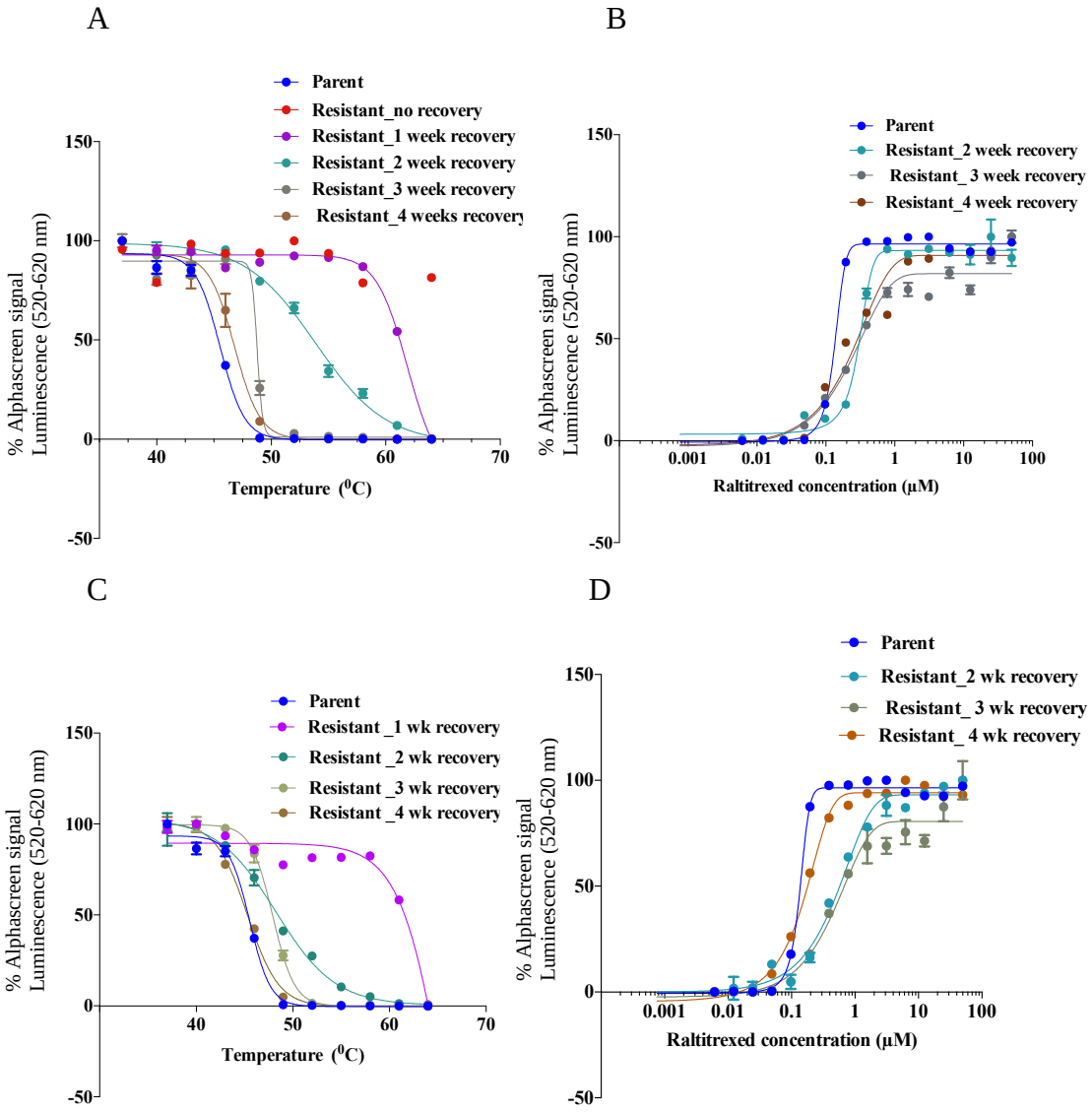

Figure 55: CETSA to study raltitrexed resistance in the RX_pulse(low) and RX_pulse (high) cell lines

CETSA melt curves of TS in parent cells and RX_pulse (low) resistant cells at different stages of recovery (A) and $ITDRF_{CETSA}$ of RX at 50^0C in parent and RX_pulse (low) resistant cells (B). CETSA melt curves of TS in parent cells and RX_pulse (high) resistant cells at different stages of recovery (C) and $ITDRF_{CETSA}$ of RX at 50^0C in parent and RX_pulse (high) resistant

cells (D). The melt curve data and ITDRF$_{CETSA}$ data are representative of two technical replicates from single experiment.

CETSA results from the three RX resistant cells showed that RX stayed in the cells for a week or more after the drug treatment and caused target engagement in thymidylate synthase. TS is the enzyme that is essential for thymidylate production in cells, which is required for DNA synthesis and cell growth. The interesting finding from the CETSA results was that, even when thymidylate synthase is fully engaged, and presumably inhibited, by raltitrexed the resistant cells can still survive and proliferate. This suggests another source for the thymidine nucleotides needed for DNA synthesis.

To shed further light on the raltitrexed resistance mechanism, we did a proteome profiling of the parent and the RX_pulse (low) resistant cell lines using mass spectrometry (Figure 56). The aim of this experiment was to monitor changes in the expression levels of specific proteins, which could be a reason for the observed resistance.

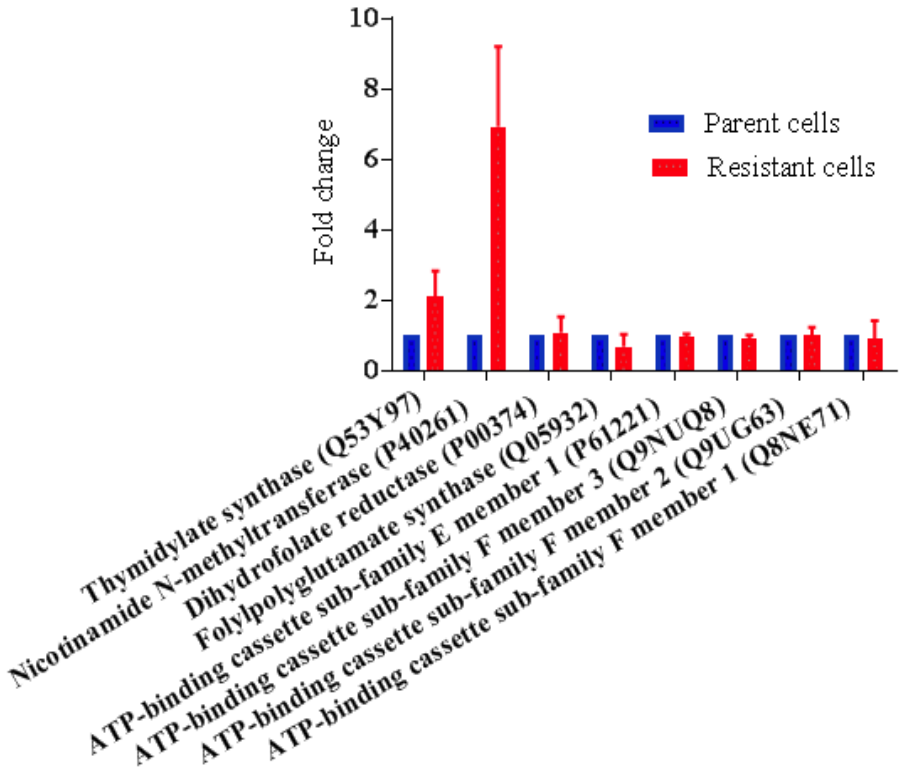

Figure 56: Proteome profiling of the parent and RX resistant cells

It shows upregulation of TS and NNMT in the RX_pulse (low) resistant cells. The data is representative of three biological replicates.

For the above thermal profiling experiment, the resistant cells were taken after drug treatment without any recovery. We treated the K562 parent cells with 1µM RX for 4 hours and compared the expression levels of proteins with the K562 cells without treatment, RX resistant cells that are not recovered and that are 1 week recovered (Figure 57). In the initial experiment, we did see significant differences in, for example, TS and nicotinamide N-methyltransferase (NNMT). We observed that the RX treatment in the parent cells did not trigger the upregulation of these enzymes. We found over-expression of these enzymes only in the resistant cell data. This confirmed that this upregulation is not just because of drug treatment but has some association to drug resistance development.

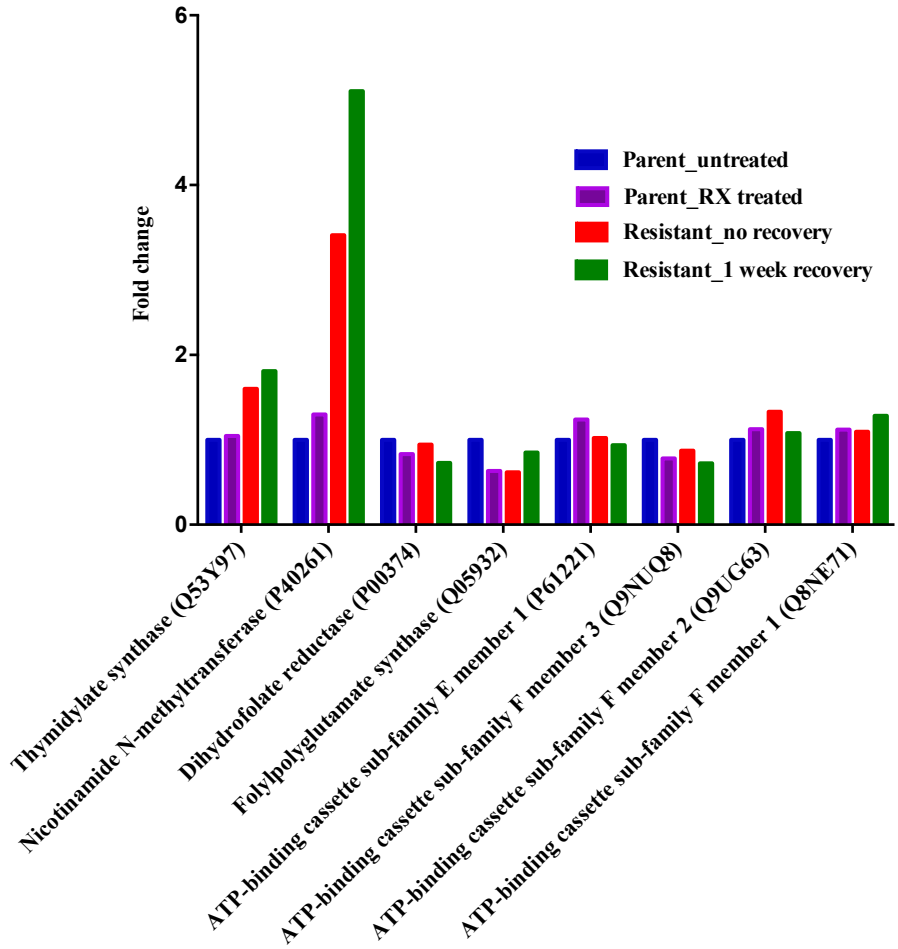

Figure 57: Proteome profiling of parent cells with RX treatment Vs resistant cells

Comparison of protein expression levels in parent cells with and without RX treatment and resistant cells after no recovery and 1 week recovery.

The proteome profiling data showed that the TS levels in resistant cells is one-fold higher compared to the parent cells while NNMT is seven-fold higher.

NNMT belongs to the methyltransferase class of enzyme, which catalyzes the N-methylation of nicotinamide to 1-methylnicotinamide (1-MNA), using S-adenosyl-L-methionine (SAM) as the methyl donor. N-methylation is the process by which the liver metabolizes drugs for detoxification.

S-adenosyl-L-methionine + nicotinamide = S-adenosyl-L-homocysteine + 1-methylnicotinamide.

NNMT has been implied in drug metabolism/degradation but when we do not note major changes in drug metabolism in these cells there might be other mechanism. We instead tested the hypothesis that NNMT could use uracil/uridine as a substrate to generate thymine/thymidine. However, binding and enzyme assays on a purified NNMT did not support this hypothesis.

We also sequenced TS in the parent and RX resistant cells to find out if the protein is mutated in the resistant cells. The sequenced region of the protein was compared with the wild type TS sequence using a multiple sequence alignment tool. We observed that there is no change in TS in the resistance cells and therefore it is not the reason of RX resistance.

2.4. CETSA to study 5-fluorouracil resistance

5-Fluorouracil (5-FU) is an important drug used in the treatment of cancer. Drug resistance often develops to 5-FU therapy.

Fluorodeoxyuridine monophosphate (FdUMP), the active metabolite of 5-FU binds to the nucleotide-binding site of TS forming a stable complex with methylene tetrahydrofolate (CH_2THF) and TS. This blocks dUMP from binding to the nucleotide-binding site leading to inhibition in dTMP synthesis. TS inhibition gives rise to deoxynucleotide (dNTP) pool imbalances and an increase in the levels of deoxyuridine triphosphate (dUTP), both causing DNA damage and cell death.

We used CETSA to study 5-FU drug resistance in HCT15 parent and 16μM 5-FU resistant cell line pairs. These cell lines were obtained from a cell repository and resistance to 5-FU was confirmed by performing the growth curve experiment (Figure 48E). To understand how long the drug is retained in the cells after treatment, the HCT15 parent cells were treated with 16μM 5-FU for 90 minutes and then the TS melt curves were generated at different stages of recovery (Figure 58). TS melt curve showed more than 10-degree stabilization at 1 hour of recovery and reverted to the parental form by the 3rd day of recovery. 5-FU binds covalently

to TS and we hypothesized that the non-resistant clones in the population outgrew the resistant clones and caused the reversion during the recovery phase.

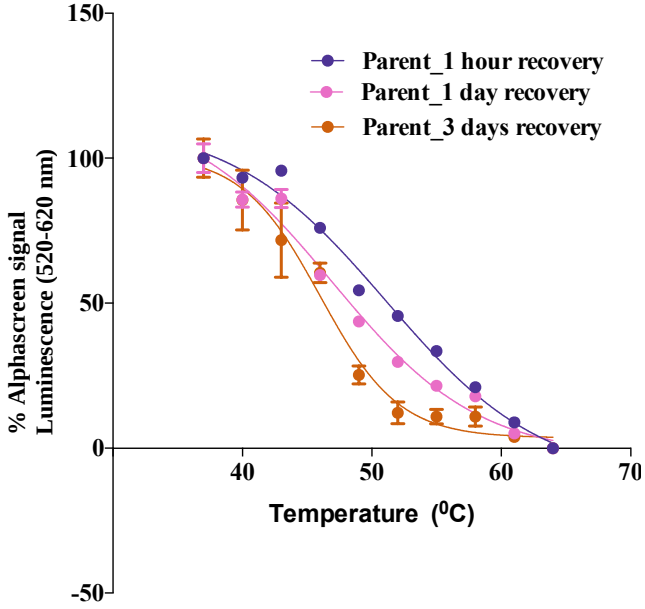

Figure 58: CETSA curves of TS in HCT15 parent cells

Melt curves of TS at different stages of recovery after 5-FU treatment. The data is representative of two technical replicates from single experiment.

The 5FU resistant cells were then characterized by looking at the CETSA melt curves and $ITDR_{CETSA}$ curves (Figure 59). We compared the CETSA melt curves of TS in the parent cells and resistant cells at different stages of recovery. The resistant cells maintained in 5FU containing media showed a 15-degree stabilization in the TS melt curve and reverted to the parental form rapidly over the recovery period. At the 4^{th} week of recovery of the resistant cells, the TS melt curve overlapped with that of the parent cells. After 3 days of recovery of the resistant cells, we studied the $ITDR_{CETSA}$ of 5FU at 50^0C and no major difference in the ic50 of the drug was observed.

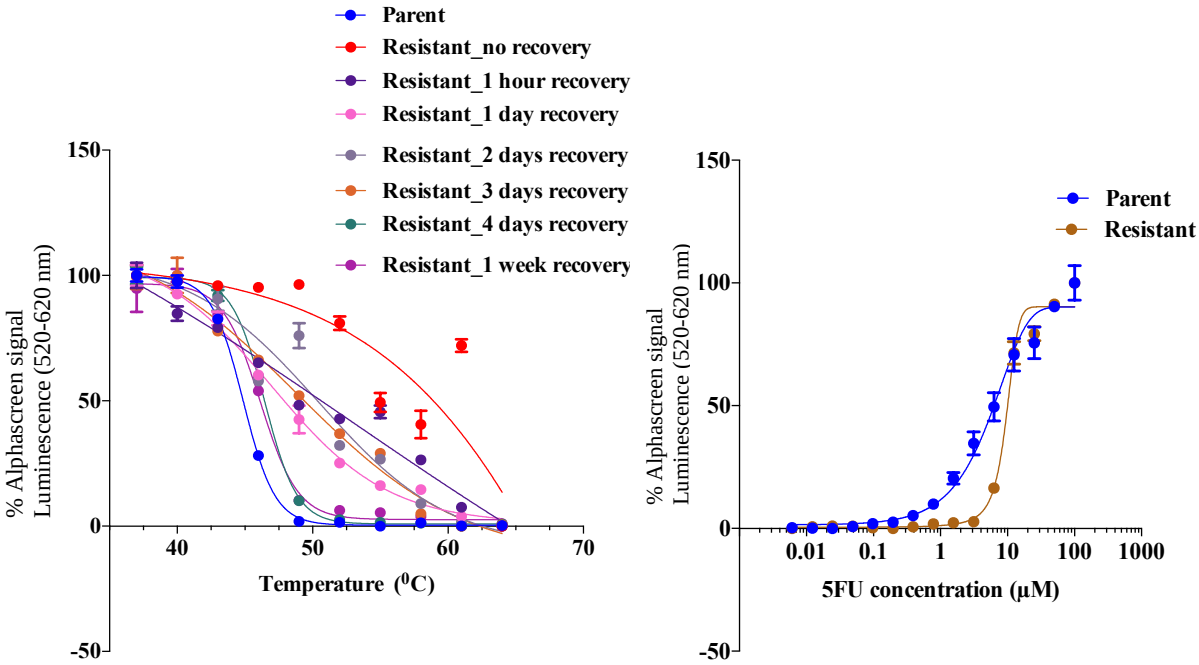

Figure 59: CETSA to study 5FU resistance

CETSA melt curves of Thymidylate synthase in parent cells and 5FU resistant cells at different stages of recovery and $ITDRF_{CETSA}$ of 5FU at 50^0C in parent and resistant cells. The data is representative of two technical replicates from single experiment.

At this stage, we performed the $ITDR_{CETSA}$ again with 5-Fluoro-2′-deoxyuridine (5FdU), the nucleoside version of 5-FU that is rapidly transported in to the cells (Figure 60). 5FdU gets converted in the cells to the active metabolite 5-FdUMP that inhibits TS. We looked at $ITDR_{CETSA}$ of 5FdU in parent and resistant cells. More than a 10-fold shift was observed in the dose response of 5FdU in the resistant cells as compared to the parental cells.

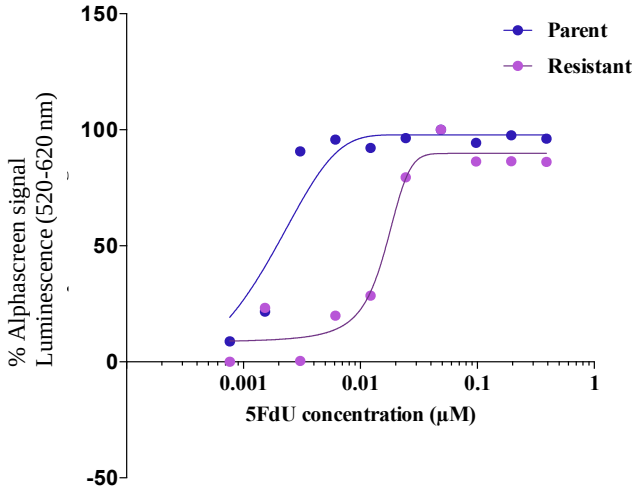

Figure 60: $ITDRF_{CETSA}$ of 5FdU

Dose response of 5FdU in parent and 5FU resistant cells at 50^0C.

Profiling the protein levels on the proteome of the parent and resistant cells was performed to detect significantly upregulated or downregulated proteins in the resistant cells that can be associated to resistance. The expression levels of few selected proteins are showed in figure 61. The proteome profiling data showed that the target protein TS is present at two-fold higher levels in the resistant cells. Target overexpression can contribute to resistance development as the drug administered becomes insufficient to completely inhibit the target due to its increased levels, but protein levels could potentially also be increased by drug binding stabilising the target protein.

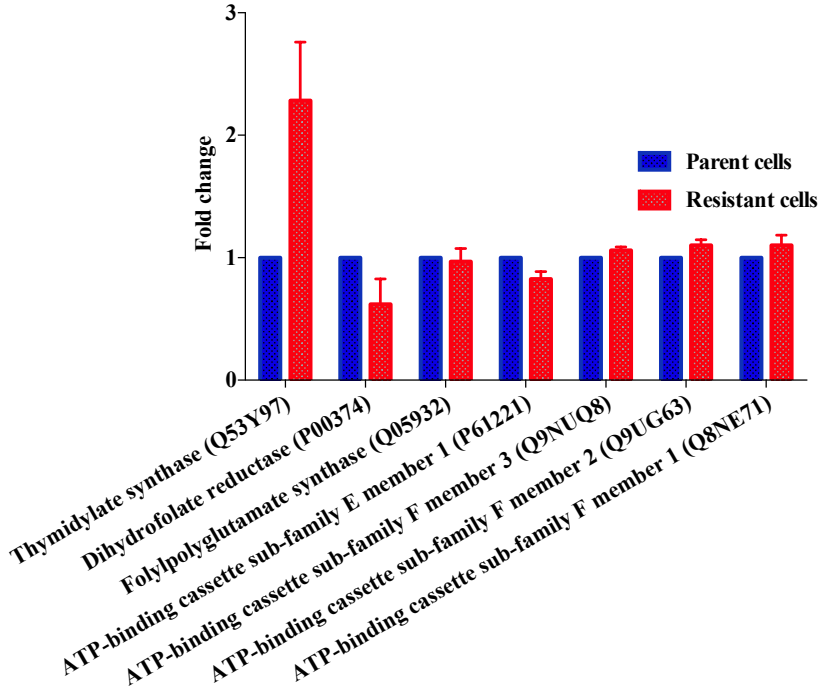

Figure 61: Proteome profiling of parent and 5FU resistant cells

The data showed upregulation of TS and down regulation of DHFR in the 5FU resistant cells. The data is representative of three biological replicates.

We determined the effect of antifolate drugs such as raltitrexed, methotrexate, pemetrexed and nolatrexed in the parent and 5FU resistant cells (Figure 62). $ITDR_{CETSA}$ curves of all four drugs showed no difference in the drug dose threshold. Hence, the 5FU resistant cells did not have a shift in the dose dependent target engagement with these antifolate drugs. This suggest no cross resistance with these compounds (not tested at the viability level) but also that higher TS levels does not affect the dose needed to get target engagement.

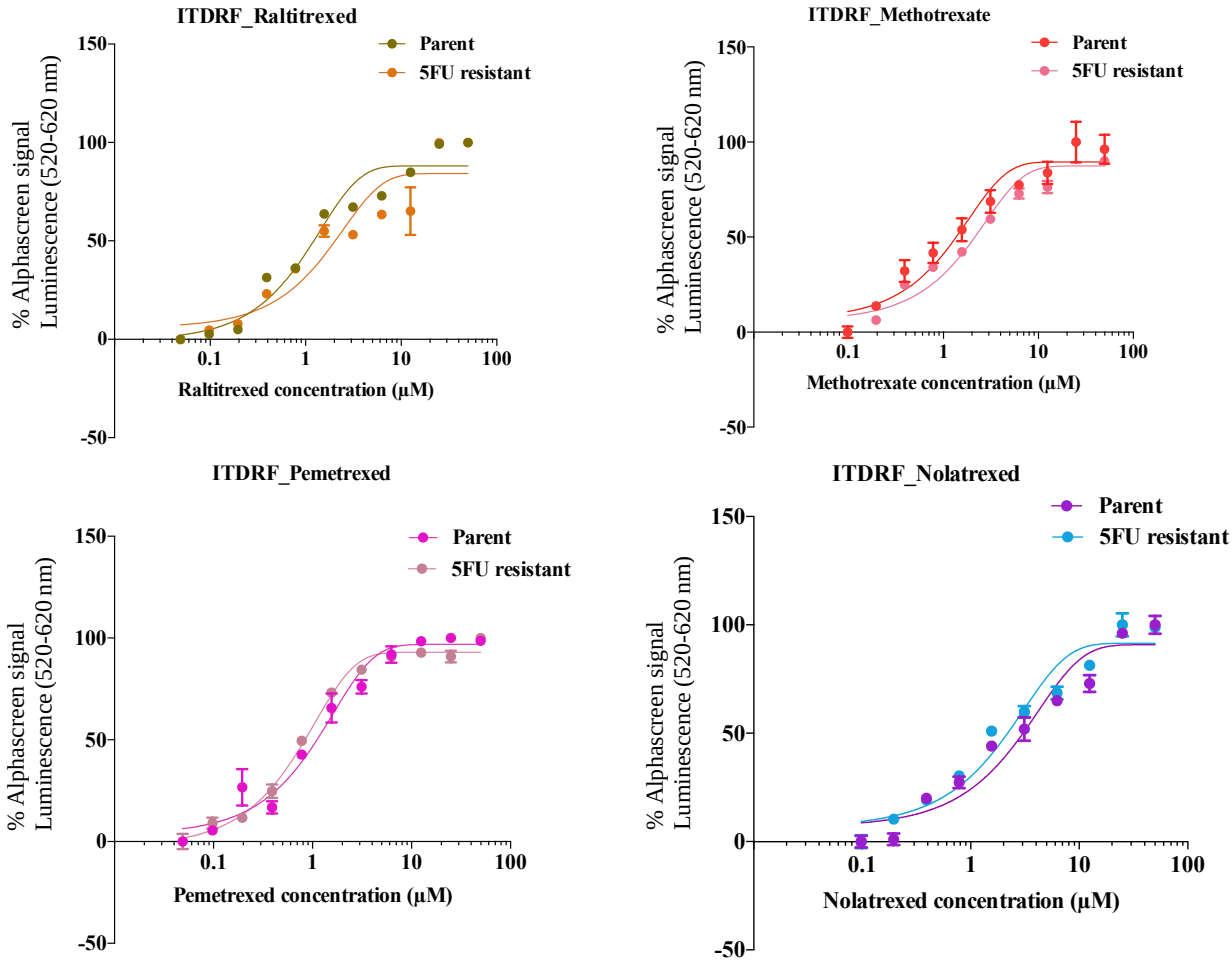

Figure 62: ITDR$_{CETSA}$ of RX, MX, PX and NX

Dose response of the drugs at 50^{0}C in parent and 5FU resistant cells. The data is representative of two technical replicates from single experiment.

2.5 CETSA to study nolatrexed resistance

Nolatrexed, the non-classical antifolate drug was designed to eliminate the development of common resistance mechanisms related to active transport and polyglutamation, associated with the classical antifolates. Nolatrexed does not require active transport to enter the cells and is also not a substrate for enzyme FPGS. To study drug resistance to nolatrexed, we developed 50µM nolatrexed resistant K562 cell line using the pulse strategy. We subsequently did some preliminary characterization of the parent and resistant cell pair by generating CETSA melt curves and ITDR$_{CETSA}$ curves.

We treated K562 cells with 50µM nolatrexed for 1 hour and observed nearly a 10-degree stabilization in the melting temperature of TS (Figure 63A). The NX resistant cells were then characterized and melting profile of TS was studied with and without NX treatment (Figure

63B). We observed that in the control TS melted around at 50^0C and there is no stabilization in the TS melting temperature when the resistant cells were treated with 50µM nolatrexed. The resistant cells were then recovered for 1 day in drug free media and the TS melt curve was generated (Figure 63C). We saw that already after a day of recovery, the TS melt curve showed a similar behavior as the parental cells with a strong response upon NX treatment.

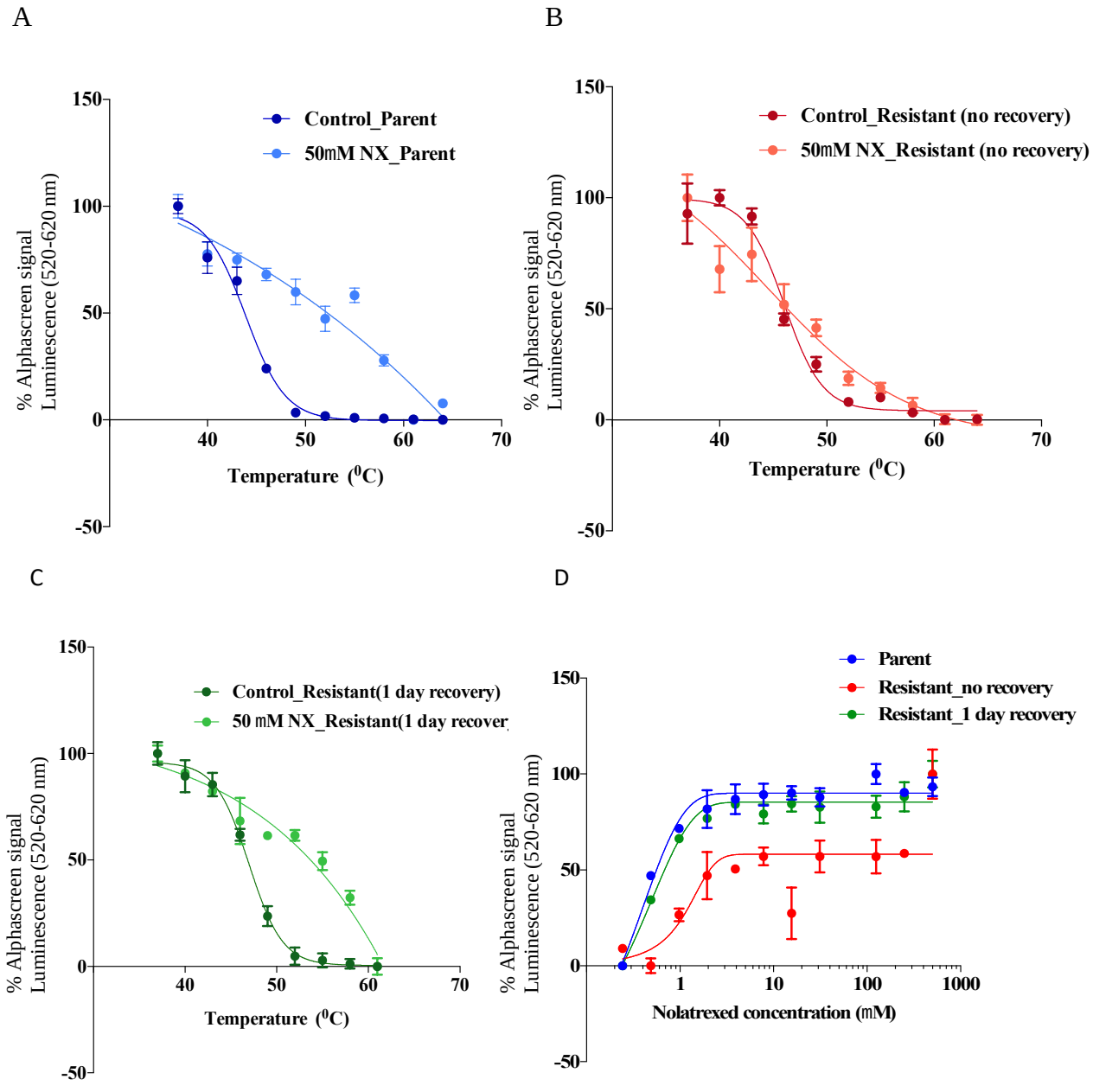

Figure 63: CETSA to study nolatrexed resistance

CETSA melt curve of TS in K562 parent cells, with and without 50 µM nolatrexed treatment (A), TS CETSA melt curve in resistant cells_not recovered, with and without 50 µM NX treatment (B), TS melt curve in resistant cells_1 day recovered, with and without 50 µM NX

treatment (C). $ITDRF_{CETSA}$ of NX at 50^0C in parent and nolatrexed resistant cells (D). The data is representative of two technical replicates from single experiment.

We generated the $ITDR_{CETSA}$ curves of NX in the parental and resistant cells (Figure 63D). It was observed that after 1 day of recovery, the $ITDR_{CETSA}$ curve in resistant cells overlaps with the parental curve. When the $ITDR_{CETSA}$ curves did not have a clear baseline the exact shift of the dose threshold remains to be determined. Although the NX CETSA data is preliminary, it supports a mechanism where the drug is rapidly degraded or exported to minimize target engagement. The data also support that the cells already within 1 day revert to a drug target engagement behavior similar as the parental cells. This response indicates that this mechanism of resistance is induced as a regulatory response, rather than hardwired mutations. The induction of catabolic enzymes and efflux pumps are possible resistance mechanisms in this case that remains to be tested.

3. Mapping interactions of nucleotide metabolites with the human proteome using MS-CETSA

CETSA assesses drug target engagement in cells based on ligand-induced changes in protein thermal stability and have above been discussed when protein quantification is made with immune assays. CETSA combined with quantitative mass spectrometry permits to study the effect of drugs of with cellular proteomes constituting 6000 or more proteins [77]. The MS-CETSA approach can be used to study drug interaction and downstream effects of such interactions [77,132] but also for physiological protein ligands interactions such as with metabolites, the latter being studied by us (Lim et al, submitted).

Metabolites play essential roles in many cellular processes such as synthesis of proteins, lipids and nucleic acids and regulation of cell signaling and metabolism. Metabolites interact with the target enzymes and, the dysregulation of metabolite-protein interactions can lead to diseases. The interaction between proteins and metabolites are studied by performing biochemical assays on purified recombinant protein. Affinity proteomics can be used to identify novel proteins interacting with the metabolites in lysates. However, efficient approaches to discover and study novel metabolite interactions with the human proteome in cells and tissues have largely been lacking.

We have developed a stringent strategy for studying the interactions of metabolites with the human proteome using CETSA. This can lead to the discovery of previously unknown proteins, which bind nucleotides as receptors or as enzymes.

We studied the metabolite interactions with proteome in the K562 cell lysate. The cell lysate was treated with the nucleotides, CETSA melt curve and ITDR experiments were performed and, quantitative mass spectrometry was used for detecting protein hits responding to the nucleotide treatment. The aim of this study was to study the nucleotide-protein interactions in the proteome, validate the method with known interactions and most importantly discover novel interactions. This is a collective work of our CETSA team where I was involved in looking at the interactions of nucleotides dUMP, dTMP and dCMP with the human proteome. We analyzed and examined the datasets for known interactions. The protein thymidylate synthase showed a shift in the melting temperature when treated with dUMP and dTMP. The protein Thymidylate Kinase showed stabilization in the melt curve upon dTMP treatment and, dCMP stabilized Deoxycytidine Kinase. The detection of these known interactions added confidence to the data and validated the method (Figure 64A, 64B and 64C).

A

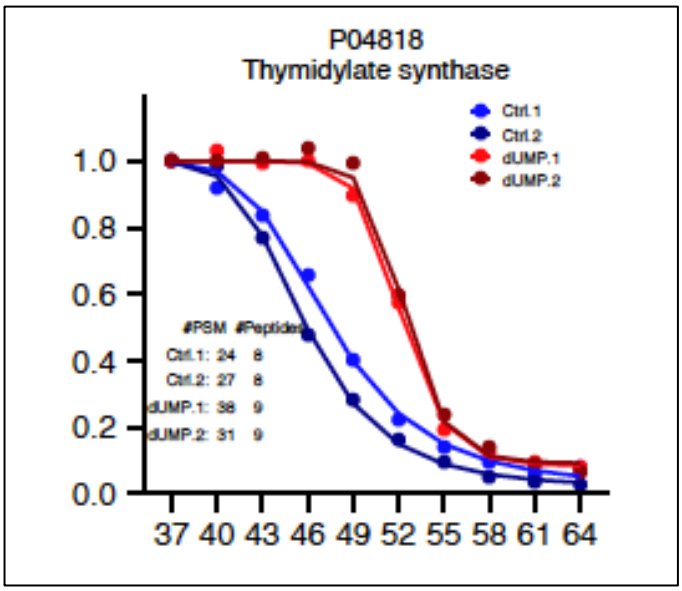

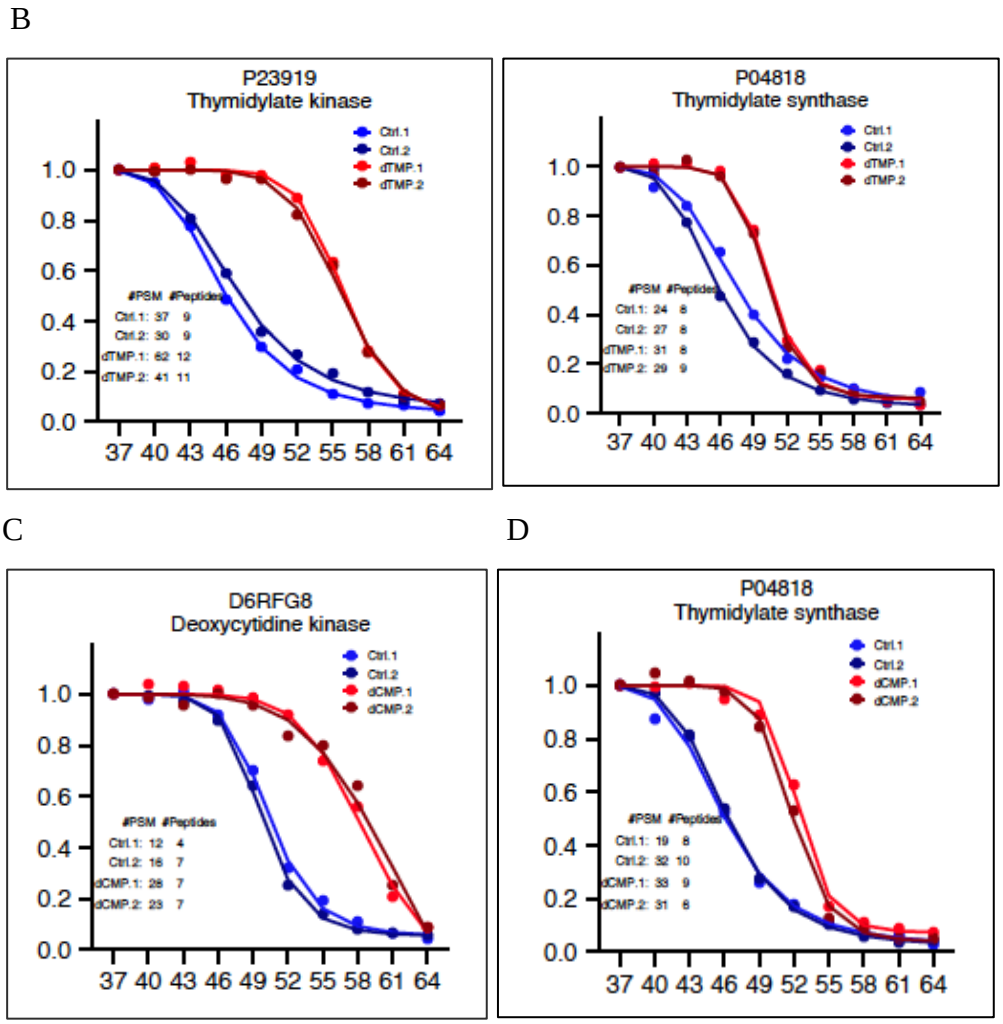

Figure 64: CETSA melt curves of proteins known to interact with nucleotides: dUMP (A), dTMP (B) and dCMP (C). Unanticipated interaction of dCMP with TS (D).

We observed that in the dCMP dataset TS responds to dCMP treatment (Figure 62D). We investigated this interaction further by doing in cell experiments. Nucleoside versions of the three nucleotides dU, dT and dC were used for these studies. These nucleosides are rapidly transported in to the cells. In the cells, they get converted in to the corresponding monophosphate forms by the action of responsible enzymes. We treated the K562 cells with 50mM of the above-mentioned nucleosides for 30 minutes and studied the melting profile of TS using alphascreen detection (Figure 65).

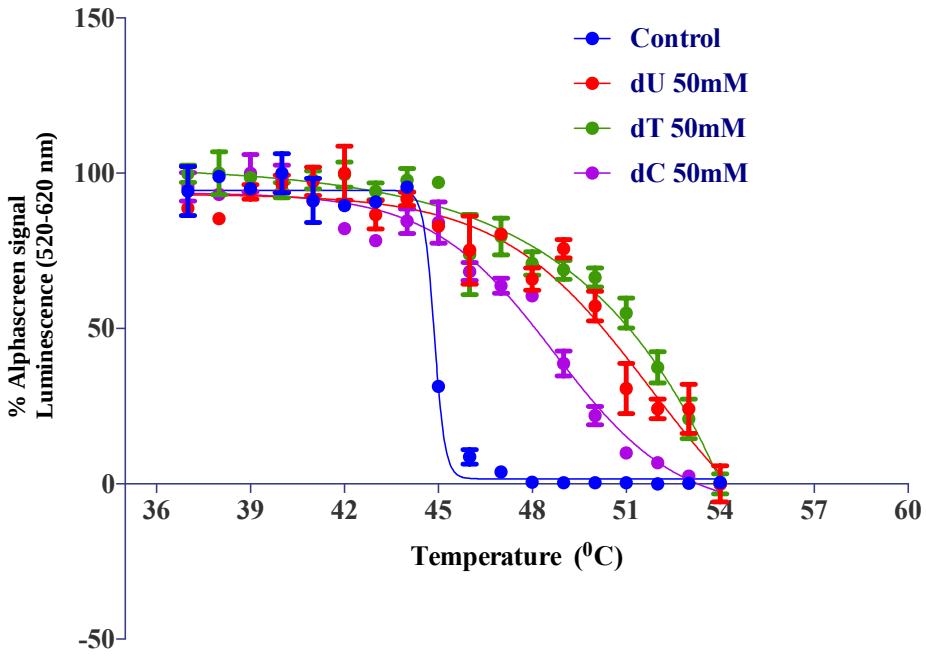

Figure 65: TS melt curve in K562 cells with and without dU dT and dC treatment.

The data is representative of two technical replicates from single experiment.

The melt curves showed that TS gets stabilized significantly upon the treatment with the nucleosides. dC induced a shift of about 6 degrees to the TS melt curve in K562 cells. Next, we looked at the $ITDR_{CETSA}$ curves of all the three nucleosides in K562 cells at 48^0C after 30 minutes' treatment (Figure 66A). From the ITDR data we confirmed that dC interacts with TS. In order to further examine the time course import of dC in to the cells, $ITDR_{CETSA}$ experiment was performed at 48^0C by treating the cells with a range of dC concentrations at different time intervals (Figure 66B). The data showed that dC gets imported in to the cells in a faster rate, within 10 minutes of treatment. However, no saturation was observed in dC accumulation even after 60 minutes of treatment.

A

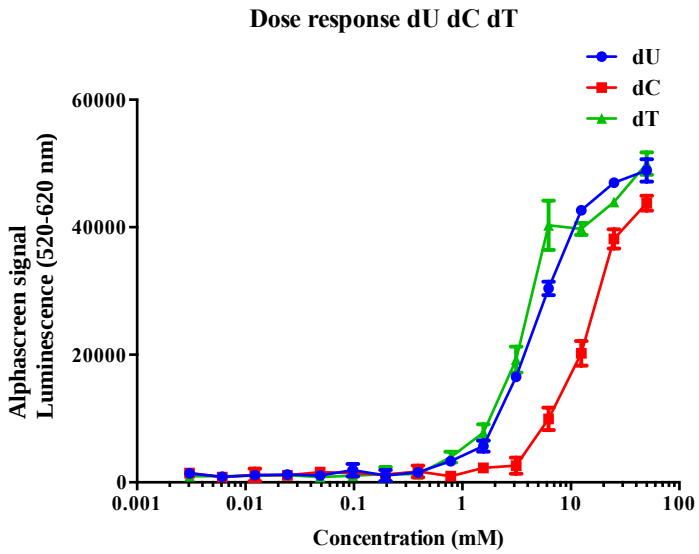

B

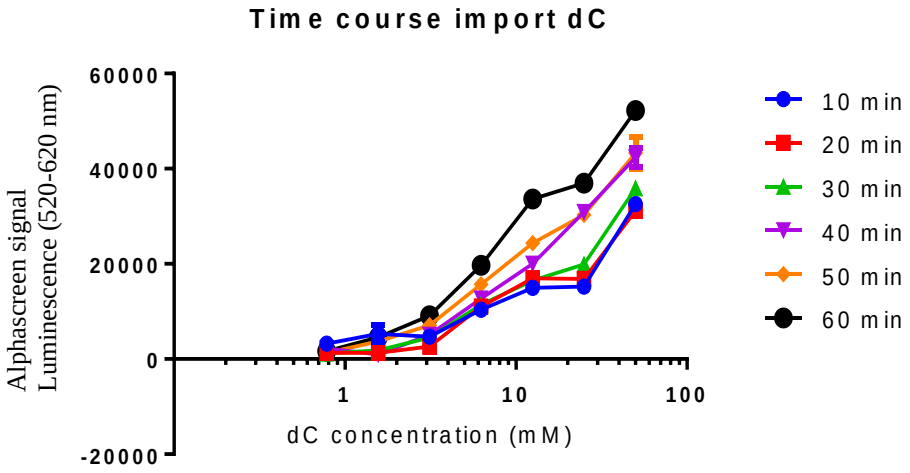

Figure 66: ITDR$_{CETSA}$ and time course import of nucleosides

ITDR$_{CETSA}$ of dU, dC and dT in K562 cells at 48^{0}C (A) and time course import of dC in K562 cells (B). The ITDR$_{CETSA}$ is representative of two technical replicates from single experiment.

We performed further studies to understand the dCMP interaction with TS, as it was unexpected. To examine this interaction further, an enzymatic assay was done on recombinant TS with dCMP. The enzymatic assay results demonstrated that dCMP inhibits TS activity and it induced a thermal shift at a much higher concentration as compared to dTMP (Figure 67A). The crystal structure of TS in presence of dCMP was determined by Dr. Chen Dan in our group, which shows that dCMP indeed binds to the active site of TS (Figure 67B). There was a difference in the thermal response of dCMP and dTMP, which suggests that the dominant TS species in the lysate and the recombinant protein is different. To understand the role of dCMP as a TS regulator, further studies need to be done.

This interaction may not be involved in the drug resistance mechanisms to TS specific drugs as the drugs have a higher affinity (lower nanomolar range) to TS when compared to dCMP (micromolar range). Therefore it is not correlative to TS interaction with the protein specific drugs.

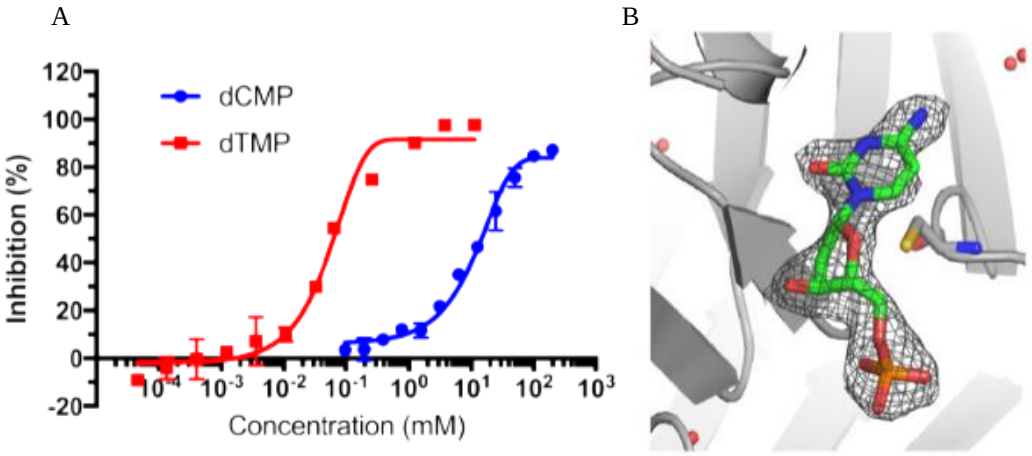

Figure 67: dCMP interaction with TS

Effect of dCMP versus dTMP on TS activity (A). Binding site of dCMP and dUMP to TS. Crystal structure of TYMS complexed with dCMP, shown with 2Fo-Fc density map around dCMP contoured at 1.0 sigma (B).

We also discovered several novel metabolite-protein interactions from these studies (Figure 68). The $ITDR_{CETSA}$ data of dNMPs showed that the enzyme UMP-synthase (UMPS), a bifunctional enzyme involved in the de novosynthesis of UMP interacted with all the dNMPs except dAMP. This suggests that UMP synthesis is regulated by dNMP pools at higher concentrations. The 7-methylguanosine specific 5' -nucleotidase (NT5C3B) exhibited an unexpected interaction with dTMP, which indicates that it has a wider specificity than reported in existing studies.

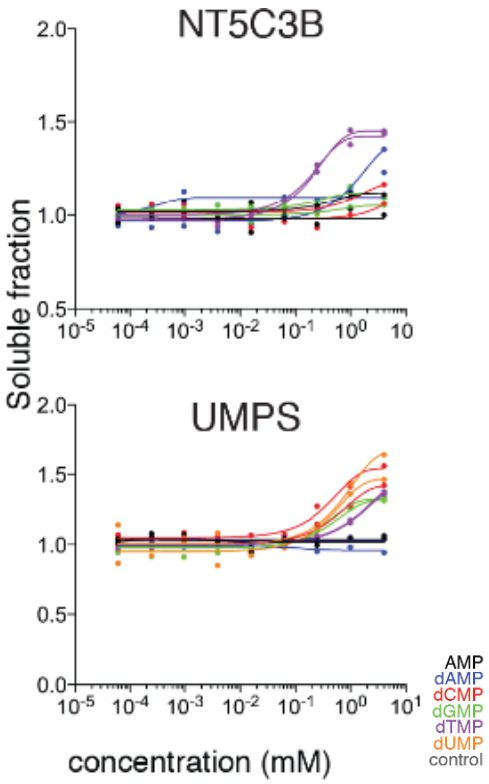

Figure 68: The unanticipated protein hits from the dNMP-ITDR data

The proteins that are associated with nucleotide metabolism; 7-methylguanosine specific 5' -nucleotidase (NT5C3B) and UMP synthase (UMPS).

The in cell ITDR$_{CETSA}$ experiment with dU, dC, dT followed by mass spectrometry revealed that CETSA could pick up the important enzymes associated with the nucleotide synthesis pathway. Enzymes such as Ribonucleoside-diphosphate reductase (RNR), Deoxyuridine 5'-triphosphate nucleotidohydrolase (dUTPase), Thymidylate synthase (TS) and Thymidylate Kinase (TK), the major enzymes related to nucleotide synthesis responded to the nucleoside treatment and gave dose-dependent stabilization (Figure 69).

A

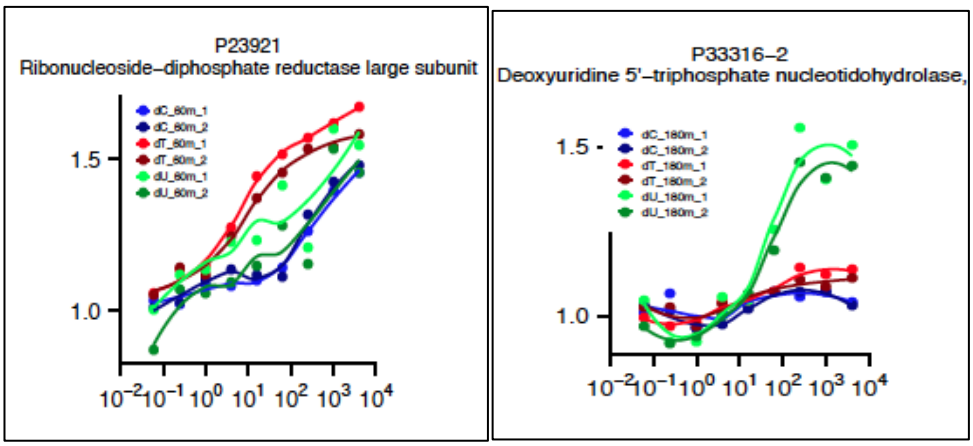

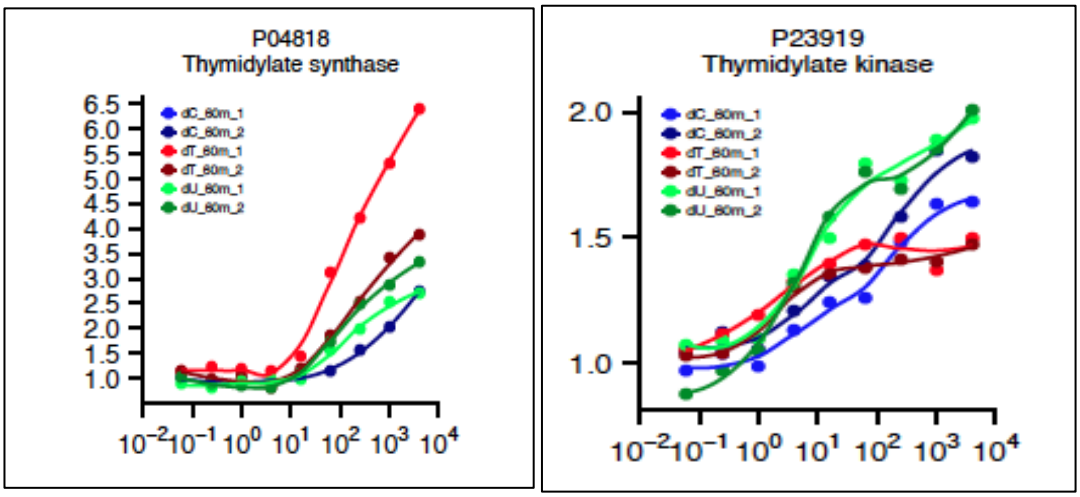

B

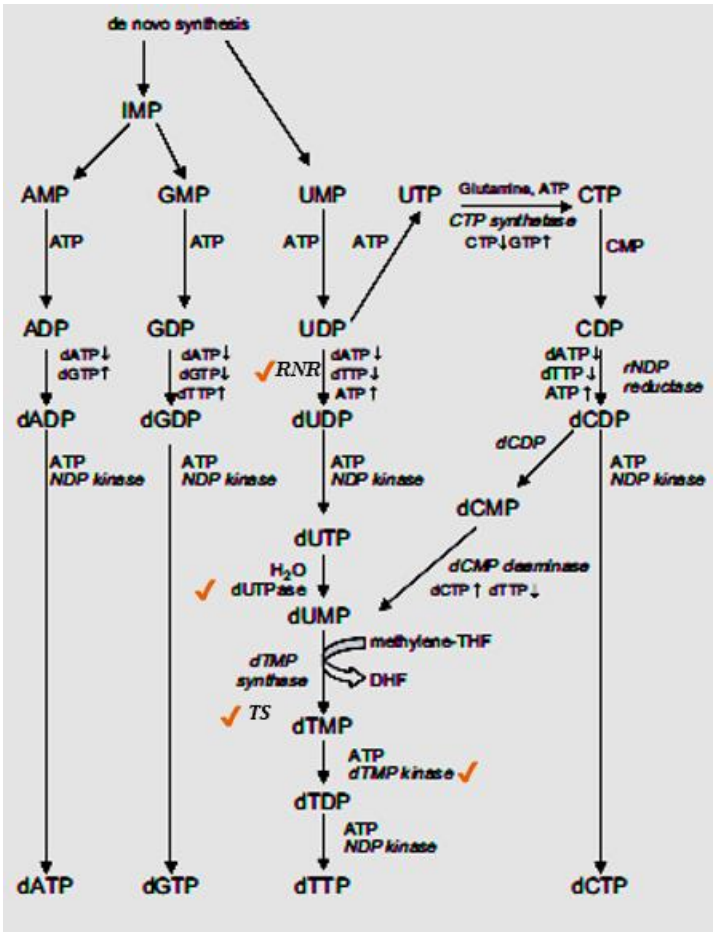

Figure 69: Enzymes in the nucleotide synthesis pathway

Important enzymes associated with the nucleotide synthesis pathway responding to the in-cell nucleoside treatment (A). The nucleotide synthesis pathway in cells and the proteins involved in it (B).

We also showed that CETSA could identify known and novel redox proteins. This study was done using NAD(P)H, the nucleotide-based redox metabolite. The $ITDRF_{CETSA}$ data of NADPH was collected to validate the known interactions and to discover the novel ones. A hit list consisting of 40 proteins was generated, out of which 30 were mostly reductases and dehydrogenases that are predicted NAD(P) binding proteins. One of the hits was a fatty acid synthase with 2500 amino acid residues and six catalytic domains. Only two out of the six catalytic domains are predicted to interact with NADP [133]. This showed that even large proteins can produce informative CETSA data. An unexpected protein coronin 1c was found to interact with NADPH that suggests a previously unrevealed interaction. We also performed in-cell CETSA studies to identify protein-metabolite interactions associated with changes in proteome due to thymine-induced cell cycle arrest. In cells treated with thymidine, CETSA identified the intracellular interaction of thymidine metabolites to critical proteins in the deoxyribonucleotide metabolism. Novel interactions were also discovered and validated.
These studies support that MS-CETSA can be implemented to understand the intracellular metabolite interactions that were previously difficult to map.

CHAPTER 4: DISCUSSION

Monitoring drug-target engagement in cells and tissues is playing an increasingly important role in drug discovery to optimize drug binding and to confirm that the effects seen of novel drug candidates are indeed due to the anticipated drug target. In this work, we show that CETSA can be used for a variety of applications: for example, confirming drug target engagement in cells, monitor the complex processes involved in the drug transport, drug efflux and influx, the development of drug resistance towards cancer drugs and interaction of metabolites with the human proteome. The studies performed using CETSA suggest that this method could be applicable for a wide range of soluble intracellular and extracellular drug targets. However, CETSA is not likely to work for highly inhomogeneous proteins or for proteins that do not aggregate upon the unfolding of the ligand-binding domain [75].

TPA, developed in parallel with CETSA could be used as a highly sensitive screening assay for high throughput fragment screening. TPA enables screening at a very low protein concentration, using simple and low-cost equipment. A buffer screen can also be performed with TPA before purification to determine at which buffer conditions (pH, salt etc.) the protein is more stable. TPA was used for fragment screening of several targets such as hPARP1, hTNKS2 and hCA2 and, the hits were validated using dose response experiments. The overlap of TPA hits from the hPARP1 screen in two different matrices shows that TPA can be used for screening purified proteins as well as over-expressed, unpurified proteins in lysates. This enables the screening of low expressing targets that are hard to purify. The hits from hPARP1 screen were validated using DSF and DSLS and good correlation was observed. This demonstrates that TPA is a good alternative to other commonly used thermal shift assays such as DSF and DSLS. When the prominent hPARP1 hits were tested in HeLa lysate using CETSA, they showed stabilization in the protein melt curve. This example shows how TPA screen can be extended to a CETSA study to monitor target engagement in cell lysate and whole cells.

TPA results showed good correlation to DSLS results when used to compare the melting profile of thymidylate synthase in buffer, *e-coli* lysate and mammalian cell lysate. The melting temperature of TS was found to be different in different matrices. This is because the environment in which the protein is present acts on its stability. The protein would have a different melting profile in a complex system such as cell lysate and intact cells when compared to a buffer system due to the presence of substrates, co-factors and other proteins.

CETSA was developed and used to validate several clinical drug targets. Iniparib, the proposed PARP1 inhibitor failed in the phase III clinical trials, where it demonstrated lack of activity to PARP1 in living cells [75]. Apparently, it was later found that iniparib kills cancer cells by unspecific alterations of cysteine residues [134]. Our CETSA studies showed that olaparib, the well-established PARP1 inhibitor produced a large thermal shift in the protein melt curve, while iniparib failed to produce a shift. This study using hPARP1 and inhibitors showed that using CETSA, Drug targets can be validated before making big investments in clinical trials.

CETSA was implemented to study drug resistance, which is a major hindrance in cancer therapy. Thymidylate synthase and the antifolate and fluoropyrimidine inhibitors were used to demonstrate that CETSA is a useful tool to study resistance development. With the CETSA melt curves we could directly monitor drug target engagement in the resistant cells. For example, we observed slow washout of raltitrexed and the 5FU both in RX resistant and 5FU resistant cells. We observed using CETSA, the likely reversion of the resistant cells back to the parental form during recovery from drug treatments, where the non-resistant clones overtook the resistant clones during recovery. On the other hand, in the methotrexate resistant cells we did not see any target engagement after treatment. Later, we found that the RFC protein responsible for the MX transport in to the cells is strongly downregulated in the MX resistant cells likely explaining the resistance in these cell lines. Studies show that downregulation of RFC is a very common and well-studied mechanism that causes resistance to antifolate drugs [128], and with CETSA we could directly monitor this mechanism of antifolate resistance. Because of the RFC downregulation, the methotrexate resistant cells were resistant also to other classical antifolates that require active transport to enter the cells. The significant downregulation of RFC in the resistant cells is the or one of the possible reasons for resistance development that was monitored by CETSA.

In the RX resistant cells, we observed that even when TS is inhibited, the cells could proliferate. This means that even when TS, the enzyme essential for thymidine synthesis is inhibited, the resistant cells obtained thymidine from another source. One possibility is that there could be a backup enzyme for TS in the resistant cells, which is producing thymidine for these cells to survive and proliferate. We tested the hypothesis that NNMT could use uracil/uridine as a substrate to generate thymine/thymidine. However, binding and enzyme assays on the purified NNMT did not support this hypothesis. But there is a possibility that NNMT in the resistant

cells might have undergone some modifications such as phosphorylation or post translational modification, which is essential for it to act as the backup enzyme for TS. To test this, we are currently looking at NNMT in the resistant cells using western blot to see if there is dose response behaviour when the cells are treated with the TS substrate uridine. Another efficient way to understand if this hypothesis is true is by doing an NNMT knock down in the resistant cells. If NNMT helps to maintain the in-cell thymidine levels during the absence of TS in the resistant cells, knock down of this protein should lead to cell death.

The de novo pathway and salvage pathway are the two sources of dNTP pools within the cells. Thymidylate synthase does the de novo synthesis of thymidylate from deoxyuridylate and methylenetetrahydrofolate. In the salvage pathway, the bases and nucleosides from RNA or DNA catabolism are recycled to produce dNTPs. The de novo synthesis of thymidine is shut down in the RX resistant cells due TS inhibition. If the hypothesis of NNMT or other proteins acting as back up enzyme for TS in the resistant cells is false, then the only source of thymidylate for these cells is through the salvage pathway.

The transport of nucleosides in to the cells is via the nucleoside transporter proteins. These compounds are then phosphorylated by nucleoside kinases such as thymidine kinase 1 and 2, deoxycytidine kinase or deoxyguanosine kinase [135]. Another hypothesis that explains the survival and proliferation of the RX resistant cells during the absence of TS is that the nucleoside transporters and/or the nucleoside kinases mentioned above are modified in these cells. The upregulation or mutations in these proteins can cause increased thymidine production via the salvage pathway. This thymidine produced could be sufficient for the resistant cells to proliferate even when TS is inhibited. Sequencing the nucleoside transporters and nucleoside kinases in the parent and resistant cells will help to test this hypothesis. Also, the expression levels of these proteins can be compared in the parent and resistant cell lines to see if there is a difference that can contribute to resistance. The in-cell thymidine levels of parent and resistant cells should be compared to answer this question, experiments which are in progress.

RFC protein is responsible for transporting both RX and MX and both these drugs undergo polyglutamation and retention in the cells. It was interesting to observe that the resistance mechanisms for these drugs are different in our studies. Downregulation of RFC contributed to low target engagement and therefore resistance to methotrexate, while target engagement

was observed in the RX resistant cells that seemed to invoke resistance by a different mechanism. A possible reason for this difference could be that the technique used for developing drug resistance was different in these cell lines. We developed RX resistant cell lines in house using pulse strategy, while the MX resistant cells were obtained from a cell repository. Because of this difference it is possible that the cells get reprogrammed in different ways, which lead to different mechanisms of resistance. Also, the parent cell lines used for developing RX and MX resistance are different. RX resistance was developed on leukaemia cell lines (K562), whereas breast cancer cell line (HCC1806) was used for developing MX resistance. These different resistant mechanisms are true only for these cell lines and could be different in other cell lines.

Upregulation of the target protein itself is a well-studied mechanism causing drug resistance [136]. In the 5FU resistant cells it was observed that the upregulation of the target enzyme TS lead to development of drug resistance because the drug administered was not enough to completely inhibit the target.
The nolatrexed resistant cells revert to the parental form within a day of recovery. This reversion supports mechanisms where the drug is rapidly exported out of the cells causing minimal target engagement. The possible reasons for this reversion are activation of efflux pumps and catabolic enzymes.

In conclusion, the study of antifolate and fluoropyrimidine drug resistance using CETSA revealed several well studied mechanisms of drug resistance and also other potential processes that needs further investigation. The reported mechanisms such as downregulation of RFC contributing to MX resistance and upregulation of TS causing 5FU resistance were monitored in our studies. The potential mechanisms causing RX resistance in our study is being investigated and the two hypotheses: presence of backup enzyme for TS and hyperactivation of the salvage pathway are being tested. The study of NX resistance using CETSA is still in the preliminary stage and more data needs to be collected to find out the resistance mechanism.

Our studies show that CETSA has the potential to monitor drug efficiency at the target level in patients. These drug resistance studies were performed on different human cancer cell lines and eventually we would like to apply CETSA on patient biopsies collected at different stages of drug treatment. This would help in understanding the appropriate drug dosage and usage during cancer therapy. We can also monitor the development of acquired drug resistance at the

target engagement level during cancer therapy. In our methotrexate resistance study, we observed that these cell lines are resistant to other antifolate drugs as well due to downregulation of RFC. However, target engagement was observed when these cells were treated with 5FU and nolatrexed, which does not require RFC transport. These studies support that CETSA would be useful to determine the class of drugs to which a patient is resistant, and to propose an alternate drug to which the patient will respond.

We also introduced a stringent technique based on CETSA to study metabolite interactions in the human proteome. Hit generation was done looking at the $ITDR_{CETSA}$ curves, rather than the melt curves and it was proved that CETSA can detect many known metabolite-protein interactions in intact cells that were previously characterized using traditional techniques on purified proteins. From the CETSA studies, we also discovered novel metabolite-protein interactions that were validated using studies on purified proteins.
CETSA is applicable for a wide range of metabolites. Previously, it was not possible to directly monitor the different metabolite interactions in cells and CETSA now enables the discovery and study of novel metabolic steps in cells. As other cell biology, the protein-metabolite interactions should be studied in cells to understand details of such processes. CETSA therefore has the potential to help us understand modulations of cellular metabolic processes that can be associated to certain diseases and proteins that responded to CETSA could potentially be used as biomarkers for specific cellular metabolic distortions. CETSA can also help in discovering novel enzymes associated with metabolic pathways that can be important therapeutic targets.
$ITDR_{CETSA}$ curves were analyzed for selecting the hits in the CETSA experiments. This is a much more distinct strategy compared to the previous approach based on CETSA shifts mainly because by using the ITDR approach, the weak metabolite protein interactions can be detected. The reference and the treated conditions are combined to enable simultaneous sampling, which decreases any inconsistency due to the mass spectrometry runs.

In this thesis, CETSA was used for various applications such as: to study drug target engagement in cancer cells for several important clinical targets, to monitor processes of drug transport and activation in cells, to study drug resistance development in cancer therapy and to study the interactions of metabolites with the human proteome. TPA, the method derived from CETSA was used to perform fragment screening for several protein targets.
The versatility of CETSA would make it an important tool in the field of drug research and development.

CHAPTER 5: FUTURE INVESTIGATIONS

The main future work plans for my project would be the following:

1. To understand the mechanism contributing to RX resistance. The RX resistant cells survive and proliferate even when TS is inhibited. This means these cells are obtaining thymidine from some other source and that could be a backup enzyme for TS or the hyperactivation of proteins in the salvage pathway.
2. To check if NNMT can produce thymine using the substrates of TS in the raltitrexed resistant cells where TS is inhibited. We are currently developing a method that uses mass spectrometry to quantify thymine production, if there is any, when TS substrates are used to carry out the reaction catalysed by NNMT.
3. To compare the in-cell thymine levels of the parent and raltitrexed resistant cells using mass spectrometry. This will help us understand whether the resistant cells receive equal or more thymidine compared to the parent cells.
4. To monitor DHFR in the methotrexate resistant cells using CETSA. DHFR is the enzyme that generates tetrahydrofolates from dihydrofolates and is the primary target of MX.
5. To use CETSA to study the phenomenon of drug resistance development in other class of drugs.
6. To implement CETSA for clinical studies. To obtain patient cell lines/biopsies at different stages of cancer therapy and use CETSA to study the interesting mechanisms that contribute to drug resistance. Also, to find out to which class of drugs the patient is resistant to and propose alternate drugs for treatment.
7. To test new drugs on the resistant cell lines and study the response of different proteins, using mass spectrometry.
8. To perform CETSA experiments to study the effect of different metabolites/drugs/fragments on the thermal profile of cellular proteome, and to discover new target proteins, which shows stabilization in the melt curves, in presence of the metabolites/drugs/fragments.

REFERENCES

1. Anand, P., A.B. Kunnumakkara, C. Sundaram, K.B. Harikumar, S.T. Tharakan, O.S. Lai, B. Sung, and B.B. Aggarwal. (September, 2008). Cancer is a preventable disease that requires major lifestyle changes. Pharm. Res., 25(9):2097-116.
2. Myers M.H, and Ries LA. (1989). Cancer patient survival rates: SEER program results for 10 years of follow-up. CA Cancer J Clin., 39:21-32.
3. Martinez, D., Taylor Parker, M., Fultz, K.E., Ignatenko, N.A., and Gerner, E.W. (2003). Burger's Medicinal Chemistry and Drug Discovery. 6th ed. John Wiley&Sons, Inc.
4. Fearon, E., and Vogelstein, B. (1990). A genetic model for colorectal tumorigenesis. Cell., 61(5): 759-767.
5. Worthley, D. L., Whitehall, V. L., Spring, K. J., and Leggett, B. A. (2007). Colorectal carcinogenesis: Road maps to cancer. World Journal of Gastroenterology: WJG., 13(28):3784–3791.
6. Hennings, H., Glick, A., Greenhalgh, D., Morgan, D., Strickland, J., Tennenbaum, T., and Yuspa, S. 1993. Critical aspects of initiation, promotion, and progression in multistage epidermal carcinogenesis. Experimental Biology and Medicine., 202(1): 1-8.
7. Minamoto, T., Mai, M., and Ronai, Z. (1999). Environmental factors as regulators and effectors of multistep carcinogenesis. Carcinogenesis., 20(4): 519-527.
8. Hanahan, D., and Weinberg, R.A. (2011). Hallmarks of cancer: the next generation. Cell., 144(5):646-74.
9. Bearss, D.J., Hurley, L.H., and Von Hoff, D.D. (2000). Telomere maintenance mechanisms as a target for drug development. Oncogene., 19(56):6632-41.
10. Zafonte, B.T., Hulit, J., Amanatullah, D.F., Albanese, C., Wang, C., Rosen, E., Reutens, A., Sparano, J.A., Lisanti, M.P., and Pestell, R.G. (2000). Cell-cycle dysregulation in breast cancer: breast cancer therapies targeting the cell cycle. Front Biosci., 1(5): D938-61.
11. Suryadinata, R., Sadowski, M., and Sarcevic, B. (2010). Control of cell cycle progression by phosphorylation of cyclin-dependent kinase (CDK) substrates. Bioscience Reports., 30 (4).
12. Vela, L., and Marzo, I. (2015). Bcl-2 family of proteins as drug targets for cancer chemotherapy: the long way of BH3 mimetics from bench to bedside. Curr Opin Pharmacol., 23:74-81.

13. Abou-Ghali, M., and Stiban, J. (2015). Regulation of ceramide channel formation and disassembly: Insights on the initiation of apoptosis. Saudi Journal of Biological Sciences.
14. Semenza, G.L. (2000). HIF-1: mediator of physiological and pathophysiological responses to hypoxia. J Appl Physiol., 88(4):1474-80.
15. Rahimi, N. (2012). The Ubiquitin-Proteasome System Meets Angiogenesis. Mol Cancer Ther., 11(3):538-48.
16. Kandoth, C., McLellan, M.D., Vandin, F., Ye, K., Niu, B., Lu, C., Xie, M., Zhang, Q., McMichael, J.F., Wyczalkowski, M.A., Leiserson, M.D., Miller, C.A., Welch, J.S., Walter, M.J., Wendl, M.C., Ley, T.J., Wilson, R.K., Raphael, B.J., and Ding, L. (2013). Mutational landscape and significance across 12 major cancer types. Nature., 502: 333–339
17. Park, J. (2001). The Cell: A Molecular Approach, Second Edition. The Yale Journal of Biology and Medicine., *74*(5): 361.
18. Dang, C.V. (2012). MYC on the path to cancer. Cell., 149(1):22-35.
19. Chalhoub, N., and Baker, S.J. (2009). PTEN and the PI3-kinase pathway in cancer. Annu Rev Pathol., 4:127-50.
20. Lesko, A.C., Goss, K.H., and Prosperi, J.R. (2014). Exploiting APC function as a novel cancer therapy. Curr drug targets., 15(1):90-102.
21. Giacinti, C., and Giordano, A. (2006). RB and cell cycle progression. Oncogene., 25:5220-5227.
22. Ozaki, T., and Nakagawara, A. (2011). Role of p53 in cell death and human cancers. Cancers., 3:994-1013.
23. Magnol, J.P., and Achache, S. (1983) Cancerologie vétérinaire et comparée. Maloine Editeur., Paris.
24. Gillette, E.L. (1987). Principles of Radiation Therapy. Veterinary Cancer Medicine., 137-143.
25. Theilen, G.H., Madewell, B.R., and Carter, S.K. (1987). Chemotherapy. Veterinary Cancer Medicine., 157-166.
26. Baba, A.I, and Câtoi, C. (2007). Comparative Oncology. Bucharest: The Publishing House of the Romanian Academy. Chapter 19, Principles Of Anticancer Therapy. https://www.ncbi.nlm.nih.gov/books/NBK9546/.

27. Røsland, G.V., and Engelsen, A.S. (2014). Novel points of attack for targeted cancer therapy. Basic and clinical pharmacology and toxicology., 116:9-18.
28. Twomey, J.D., Brahme, N.N., and Zhang, B. (2017). Drug-biomarker co-development in oncology – 20 years and counting. Drug resistance updates., 30:48-62.
29. Boekhout, A.H., Beijnen, J.H., and Schellens, J.H.M. (2011). Trastuzumab. Oncologist., 16:800–810.
30. Pedersen, M.W., Jacobsen, H.J., Koefoed, K., Dahlman, A., Kjær, I., Poulsen, T.T., et al. (2015). Targeting three distinct HER2 domains with a recombinant antibodymixture overcomes trastuzumab resistance. Mol. Cancer Ther., 14: 669–680.
31. Bhamidipati, P.K., Kantarjian, H., Cortes, J., Cornelison, M., and Jabbour, E. (2013). Ther Adv Hematol., 4(2):103-117.
32. Tahir, S.K., Smith, M.L., Hessler, P., Rapp, L.R., Idler, K.B., Park, C.H., Leverson, J.D., and Lam, L.T. (2017). Potential mechanisms of resistance to venetoclax and strategies to circumvent it. BMC cancer., 17:399.
33. Herrera-Abreu, M.T., Palafox, M., Asghar, U., Rivas, M.A., Cutts, R.J., Garcia-Murillas, I., Pearson, A., Guzman, M., Rodriguez, O., Grueso, J., Bellet, M., Cortés, J., Elliott, R., Pancholi, S., Baselga, J., Dowsett, M., Martin, L.A., Turner, N.C., and Serra, V. (2016). Early Adaptation and Acquired Resistance to CDK4/6 Inhibition in Estrogen Receptor-Positive Breast Cancer. Cancer Res., 76(8):2301-13.
34. Sweeny K. Technology trends in drug discovery and development: implications for the development of the pharmaceutical industry in australia. Pharmaceutical Industry Project Equity, Sustainability and Industrial Development, Working Paper Series; 2002.
35. Prakash, N., and Devangi, P. (2010). Drug Discovery. J Antivirals Antiretrovirals., 2 (4).
36. Harvey, A.L. (2008). Natural products in drug discovery. Drug Discov Today., 13:894-901.
37. Morgan, S., Grootendorst, P., Lexchin, J., Cunningham, C., and Greyson, D. (2011). The cost of drug development: a systematic review. Health Policy., 100 (1):4-17.
38. Smith, C.G., and O'Donnell, J.T. (2006). Overview of the current process of new drug discovery and development. Informa healthcare., 7-13.
39. Ratti, E., and Trist, D. (2001). Continuing evolution of the drug discovery process. Pure Appl Chem., 73:67-75.

40. Verpoorte, R. (1998). Exploration of nature's chemodiversity: the role of secondary metabolites as leads in drug development. Drug Discov Today., 3:232-8.
41. Sneader, W. (2005). Drug Discovery: A history. Wiley (NY).
42. Burger, A. (1970). Medicinal Chemistry. Wiley (NY).
43. Walsh, G. (2007). Pharmaceutical biotechnology: Concepts and applications. John Wiley (UK).
44. Boehm, H.J., Boehringer, M., Bur, D., Gmuender, H., Huber, W., Klaus, W., Kostrewa, D., Kuehne, H., Luebbers, T., Meunier-Keller, N., and Mueller, F. (2000). Novel inhibitors of DNA gyrase: 3D structure based biased needle screening, hit validation by biophysical methods, and 3D guided optimization. A promising alternative to random screening. J Med Chem., 43(14):2664-74.
45. Umashankar, V., and Gurunathan, S. (2015). Drug discovery: An appraisal. International Journal of Pharmacy and Pharmaceutical Sciences., 7(4):59-66.
46. Du, G.H. (2004). Evaluation and validation of drug targets. Acta Pharmacol Sin., 25:1566.
47. Bischof, J., and HE, X. (2005). Thermal Stability of Proteins. Annals of the New York Academy of Sciences., 1066, 12-33.
48. Fields, P. (2001). Review: Protein function at thermal extremes: Balancing stability and flexibility. Comparative Biochemistry and Physiology Part A: Molecular & Integrative Physiology., 129(2-3): 417-431.
49. Ericsson, U., Hallberg, B., Detitta, G., Dekker, N., and Nordlund, P. (2006). Thermofluor-based high-throughput stability optimization of proteins for structural studies. Analytical Biochemistry., 357(2):289-298.
50. Kopec, J., and Schneider, G. (2011). Comparison of fluorescence and light scattering based methods to assess formation and stability of protein–protein complexes. Journal of Structural Biology., 175(2):216-223.
51. Ó'Fágáin, C. (2011). Protein Chromatography: Methods and Protocols, Methods in Molecular Biology (10.1007/978-1-60761-913-0_7 ed., Vol. 681). Springer science.
52. Fu, J., Momˇciloviˊc, I., and Vara Prasad, P.V. (2012). Roles of Protein Synthesis Elongation Factor EF-Tu in HeatTolerance in Plants. Journal of Botany.
53. Pantoliano, M., Petrella, E., Kwasnoski, J., Lobanov, V., Myslik, J., Graf, E., Carver, T., Asel, E., Springer, B.A., Lane, P., and Salemme, F.R. (2001). High-Density Miniaturized Thermal Shift Assays as a General Strategy for Drug Discovery. Journal of Biomolecular Screening., 6(6):429-40.

54. Senisterra, G., Markin, E., Yamazaki, K., Hui, R., Vedadi, M., & Awrey, D. (2006). Screening for Ligands Using a Generic and High-Throughput Light-Scattering-Based Assay. Journal of Biomolecular Screening., 11(8):940-8.
55. Koshland, D.E. (1958). Application of a Theory of Enzyme Specificity to Protein Synthesis. Proceedings of the National Academy of Sciences of the United States of America., **44** (2): 98–104.
56. Linderstrøm-Lang, K., and Schellman, J. A. (1959). Protein structure and enzyme activity. The Enzymes., **1** (2): 443–510.
57. Ciulli, A. (2013). Biophysical screening for the discovery of small-molecule ligands. Methods Mol Biol., 1008:357-388.
58. Semisotnov, G.V., Rodionova, N.A., Razgulyaev, O.I., Uversky, V.N., Gripas', A.F., and Gilmanshin, R.I. (1991). Study of the "molten globule" intermediate state in protein folding by a hydrophobic fluorescent probe. Biopolymers., **31** (1): 119–28.
59. Vivoli, M., Novak, H., Littlechild, J., and Harmer, N. (2014). Determination of Protein-ligand Interactions Using Differential Scanning Fluorimetry. Journal of Visualized Experiments., (91): 51809.
60. Lo, M., Aulabaugh, A., Jin, G., Cowling, R., Bard, J., Malamas, M., and Ellestad, G. (2004). Evaluation of fluorescence-based thermal shift assays for hit identification in drug discovery. Analytical Biochemistry., 332(1):153-9.
61. E. Nettleship, J., Brown, J., R Groves, M., and Geerlof, A. (2008). Methods for Protein Characterization by Mass Spectrometry, Thermal Shift (ThermoFluor) Assay, and Multiangle or Static Light Scattering. Methods Mol Biol., 426:299-318.
62. Alexandrov, A., Mileni, M., Chien, E., Hanson, M., and Stevens, R. (2008). Microscale Fluorescent Thermal Stability Assay for Membrane Proteins. Structure, 16(3):351-9.
63. Johnson, C. (2013). Differential scanning calorimetry as a tool for protein folding and stability. Archives of Biochemistry and Biophysics., 531(1-2):100-9.
64. Senisterra, G., Markin, E., Yamazaki, K., Hui, R., Vedadi, M., and Awrey, D. (2006). Screening for Ligands Using a Generic and High-Throughput Light-Scattering-Based Assay. J Biomol Screen., 11(8):940-8.
65. Drescher, D. G., Ramakrishnan, N.A., and Drescher, M.J. (2009). Surface Plasmon Resonance (SPR) Analysis of Binding Interactions of Proteins in Inner-Ear Sensory Epithelia. Methods in Molecular Biology., 493: 323–343. http://doi.org/10.1007/978-1-59745-523-7_20.

66. Patching, S.G. (2014). Surface plasmon resonance spectroscopy for characterisation of membrane protein–ligand interactions and its potential for drug discovery. Biochimica et Biophysica Acta., 1838: 43-45.
67. Perozzo, R., Folkers, G., and Scapozza, L. (2004). Thermodynamics of protein–ligand interactions: History, presence, and future aspects. J Recept Signal Transduct Res., 24(1-2):1-52.
68. Peters, W. B., Frasca, V., and Brown, R.K. (2009). Recent developments in isothermal titration calorimetry label free screening. Comb Chem High Throughput Screen., 12(8):772-90.
69. Holdgate, G. A., and Ward, W.H. (2005). Measurement of binding thermodynamics in drug discovery. Drug Discov Today., 10(22):1543-50.
70. Nunez, S., Venhorst, J., and Kruse, C.G. (2012). Target–drug interactions: First principles and their application to drug discovery. Drug Discov. Today., 17(1-2):10-22.
71. Song, C., Zhang, S., and Huang, H. (2015). Choosing a suitable method for the identification of replication origins in microbial genomes. Front. Microbiol. https://doi.org/10.3389/fmicb.2015.01049.
72. Schürmann, M., Janning, P., Ziegler, S., and Waldmann, H. (2016). Small-Molecule Target Engagement in Cells. Cell Chem Biol., 23(4):435-41.
73. Sun, Y.S., Hays, N.M., Periasamy, A., Davidson, M.W., and Day, R.N. (2012). Monitoring protein interactions in living cells with fluorescence lifetime imaging microscopy. Int J Mol Sci., 13(11): 14385–14400.
74. Simon, G.M., Niphakis, M.J., and Cravatt, B.F. (2013). Determining target engagement in living systems. Nat. Chem. Biol. 9(4), 200–205.
75. Molina, D., Jafari, R., Ignatushchenko, M., Seki, T., Larsson, E., Dan, C., Sreekumar, L., Cao, Y., and Nordlund, P. (2013). Monitoring Drug Target Engagement in Cells and Tissues Using the Cellular Thermal Shift Assay. Science, 341(6141):84-87.
76. Auld, D., Thorne, N., Maguire, W., and Inglese, J. (2009). Mechanism of PTC124 activity in cell-based luciferase assays of nonsense codon suppression. Proc Natl Acad Sci U S A., 106(9):3585-90.
77. Savitski, M.M., Reinhard, F.B., Franken, H., Werner, T., Savitski, M.F., Eberhard, D., Martinez, Molina D., Jafari, R., Dovega, R.B., Klaeger, S., Kuster, B., Nordlund, P., Bantscheff, M., and Drewes, G. (2014). Tracking cancer drugs in living cells by thermal profiling of the proteome. Science., 346(6205):1255784.

78. Alshareef, A., Zhang, H.F., Huang, Y.H., Wu, C., Zhang, J.D., Wang, P., El-Sehemy, A., Fares, M., and Lai, R. The use of cellular thermal shift assay (CETSA) to study Crizotinib resistance in ALK-expressing human cancers. Sci Rep., 6:33710.
79. Axelsson, H., Almqvist, H., Seashore-Ludlow, B., and Lundbäck, T. (2016). Screening for Target Engagement using the Cellular Thermal Shift Assay - CETSA. 2016. Assay Guidance Manual [Internet]. https://www.ncbi.nlm.nih.gov/books/NBK374282/.
80. Jafari, R., Almqvist, H., Axelsson, H., Ignatushchenko, M., Lundbäck, T., Nordlund P., and Martinez Molina, D. (2014). The cellular thermal shift assay for evaluating drug target interactions in cells. Nat Protoc., 9(9):2100-22.
81. Almqvist, H., Axelsson, H., Jafari, R., Dan, C., Mateus, A., Haraldsson, M., Larsson, A., Martinez Molina, D., Artursson, P., Lundbäck, T., and Nordlund, P. (2016). CETSA screening identifies known and novel thymidylate synthase inhibitors and slow intracellular activation of 5-fluorouracil. Nat Commun.;7:11040.
82. Touroutoglou, N., and Pazdur, R. (1996). Thymidylate Synthase Inhibitors. Clinical Cancer Research., 2:227-243.
83. Berg, R.W., Ferguson, P.J., DeMoor, J.M., Vincent, M.D., Vincent, M.D., and Koropatnick, J. The Means to an End of Tumor Cell Resistance to Chemotherapeutic Drugs Targeting Thymidylate Synthase: Shoot the Messenger. (2002). Current Drug Targets., 3(4): 297-309(13).
84. Chu, E., Koeller, D.M., Casey, J.L., Drake, J.C., Chabner, B.A., Elwood, P.C., Zinn, S., and Allegra, C.J. (1991). Autoregulation of human thymidylate synthase messenger RNA translation by thymidylate synthase. Proc Natl Acad Sci U S A., 88(20):8977-81.
85. Chu, E., Voeller, D.M., Jones, K.L., Takechi, T., Maley, G.F., Maley, F., Segal, S., and Allegra, C.J. (1994). Identification of a thymidylate synthase ribonucleoprotein complex in human colon cancer cells. Mol Cell Biol., 14(1):207-13.
86. Wilson, P.M., Danenberg, P.V., Johnston, P.G., Lenz , H.J., and Ladner, R.D. (2014). Standing the test of time: targeting thymidylate biosynthesis in cancer therapy. Nature Reviews Clinical Oncology.,11: 282–298.
87. Farber, S., and Diamond, L.K. (1948). Temporary remissions in acute leukemia in children produced by folic acid antagonist, 4-aminopteroyl-glutamic acid. N Engl J Med., 238(23):787-93.
88. Walling, J. 2006. From methotrexate to pemetrexed and beyond. A review of the pharmacodynamic and clinical properties of antifolates. Investigational New Drugs., 24(1):37-77.

89. Gonen, N., and Assaraf Y.G. (2012). Antifolates in cancer therapy: structure, activity and mechanisms of drug resistance. Drug Resist Updat., 15(4):183-210.
90. Jackman, A.L., Theti, D.S., and Gibbs, D.D. (2004). Antifolates targeted specifically to the folate receptor. Advance Drug Delivery Reviews., 56(8):1111-25.
91. Westerhof, G.R., Schornagel, J.H., Kathmann, I., Jackman, A.L., Rosowsky, A., Forsch, R.A., Hynes, J.B., Boyle, F.T., Peters, G.J., Pinedo, H.M., et al. (1995). Carrier- and receptor-mediated transport of folate antagonists targeting folate-dependent enzymes: correlates of molecular-structure and biological activity. Mol Pharmacol., 48(3):459-71.
92. Thomas, R.J., Williams, M., and Garcia-Vargas, J. (2003). Lessons learned from raltitrexed–quality assurance, patient education and intensive supportive drugs to optimise tolerability. Clin Oncol (R Coll Radiol)., 15(5):227–232.
93. Assaraf, Y.G. 2007. Molecular basis of antifolate resistance. Cancer and Metastasis Reviews., 26(1):153-81.
94. Shih, C., Chen, V.J., Gossett, L.S., Gates, S.B., MacKellar, W.C., Habeck, L.L., Shackelford, K.A., Mendelsohn, L.G., Soose, D.J., Patel, V.F., Andis, S.L., Bewley, J.R., Rayl, E.A., Moroson, B.A., Beardsley, G.P., Kohler, W., Ratnam, M., Schultz, R.M. (1997). LY231514, a pyrrolo[2,3-d]pyrimidine-based antifolate that inhibits multiple folate-requiring enzymes. Cancer Research 57 (6), 1116–1123.
95. Zhao, R., Gao, F., and Goldman, I.D. (2001). Marked suppression of the activity of some, but not all, antifolate compounds by augmentation of folate cofactor pools within tumor cells. Biochemical Pharmacology., 61: 857–865.
96. Webber, S., Bartlett, C.A., Boritzki, T.J., Hilliard, J.A., Howland, E.F., Johnston, A.L., Kosa, M., Margosiak, S.A., Morse, C.A., and Shetty, B.V. (1996). AG337, a novel lipophilic thymidylate synthase inhibitor: in vitro and in vivo preclinical studies. Cancer Chemotherapy and Pharmacology., 37(6): 509–517.
97. Longley, D.B., Harkin, D.P., and Johnston, P.G. (2003). 5-Fluorouracil: Mechanisms of action and clinical strategies. Nature reviews. Cancer., 3: 330-338.
98. Housman, G., Byler, S., Heerboth, S., Lapinska, K., Longacre, M., Snyder, N., and Sarkar, S. (2014). Drug Resistance in Cancer: An Overview. *Cancers*., *6*(3):1769–1792. http://doi.org/10.3390/cancers6031769.
99. Giaccone, G., and Pinedo, H.M. (1996). Drug Resistance. The Oncologist., 1(1,2): 82-87.
100. Belkov, V.M., Krynetski, E.Y., Schuetz, J.D., Yanishevski, Y., Masson, E., Mathew, S., Raimondi, S., Pui, C.H., Relling, M.V., and Evans, W.E. (1999). Reduced Folate

Carrier Expression in Acute Lymphoblastic Leukemia: A Mechanism for Ploidy but not Lineage Differences in Methotrexate Accumulation. Blood., 93:1643-1650.

101. Kastrup, I.B., Worm, J., Ralfkiaer, E., Hokland, P., Guldberg, P., and Grønbaek, K. (2008). Genetic and epigenetic alterations of the reduced folate carrier in untreated diffuse large B-cell lymphoma. European Journal of Haematology., 80(1), 61–66.
102. Saikawa, Y., Knight, C.B., Saikawa, T., Page, S.T., Chabner, B.A., and Elwood, P.C. (1993). Decreased expression of the human folate receptor mediates transport-defective methotrexate resistance in KB cells. Journal of Biological Chemistry., 268, 5293–5301.
103. Kaufman, Y., Ifergan, I., Rothem, L., Jansen, G., and Assara, Y.G. (2006). Coexistence of multiple mechanisms of PT523 resistance in human leukemia cells harboring 3 reduced folate carrier alleles: transcriptional silencing, inactivating mutations, and allele loss. Blood., 107 (8): 3288–3294.
104. Rothem, L., Stark, M., and Assaraf, Y.G. (2004). Impaired CREB-1 phosphorylation in antifolate-resistant cell lines with down-regulation of the reduced folate carrier gene. Molecular Pharmacology., 66 (6): 1536–1543.
105. Barakat, R.R, Li, W., Lovelace, C., and Bertino, J.R. (1993). Intrinsic resistance of cervical squamous cell carcinoma cell lines to methotrexate (MTX) as a result of decreased accumulation of intracellular MTX polyglutamates. Gynecologic Oncology., 51(1):54–60.
106. Mauritz, R., Peters, G.J., Priest, D.G., Assaraf, Y.G., Drori, S., Kathmann, I., Noordhuis, P., Bunni, M.A., Rosowsky, A., Schornagel, J.H., Pinedo, H.M., Jansen, G. (2002). Multiple mechanisms of resistance to methotrexate and novel antifolates in human CCRF-CEM leukemia cells and their implications for folate homeostasis. Biochem Pharmacol., 63(2):105-15.
107. Liani, E., Rothem, L., Bunni, M. A., Smith, C. A., Jansen, G., and Assaraf, Y. G. (2003), Loss of folylpoly-γ-glutamate synthetase activity is a dominant mechanism of resistance to polyglutamylation-dependent novel antifolates in multiple human leukemia sublines. Int. J. Cancer., 103: 587–599.
108. Barnes, M.J., Estlin, E.J., Taylor, G.A., Aherne, G.W., Hardcastle, A., McGuire, J.J., Calvete, J.A., Lunec, J., Pearson, A.D.J., and Newell, D.R. (1999). Impact of polyglutamation on sensitivity to raltitrexed and methotrexate in relation to drug-induced inhibition of de novo thymidylate and purine biosynthesis in CCRF-CEM cell lines. Clinical Cancer Research., 5: 2548–2558.

109. Stark, M., Wichman, C., Avivi, I., and Assaraf, Y.G. (2009). Aberrant splicing of folylpolyglutamate synthetase as a novel mechanism of antifolate resistance in leukemia. Blood., 113 (18): 4362–4369.

110. Schimke, R.T. (1988). Gene amplification in cultured cells. J Biol Chem., 263(13):5989-5992.

111. Jin, J., Huang, M., Wei, H.L., and Liu, G.T. (2002). Mechanism of 5-fluorouracil required resistance in human hepatocellular carcinoma cell line Bel (7402). World J Gastroenterol., 8(6):1029-34.

112. Kawate, H., Landis, D.M., and Loeb, L.A. (2002). Distribution of Mutations in Human Thymidylate Synthase Yielding Resistance to 5-Fluorodeoxyuridine. The Journal of Biological Chemistry., 277: 36304-36311.

113. Chang G., and Roth C.B. (2001). Structure of MsbA from *E. coli*: A homolog of the multidrug resistance ATP binding cassette (ABC) transporters. Science., 293 (5536):1793–1800.

114. Borst P., and Elferink O. (2002). Mammalian ABC transporters in health and disease. Annu. Rev. Biochem., 71:537–592.

115. Schinkel A., Smit J., van Tellingen O., Beijnen J., Wagenaar E., van Deemter L., Mol C., van der Valk M., Robanus-Maandag R., te Riele H., et al. (1994). Disruption of the mouse mdr1a P-glycoprotein gene leads to a deficiency in the blood-brain barrier and to increased sensitivity to drugs. Cell., 77(4):491–502.

116. Sauna Z., and Ambudkar, S. (2001). Characterization of the catalytic cycle of ATP hydrolysis by human P-glycoprotein. The two ATP hydrolysis events in a single catalytic cycle are kinetically similar but affect different functional outcomes. J. Biol. Chem., 276 (15):11653–11661.

117. Bonanno, L., Favaretto, A., and Rosell, R. (2014). Platinum drugs and DNA repair mechanism in lung cancer. Anticancer Res., 34(1):493–502.

118. Selvakumaran, M., Pisarcik, D., Bao, R., Yeung, A., and Hamilton, T. (2003). Enhanced cisplatin cytotoxicity by disturbing the nucleotide excision repair pathway in ovarian cancer cell lines. Cancer Res., 63(6):1311–1316.

119. Olaussen K., Dunant A., Fouret P., Brambilla E., Andre F., Haddad V., Taranchon E., Filipits M., Pirker R., Helmut P., et al. (2006). DNA repair by ERCC1 in non-small-cell lung cancer and cisplatin-based adjuvant chemotherapy. N. Engl. J. Med., 355(10):983–991.

120. Sarkar, S., and Faller, D.V. (2013). Telomere-homilogous G-rich oligonucleotides sensitize human ovarian cancer cells by combination therapy. Nucleic Acid Ther., 23(3):167–174.

121. Sargent, J.M. (2003). The use of the MTT assay to study drug resistance in fresh tumour samples. Recent Results Cancer Res.,161:13-25.

122. Śliwka, L., Wiktorska,K., Suchocki, P., Milczarek,M., Mielczarek,S., Lubelska, K., Cierpiał,T., Łyżwa, P., Kiełbasiński, P., Jaromin,A., Flis,A., and Chilmonczyk, Z. (2016). The comparison of MTT and CVS assays for the assessment of anticancer agent interactions. PLoS One., 11(5): e0155772.

123. Yang, N., Kaur, S., Volinia, S., Greshock, J., Lassus, H., Hasegawa, K., Liang, S., Leminen, A., Deng, S., Smith, L., et al. (2008). Micro RNA microarray identifies Let-7i as a novel biomarker and therapeutic target in human epithelial ovarian cancer. Cancer Res., 68(24):10307–14.

124. Seve, P., Reiman, T., and Dumontet, C. (2010). The role of beta III tubulin in predicting chemoresistance in non-small cell lung cancer. Lung Cancer., 67(2):136–143.

125. Hodgkinson, V.C, Eagle, G.L., Drew, P.J., Lind, M.Y., and Cawkwell, L. (2010). Biomarkers of chemotherapy resistance in breast cancer identified by proteomics: Current status. Cancer Letters., 294(1):13–24.

126. Lippert, T.H., Ruoff, H.J., and Volm, M. (2011). Current status of methods to assess cancer drug resistance. Int J Med Sci., 8(3):245-53.

127. Larsson, E., Jansson, A., Ng, F.M., Wen Then, S., Panicker, R., Liu, B., Sangthongpitag, K., Pendharkar, V., Tai, S.J., Hill, J., Dan, C., et al. (2013). Fragment-Based Ligand Design of Novel Potent Inhibitors of Tankyrases. *J. Med. Chem.*, 56 (11):4497–4508.

128. Bertino, J.R., Göker, E., Gorlick, R., Li, W.W., and Banerjee, D. (1996). Resistance Mechanisms to Methotrexate in Tumors. Oncologist., 1(4):223-226.

129. Lin, L., Asthana, S., Chan, E., Bandyopadhyay, S., Martins, M.M., Olivas, V., Jiacheng Yan, J., Pham, L., Wang, M.M., Bollag, G., Solit, D.B., Collisson, E.A., Rudin, C.M., Taylor, B.S., and Bivona, T.G. (2014). Mapping the molecular determinants of BRAF oncogene dependence in human lung cancer. PNAS., 111(7): E748-E757.

130. Hrustanovic, G., Olivas, V., Pazarentzos, E., Tulpule, A., Asthana, S., Blakely, C.M., Okimoto, R.A., Lin, L., Neel, D.S., Sabnis, A., et al. (2015). RAS-MAPK dependence underlies a rational polytherapy strategy in EML4-ALK-positive lung cancer. Nat Med., 21(9):1038-47.

131. Ohashi, K., Sequist, L.V., Arcila, M.E., Moran, T., Chmielecki, J., Lin, Y.L., Pan, Y., Wang, L., de Stanchina, E., Shien, K., et al. (2012). Lung cancers with acquired resistance to EGFR inhibitors occasionally harbor BRAF gene mutations but lack mutations in KRAS, NRAS, or MEK1. Proc Natl Acad Sci U S A., 109(31):E2127-33.
132. Becher, I., Werner, T., Doce, C., Zaal, E., Tögel, I., Khan, C., Rueger, A., Muelbaier, M., Salzer, E., Berkers, C., Fitzpatrick, P., Bantscheff, M., and Savitski, M., M. (2016). Thermal profiling reveals phenylalanine hydroxylase as an off-target of panobinostat. Nature Chemical Biology., 12:908–910.
133. Jayakumar, A., Chirala, S. S., and Wakil, S. J. (1997). Human fatty acid synthase: assembling recombinant halves of the fatty acid synthase subunit protein reconstitutes enzyme activity. Proc Natl Acad Sci U S A., 94:12326-12330.
134. Liu, X., Shi, Y., Maag, D.X., Palma, J.P., Patterson, M.J., Ellis, P.A., Surber, B.W., Ready, D.B., Soni, N.B., Ladror, U.S., Xu, A.J., Iyer, R., et al. (2012). Iniparib nonselectively modifies cysteine-containing proteins in tumor cells and is not a bona fide PARP inhibitor. Clin Cancer Res., 18(2):510-23.
135. Galmarini, C.M., Mackey, J.R., and Dumontet, C. (2001). Nucleoside analogues: mechanisms of drug resistance and reversal strategies. Leukemia., 15:875–890.
136. Oguri, T., Achiwa, H., Bessho, Y., Muramatsu, H., Maeda, H., Niimi, T., Sato, S., and Ueda, R. (2005) The role of thymidylate synthase and dihydropyrimidine dehydrogenase in resistance to 5-fluorouracil in human lung cancer cells. Lung Cancer., 49(3):345-51.

APPENDIX

Table 6: Compound hits from the TPA screen

Compound ID	Structure	Name	Molecular weight	Formula
12	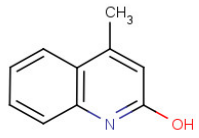	4-methylquinolin-2-ol	159.18	C10H9NO
35	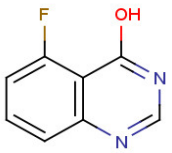	5-fluoroquinazolin-4-ol	164.14	C8H5FN2O
39	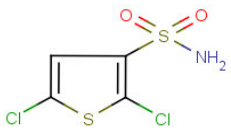	2,5-dichlorothiophene-3-sulfonamide	232.11	C4H3Cl2NO2S2
44	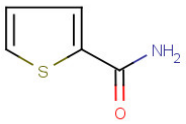	Thiophene-2-carboxamide	127.16	C5H5NOS
99	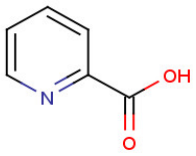	Picolinic acid	123.11	C6H5NO2
101	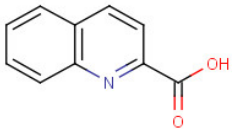	Quinaldic acid	173.17	C10H7NO2
106	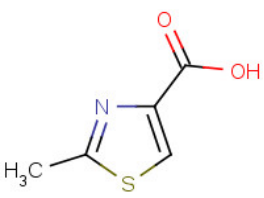	2-methyl-1,3-thiazole-4-carboxylic acid	143.16	C5H5NO2S

149	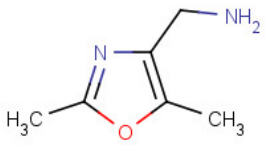	(dimethyl-1,3-oxazol-4-yl) methanamine	126.16	C6H10N2O
160	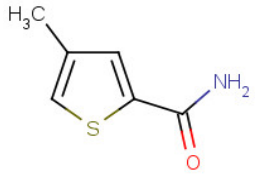	4-methylthiophene-2-carboxamide	141.19	C6H7NOS
163	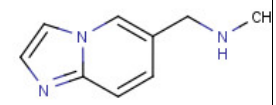	{imidazo[1,2-a]pyridin-6-ylmethyl}(methyl)amine	161.20	C9H11N3
398	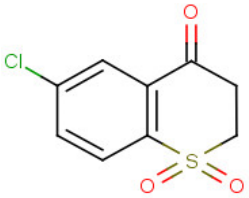	6-chloro-2,3-dihydro-1$l^{6}-benzothiopyran-1,1,4-trione	230.67	C9H7ClO3S
489	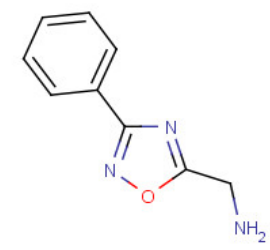	(3-phenyl-1,2,4-oxadiazol-5-yl)methanamine	175.19	C9H9N3O
495	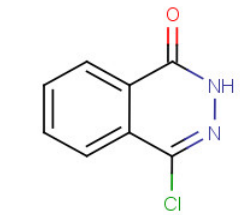	4-chloro-2H-phthalazin-1-one	180.59	C8H5ClN2O

Table 7: Protein ID and details of thymidylate synthase from the proteome profiling experiment using mass spectrometry

Accession	Description	Coverage	Peptides	PSMs	Unique peptides	Protein groups	Molecular weight
Q53Y97	Thymidylate synthase	14%	3	4	3	1	35.7

Table 8: MS/MS spectrum information of thymidylate synthase

Best PSM ambiguity	MS order	PSM	Isolation interference	Ion inject time	Precursor m/z (Da)	Precursor MH+ (Da)	Precursor charge	RT (min)	First scan
Unambiguous	MS2	1	19	46.589	730.30	2917.34	4	69.09	28308

A

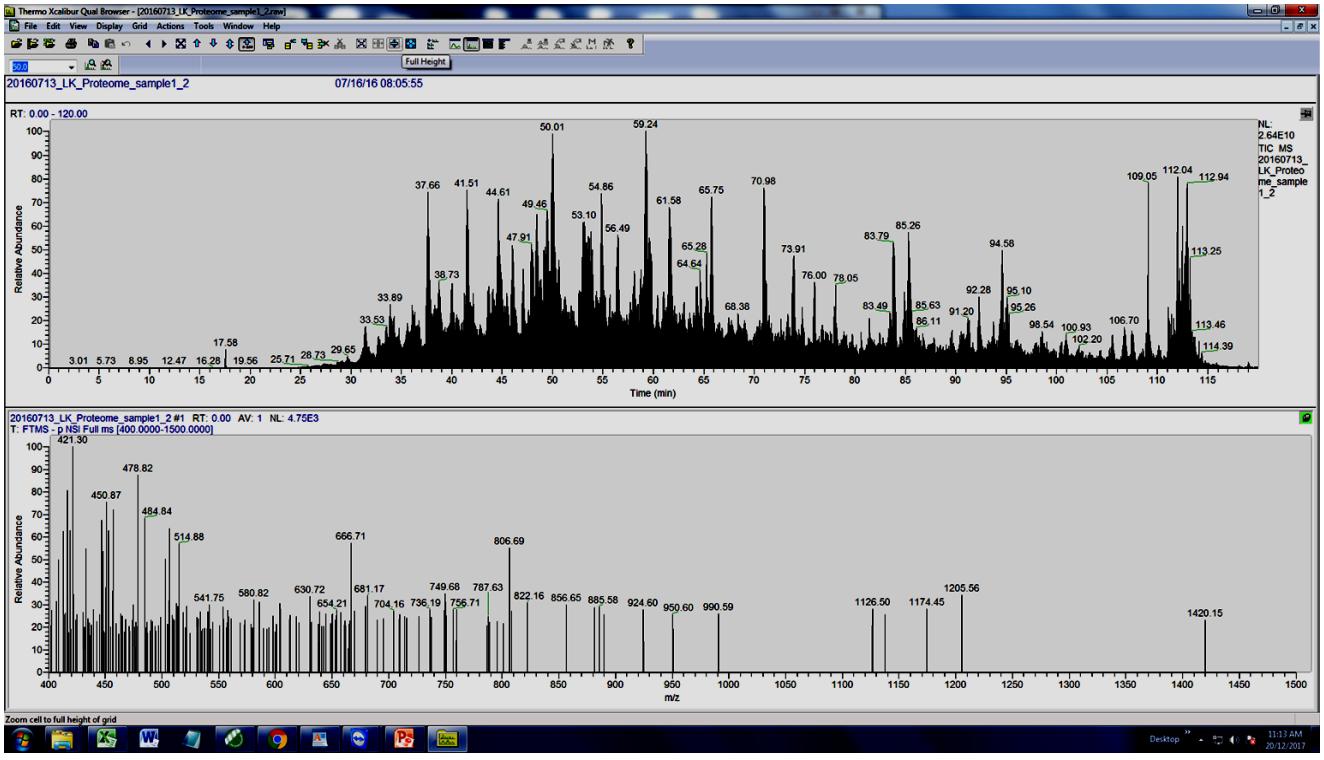

B

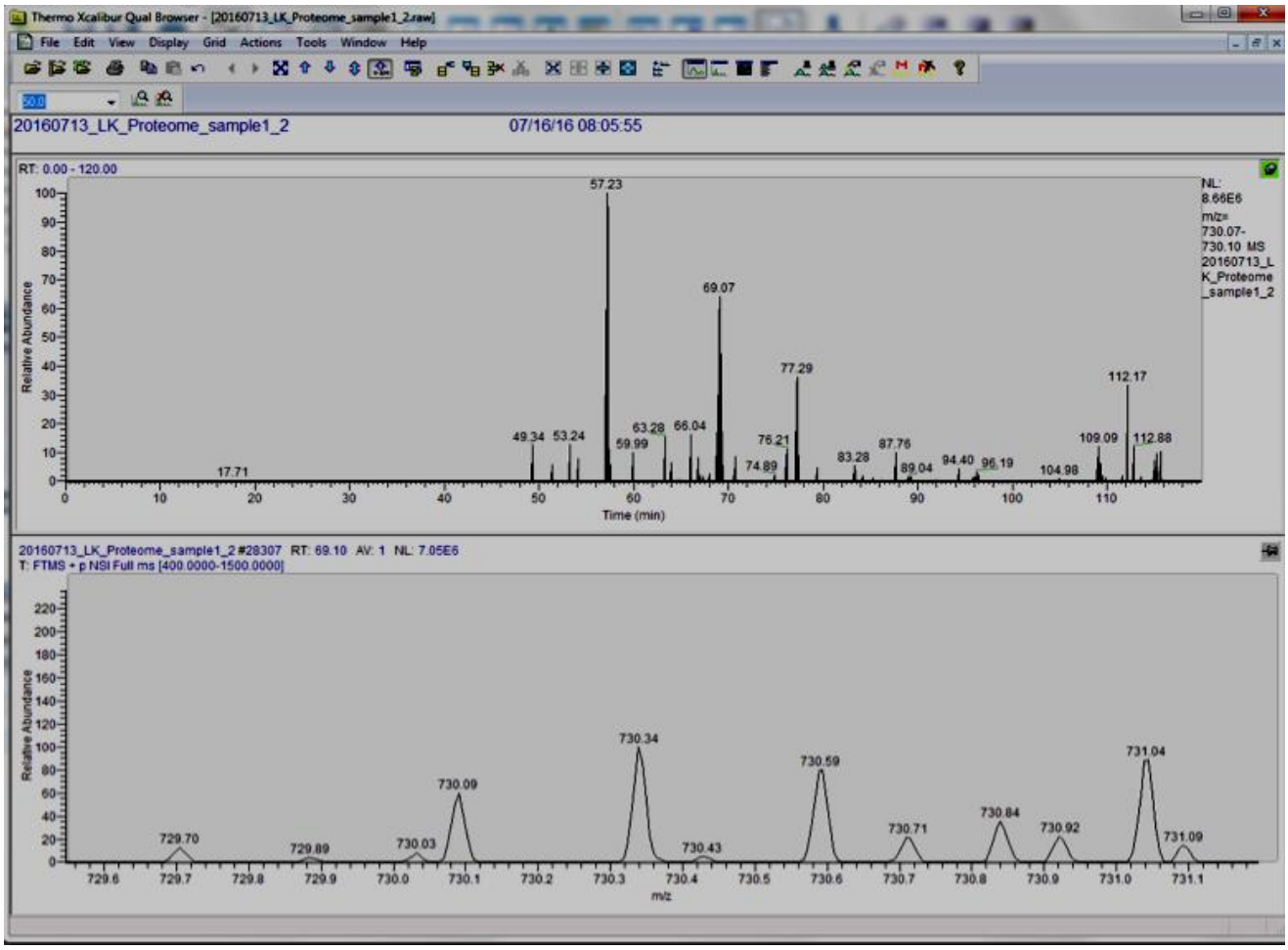
Thermo Xcalibur Qual Browser - [20160713_LK_Proteome_sample1_2.raw]
File Edit View Display Grid Actions Tools Window Help
20160713_LK_Proteome_sample1_2
07/16/16 08:05:55
RT: 0.00 - 120.00
Relative Abundance
Time (min)
NL: 8.66E6 m/z= 730.07-730.10 MS 20160713_LK_Proteome_sample1_2
57.23
69.07
77.29
112.17
49.34
53.24
59.99
63.28
66.04
74.89
76.21
83.28
87.76
89.04
94.40
96.19
104.98
109.09
112.88
17.71
20160713_LK_Proteome_sample1_2 #28307 RT: 69.10 AV: 1 NL: 7.05E6
T: FTMS + p NSI Full ms [400.0000-1500.0000]
730.34
730.09
730.59
731.04
729.70
729.89
730.03
730.43
730.71
730.84
730.92
731.09
m/z

C

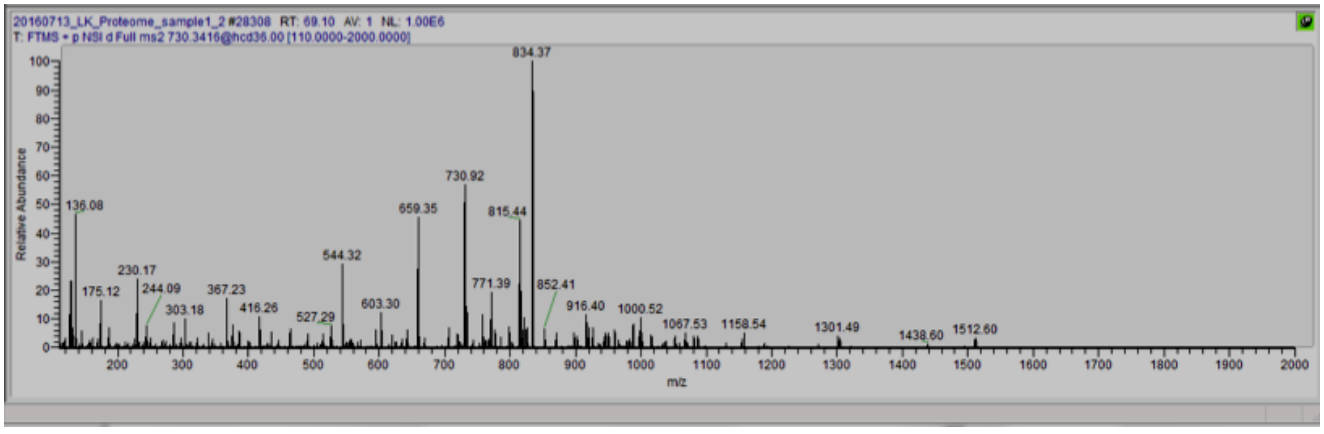
20160713_LK_Proteome_sample1_2 #28308 RT: 69.10 AV: 1 NL: 1.00E6
T: FTMS + p NSI d Full ms2 730.3416@hcd36.00 [110.0000-2000.0000]
Relative Abundance
m/z
834.37
730.92
136.08
659.35
815.44
544.32
230.17
175.12
244.09
367.23
303.18
416.26
527.29
603.30
771.39
852.41
916.40
1000.52
1067.53
1158.54
1301.49
1438.60
1512.60

D

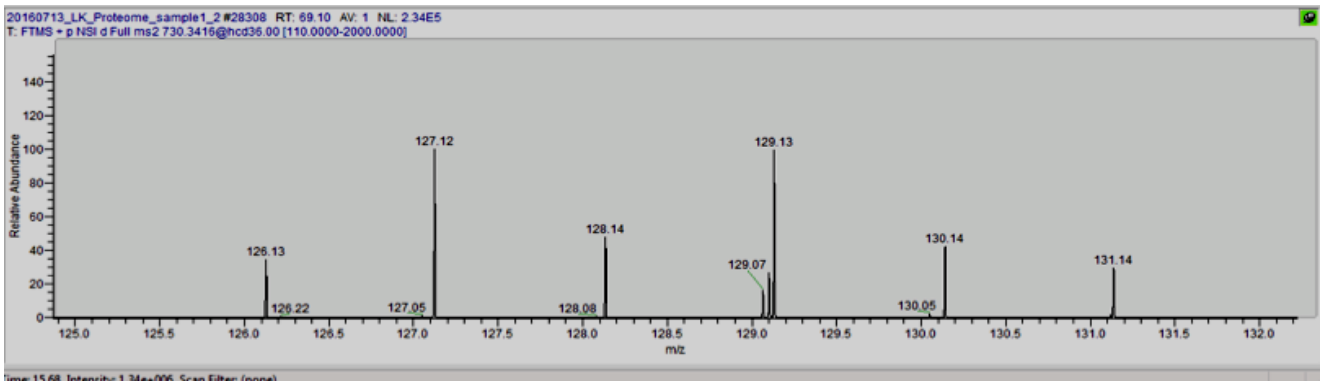

Figure 70: Representative mass spectra of thymidylate synthase in the proteome profiling experiment using mass spectrometry

Total ion chromatogram (TIC) of the scan (A), full MS1 spectra at RT 69.09 min (B), full MS2 spectra at precursor m/z 730.34 Da and first scan number 28308 (C) and the TMT6 labels (D).

AUTHOR'S PUBLICATIONS

1. Molina, D., Jafari, R., Ignatushchenko, M., Seki, T., Larsson, E., Dan, C., Sreekumar, L., Cao, Y. and Nordlund, P. (2013). Monitoring Drug Target Engagement in Cells and Tissues Using the Cellular Thermal Shift Assay. *Science.*, 341(6141):.84-87.
2. Sreekumar, L., Young Mee, K., Larsson, E., Nordlund, P. (2017). Thermal Precipitation Assay (TPA), a highly sensitive, flexible and instrument-free thermal shift technique for biophysical screening and characterization of proteins in complex mixtures. *(Manuscript in preparation).*
3. Sreekumar, L., Veerappan, S., Yan Ting, L., Nordlund, P. (2017). Exploring the potential of CETSA to study drug resistance development during cancer therapy. *(Manuscript in preparation).*
4. Yan Ting, L., Prabhu, N., Lingyun, D., Ka Diam, G., Dan, C., Sreekumar, L., Egeblad, L., Eriksson, S., Hsiang Ling, T., Soon Heng Tan, C., Lengqvist, J., Larsson, E., Sobota, R., Nordlund, P. (2017). Mapping specificities of nucleotide-protein interactions at the proteome level using CETSA. *(Manuscript).*
5. Soon Heng Tan, C., Ka Diam, G., Bisteau, X., Lingyun, D., Prabhu, N., Burak Ozturk, M., Yan Ting, L., Sreekumar, L., Han Yong, C., Lengqvist, J., Tergaonkar, V., Kaldis, P., Sobota, R., Nordlund, P. (2017). Protein Complex Dynamics in Intact Cells Monitored by MS-CETSA Based Thermal Proximity Co-Aggregation. *(Manuscript).*

POSTERS

2017. Exploring the potential of cellular thermal shift assay (CETSA) to study drug resistance during cancer therapy. American Association for Cancer research (AACR) annual meeting. Washington D.C, USA.